

องค์ประกอบทางเคมีและฤทธิ์ต้านการเพิ่มจำนวนของเซลล์มะเร็งของซีรูเมนจากชันโรง
Tetragonula laeviceps ในจังหวัดจันทบุรี



นายพงศวิช นุกิจรังสรรค์

จุฬาลงกรณ์มหาวิทยาลัย

CHULALONGKORN UNIVERSITY

วิทยานิพนธ์นี้เป็นส่วนหนึ่งของการศึกษาตามหลักสูตรปริญญาวิทยาศาสตรมหาบัณฑิต

สาขาวิชาเทคโนโลยีชีวภาพ

คณะวิทยาศาสตร์ จุฬาลงกรณ์มหาวิทยาลัย

ปีการศึกษา 2556

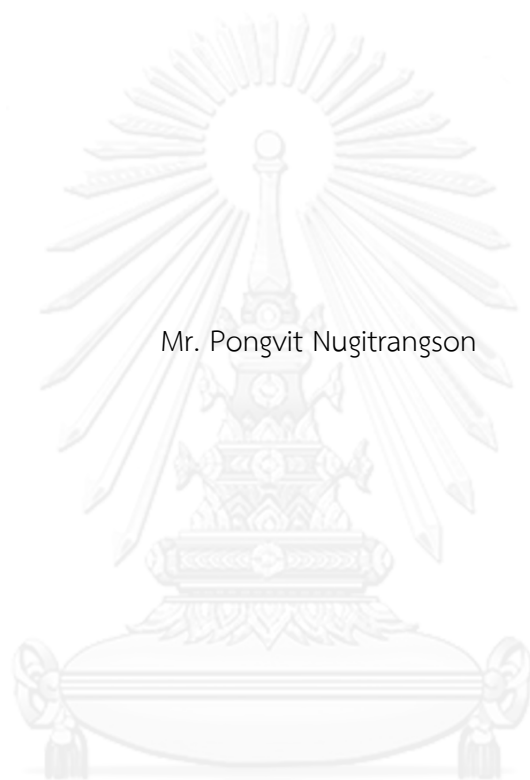
ลิขสิทธิ์ของจุฬาลงกรณ์มหาวิทยาลัย

บทคัดย่อและแฟ้มข้อมูลฉบับเต็มของวิทยานิพนธ์ตั้งแต่ปีการศึกษา 2554 ที่ให้บริการในคลังปัญญาจุฬาฯ (CUIR)

เป็นแฟ้มข้อมูลของนิสิตเจ้าของวิทยานิพนธ์ ที่ส่งผ่านทางบัณฑิตวิทยาลัย

The abstract and full text of theses from the academic year 2011 in Chulalongkorn University Intellectual Repository (CUIR) are the thesis authors' files submitted through the University Graduate School.

CHEMICAL COMPOSITION AND ANTIPROLIFERATIVE ACTIVITY ON CANCER CELL
LINES OF CERUMEN FROM STINGLESS BEE *Tetragonula laeviceps* IN CHANTHABURI
PROVINCE



Mr. Pongvit Nugitrangson

จุฬาลงกรณ์มหาวิทยาลัย

CHULALONGKORN UNIVERSITY

A Thesis Submitted in Partial Fulfillment of the Requirements
for the Degree of Master of Science Program in Biotechnology

Faculty of Science

Chulalongkorn University

Academic Year 2013

Copyright of Chulalongkorn University

Thesis Title	CHEMICAL COMPOSITION AND ANTIPROLIFERATIVE ACTIVITY ON CANCER CELL LINES OF CERUMEN FROM STINGLESS BEE Tetragonula laeviceps IN CHANTABURI PROVINCE
By	Mr. Pongvit Nugitrangson
Field of Study	Biotechnology
Thesis Advisor	Associate Professor Surachai Pornpakakul, Ph.D.
Thesis Co-Advisor	Associate Professor Chanpen Chanchao, Ph.D.

Accepted by the Faculty of Science, Chulalongkorn University in Partial
Fulfillment of the Requirements for the Master's Degree

.....Dean of the Faculty of Science
(Professor Supot Hannongbua, Dr.rer.nat.)

THESIS COMMITTEE

.....Chairman
(Associate Professor Vudhichai Parasuk, Ph.D.)

.....Thesis Advisor
(Associate Professor Surachai Pornpakakul, Ph.D.)

.....Thesis Co-Advisor
(Associate Professor Chanpen Chanchao, Ph.D.)

.....Examiner
(Noppadon Kitana, Ph.D.)

.....Examiner
(Assistant Professor Sanit Piyapattanakorn, Ph.D.)

.....External Examiner
(Ubolsree Laertsakulpanich, Ph.D.)

พงศวีช นุกิจรังสรรค์ : องค์ประกอบทางเคมีและฤทธิ์ต้านการเพิ่มจำนวนของเซลล์มะเร็งของซีรูเมนจาก
 ชันโรง *Tetragonula laeviceps* ในจังหวัดจันทบุรี. (CHEMICAL COMPOSITION AND
 ANTIPROLIFERATIVE ACTIVITY ON CANCER CELL LINES OF CERUMEN FROM STINGLESS BEE
Tetragonula laeviceps IN CHANTHABURI PROVINCE) อ.ที่ปรึกษาวิทยานิพนธ์หลัก: รศ. ดร.สุรัชย์
 พรภคกุล, อ.ที่ปรึกษาวิทยานิพนธ์ร่วม: รศ. ดร.จันทร์เพ็ญ จันทร์เจ้า, 133 หน้า.

Tetragonula laeviceps เป็นชันโรงประจำถิ่นชนิดหนึ่งของไทย ภายในรังประกอบด้วยเซลล์ที่เรียกว่า
 หม้อ ใช้เก็บผลิตภัณฑ์ต่างๆ วัสดุที่ใช้สร้างหม้อเรียกว่า ซีรูเมน เป็นของผสมของไขผึ้งและพอรพอลิส มีรายงานว่า
 ผลิตภัณฑ์ร่วมของผึ้งมีฤทธิ์ทางชีวภาพมากกว่าผลิตภัณฑ์เดี่ยว ในที่นี้จึงเน้นที่ฤทธิ์ต้านการเพิ่มจำนวนของเซลล์มะเร็ง
 ของซีรูเมน ทำการเก็บซีรูเมนจากจังหวัดจันทบุรี และทำการสกัดด้วย 80% เมทานอล ไดคลอโรมีเทนและเฮกเซน
 ตามลำดับ นอกจากนี้ยังทำการสกัดโดยสลับลำดับตัวทำละลาย จากนั้นนำสารสกัดอย่างหยาบทั้งหมดไปทดสอบฤทธิ์
 ต้านการเพิ่มจำนวนของเซลล์มะเร็ง 5 ชนิดในระดับหลอดทดลองด้วยวิธี MTT พิจารณาความเป็นพิษต่อเซลล์จากค่า
 ความเข้มข้นที่ยับยั้งการเจริญที่ 50% (IC_{50}) ผลการทดลองแสดงให้เห็นว่าสารสกัดอย่างหยาบด้วยไดคลอโรมีเทนแบบ
 กลับซ้ำ (reCDE) แสดงความเป็นพิษต่อเซลล์ดีที่สุดในการยับยั้งเซลล์มะเร็งทั้ง 5 ชนิด โดยมีค่า IC_{50} อยู่ในช่วง 0.56 -
 5.25 ไมโครกรัม/มิลลิลิตร ดังนั้นจึงนำ reCDE ไปทำการสกัดบริสุทธิ์ต่อด้วยซิลิกาเจลโครมาโทกราฟี ได้ 16 ส่วนแยก
 (แฟรกชัน) จากการทดสอบฤทธิ์ต้านการเจริญของเซลล์มะเร็ง พบว่าแฟรกชัน VII และ VIII มีฤทธิ์ดีที่สุด โดยมีค่า IC_{50}
 อยู่ในช่วง 3.38 - 6.46 และ 5.37 - 6.60 ไมโครกรัม/มิลลิลิตร ตามลำดับ นำแฟรกชันทั้งสองชนิดไปทำการสกัดบริสุทธิ์
 ต่อด้วยซิลิกาเจลโครมาโทกราฟีจนได้สารประกอบบริสุทธิ์ จากการวิเคราะห์ด้วยเทคนิค Nuclear magnetic
 resonance spectroscopy จำแนกได้ว่าเป็น alpha-mangostin สารชนิดนี้มีฤทธิ์ต้านการเจริญของเซลล์ BT474,
 Chago, Hep-G₂, KATO-III และ SW620 ด้วยค่า IC_{50} ที่ 0.50, 0.92, 0.39, 0.36 and 0.62 ไมโครกรัม/มิลลิลิตร
 ตามลำดับ ขณะที่ doxorubicin แสดงค่า IC_{50} ที่ 0.42, 0.35, 0.32, 0.56 and 0.07 ไมโครกรัม/มิลลิลิตร ตามลำดับ
 หลังจากเลี้ยงเซลล์มะเร็งต่าง ๆ ร่วมกับ alpha-mangostin แบบเดี่ยวๆ ด้วยความเข้มข้นที่ค่า IC_{50} สันฐานวิทยาของ
 เซลล์ที่ถูกทดสอบ พบว่ามีลักษณะใกล้เคียงแบบ apoptosis จากงานวิจัยนี้ จึงกล่าวได้ว่า alpha-mangostin ที่พบในซี
 รูเมนของ *T. laeviceps* เป็นทางเลือกใหม่ในการพัฒนาเป็นสารต้านมะเร็งได้

จุฬาลงกรณ์มหาวิทยาลัย
 CHULALONGKORN UNIVERSITY

สาขาวิชา เทคโนโลยีชีวภาพ

ปีการศึกษา 2556

ลายมือชื่อนิสิต

ลายมือชื่อ อ.ที่ปรึกษาวิทยานิพนธ์หลัก

ลายมือชื่อ อ.ที่ปรึกษาวิทยานิพนธ์ร่วม

5472192423 : MAJOR BIOTECHNOLOGY

KEYWORDS: ANTIPROLIFERATIVE ACTIVITY / CERUMEN / MTT ASSAY / ALPHA-MANGOSTIN /
CHROMATOGRAPHY

PONGVIT NUGITRANGSON: CHEMICAL COMPOSITION AND ANTIPROLIFERATIVE ACTIVITY ON
CANCER CELL LINES OF CERUMEN FROM STINGLESS BEE *Tetragonula laeviceps* IN
CHANTHABURI PROVINCE. ADVISOR: ASSOC. PROF. SURACHAI PORNPAAKAKUL, Ph.D., CO-
ADVISOR: ASSOC. PROF. CHANPEN CHANCHAO, Ph.D., 133 pp.

Tetragonula laeviceps is one of Thai native stingless bees. A hive is composed of cells called pots, that are used to store products. The material used in the construction called cerumen is a mixture of wax and propolis. It was reported that the mixed products of bees had the better bioactivities than a single product. Here, this research was focused on the antiproliferative activity of cerumen. The cerumen was collected from Chanthaburi province and extracted by 80% methanol, dichloromethane, and hexane, respectively. Also, the reversed order of solvents was used to extract. Next, all of crude extracts were examined the in vitro antiproliferative activity against 5 human cancer cell lines by MTT assay. The cytotoxicity was determined by 50% inhibition concentration (IC₅₀) values. The result showed that reverse crude dichloromethane extract (reCDE) presented the best cytotoxicity against 5 cancer cell lines with the IC₅₀ values in the range of 0.56 - 5.25 µg/mL. Thus, reCDE was further purified by silica gel chromatography to give 16 fractions. By the antiproliferative assay, it showed that fraction VII and VIII exhibited the best cytotoxicity against those cell lines with the IC₅₀ value in the range of 3.38 - 6.46 and 5.37 - 6.60 µg/mL, respectively. Both fractions were further purified by silica gel chromatography until gaining a pure compound. By Nuclear Magnetic Resonance Spectroscopy analysis, it was identified as alpha-mangostin. This compound was exhibited antiproliferative activity against BT474, Chago, Hep-G₂, KATO-III and SW620 with IC₅₀ values at 0.50, 0.92, 0.39, 0.36 and 0.62 µg/mL, respectively. While doxorubicin showed IC₅₀ values at 0.42, 0.35, 0.32, 0.56 and 0.07 µg/mL, respectively. After cancer cell lines were treated with the isolated alpha-mangostin at IC₅₀ concentration, cell morphology of the treated cell lines was revealed an apoptotic-like character. From this research, alpha-mangostin in *T. laeviceps* cerumen was a new choice to develop to be an anticancer agent.

จุฬาลงกรณ์มหาวิทยาลัย
CHULALONGKORN UNIVERSITY

Field of Study: Biotechnology

Academic Year: 2013

Student's Signature

Advisor's Signature

Co-Advisor's Signature

ACKNOWLEDGEMENTS

I would like to express my respective thank to my advisor, Assoc. Prof. Dr. Surachai Pornpakakul who gave me instructions and advices for a basic knowledge in chemistry method and important techniques used in this research.

I would like to express my respective thank my co-advisor, Assoc. Prof. Dr. Chanpen Chanchao who gave me instructions and advices in this research.

I would like to give my respective thank to Ms. Songchan Puthong and members of the institute of biotechnology and genetic engineering for cell culture.

I would like to give a special thank to a chairman and all committee for their suggestions and advices on my proposal and thesis.

I would like to thank Mr. Supongphan Srisurichan and members of research center for bioorganic chemistry, Department of Chemistry, Faculty of Science, Chulalongkorn University for helping in analyzing chemical structure of active compounds.

I would like to thank Ms. Pattaporn Boonsai and members of molecular biology research laboratory, Department of Biology, Faculty of Science, Chulalongkorn University for helping in extraction of cerumen.

I would like to thank Mr. Sawas and Mrs. Alai Jittajaroen, an owner of orchard and meliponiculture farm in Chantaburi province for sample collection.

I would like to thank the 90th Anniversary of Chulalongkorn University Fund (Ratchadaphiseksomphot Endowment Fund) and National Research Unit (AS613A) for financial supports.

I would like to thank Program in Biotechnology, Department of Chemistry, Department of Biology, Faculty of Science, Chulalongkorn University for all academic matters.

Finally, I am always thankful to my family members for all support and encouragement throughout my life.

CONTENTS

	Page
THAI ABSTRACT	iv
ENGLISH ABSTRACT	v
ACKNOWLEDGEMENTS	vi
CONTENTS	vii
FIGURE CONTENTS	xi
TABLE CONTENTS	xiii
Chapter I Introduction	1
Chapter II literature review	3
2.1 Biology of stingless bees <i>Tetragonula laeviceps</i>	3
2.2 Bioactivity of bee and stingless bee products	7
2.2.1 Antimicrobial activity	7
2.2.2 Antiviral activity	8
2.2.3 Anti-inflammatory activity	8
2.2.4 Anti-cholesterol activity	9
2.2.5 Anti-oxidant activity	9
2.2.6 Antiproliferative activity	10
2.3 Xanthone derivatives	10
2.4 Cancer disease	15
2.4.1 Overview of cancer patients	15
2.4.2 Apoptosis and cancer	16
2.4.3 Angiogenesis	17
2.4.4 Treatment of cancer	18
Chapter III Materials and Methods	21
3.1 Equipments & Supplies	21
3.2 Chemicals	24
3.3 Cerumen collection	25
3.4 Bioassay guided partition extraction	25

	Page
3.5 The Isolation and Identification of bioactive compounds	26
3.5.1 The Isolation of bioactive crude extracted from cerumen of <i>T. laeviceps</i>	26
3.5.2 The Isolation of bioactive fractions.....	28
3.5.3 The Isolation of subfractions that originated from bioactive fractions.....	31
3.5.4 Thin layer chromatography (TLC) identification	34
3.5.5 Identification of chemical structure.....	34
3.6 The antiproliferative activity.....	35
3.6.1 Cancer cell lines.....	35
3.6.2 Cancer cell line preparation.....	36
3.6.3 Antiproliferative activity assay.....	37
3.6.4 [3-(4,5-dimethyl-thiazol-2-yl)2,5-diphenyl-tetrazolium bromide] (MTT) assay	38
3.6.5 Calculation for 50% inhibition concentration (IC ₅₀) value.....	39
3.6.6 Statistical analysis.....	40
3.7 Cell morphology analysis.....	40
Chapter IV Results	41
4.1 Crude extract of cerumen.....	41
4.2 Antiproliferative activity of crude extracts.....	42
4.3 Chemical composition of the reverse crude dichloromethane extract.....	47
4.4 Antiproliferative activity of merged fractions from reCDE.....	48
4.5 Chemical composition from fraction VII and VIII.....	57
4.6 The antiproliferative activity of the combined fraction from fractions VII and VIII	58
4.7 Chemical composition from F7F and F8E subfractions	62
4.8 Antiproliferative activity of combined fractions from F7F and F8E.....	63
4.9 The antiproliferative activity of chemotherapeutic drugs	70
4.10 CRL-1947 fibroblast cytotoxicity.....	72

	Page
4.11 Morphology of untreated cancer cell lines	73
4.11.1 Untreated BT474 cell line.....	75
4.11.2 Untreated Chago cell line.....	76
4.11.3 Untreated Hep-G ₂ cell lines	77
4.11.4 Untreated KATO-III cell line.....	78
4.11.5 Untreated SW 620 cell line	79
4.12 Morphology of treated cancer cell lines	80
4.12.1 Treated BT474 cell line.....	81
4.12.2 Treated Chago cell line.....	82
4.12.3 Treated Hep-G ₂ cell line	83
4.12.4 Treated KATO-III cell line	84
4.12.5 Treated SW620 cell line.....	85
4.13 Chemical structure of a bioactive compound.....	87
Chapter V Discussion.....	90
Chapter VI Conclusions	98
REFERENCES	100
Appendix A.....	108
Appendix B.....	118
Appendix C.....	130
Appendix D.....	132
VITA.....	134

FIGURE CONTENTS

Figure 2.1 <i>Tetragonula laeviceps</i> Smith 1857	4
Figure 2.2 Overview of stingless bee's nest.....	5
Figure 2.3 Honey pot of <i>T. laeviceps</i>	5
Figure 2.4 Overview of <i>T. laeviceps</i> nest in bamboo stem.....	6
Figure 2.5 A pathway of xanthone biosynthesis	11
Figure 2.6 Nucleus structure of xanthone group.....	11
Figure 2.7 Chemical structure of mangostin group.....	19
Figure 2.8 Garcinone E.....	14
Figure 2.9 Gartanin.....	15
Figure 2.10 Extrinsic and intrinsic apoptosis pathway.....	17
Figure 2.11 Angiogenesis overview.....	18
Figure 2.12 Paclitaxel	18
Figure 2.13 5-fluorouracil.....	19
Figure 2.14 Doxorubicin.....	19
Figure 3.1 <i>T. laeviceps</i> 's honeypot cerumen.....	25
Figure 3.2 NMR spectroscopy.....	35
Figure 3.3 Image from microscope (20X magnification) showing morphology of five cancer cell lines.....	36
Figure 3.4 The chemical structure of anti-cancer drugs.....	38
Figure 3.5 Overview of [3-(4, 5-dimethyl-thiazol-2-yl) 2, 5-diphenyl-tetrazolium bromide] (MTT) assay.....	39
Figure 3.6 An inverted light microscope connecting to a camera.....	40
Figure 4.1 Percentage of viable cells presenting graph of 6 crude extracts against 5 different cancer cell lines.....	46
Figure 4.2 Percentage of viable cells presenting graph of 12 fractions of reverse crude dichloromethane extracts against 5 cancer cell lines	56
Figure 4.3 The percentage of viable cells of subfraction F7E and F7F against different 5 cancer cell lines.....	60

Figure 4.4 The percentage of viable cells of subfraction F8E against different 5 cancer cell lines.....	61
Figure 4.5 The graphs presenting the percentage of viable cells of combined fraction from subfraction F7F against different 5 cancer cell lines.....	67
Figure 4.6 The graphs presenting the percentage of viable cells of combined fraction from subfraction F8E against different 5 cancer cell lines.....	69
Figure 4.7 The graphs presenting the percentage of viable cells from chemotherapeutic drugs against 5 different cancer cell lines.....	71
Figure 4.8 Fibroblast cytotoxicity by purified compounds.....	73
Figure 4.9 The morphology of untreated BT474 cell line.....	75
Figure 4.10 The morphology of untreated Chago cell line	76
Figure 4.11 The morphology of untreated Hep-G2 cell line	77
Figure 4.12 The morphology of untreated KATO-III cell line.....	78
Figure 4.13 The morphology of untreated SW620 cell line.	79
Figure 4.14 The morphology of treated BT474 cell line	81
Figure 4.15 The morphology of treated Chago cell line.....	82
Figure 4.16 The morphology of treated Hep-G2 cell line.....	83
Figure 4.17 The morphology of treated KATO-III cell line	84
Figure 4.18 The morphology of treated SW620 cell line.....	85
Figure 4.19 The chemical structure of fraction F7F-3 by NMR analysis.	87
Figure 4.20 HMBC correlation of carbon position of F7F-3.....	89

TABLE CONTENTS

Table 3.1 The stepwise gradient of mobile phase used in the column chromatography for active crude extracts	27
Table 3.2 The stepwise gradient of mobile phase used in the column chromatography for the bioactive fraction (the combined fraction VII).	29
Table 3.3 The stepwise gradient of mobile phase used in the column chromatography for bioactive fraction (the combined fraction VIII).	30
Table 3.4 The stepwise gradient of mobile phase used in the column chromatography for bioactive subfraction (combined subfraction F7F).	32
Table 3.5 The stepwise gradient of mobile phase used in the column chromatography for bioactive subfraction (combined subfraction F8E).	33
Table 4.1 Mass, yield, and appearance of crude extracts.	41
Table 4.2 Mass, yield, and appearance of crude reverse polarity extracts.	41
Table 4.3 The IC ₅₀ values of 6 crude extracts on the cancer cell lines.	43
Table 4.4 Mass, yield, and appearance of merged fractions from reCDE extract after isolation with column chromatography.	47
Table 4.5 The IC ₅₀ values of merged fractions from reverse crude dichloromethane extract.	50
Table 4.6 Mass, yield, and appearance of 10 subfractions (fraction VII as origin).	57
Table 4.7 Mass, yield, and appearance of 9 compositions (fraction VIII as origin).	58
Table 4.8 The IC ₅₀ values of subfraction F7E and F7F originated from fraction VII.	59
Table 4.9 The IC ₅₀ values of subfraction F8E originated from fraction VIII.	61
Table 4.10 Mass, yield, and appearance of 13 combined fractions originated from subfraction F7F.	62
Table 4.11 Mass, yield, and appearance of 13 combined fractions originated from subfraction F8E.	63
Table 4.12 The IC ₅₀ values of the F7F-3, F7F-4, F7F-5, and F7F-6 originated from subfraction F7F.	65
Table 4.13 The IC ₅₀ values of F8E-5, F8E-6, and F8E-7 originated from subfraction F8E.	68

Table 4.14 The IC ₅₀ values of doxorubicin and 5-fluorouracil in µg/mL and µmol/mL.	70
Table 4.15 Cytotoxicity of the isolated compounds and drugs to fibroblast.....	72
Table 4.16 The IC ₅₀ value of F7E, F7F-3 and F8E-5.....	74
Table 4.17 NMR spectroscopic data of F7F-3.....	88
Table 4.18 IC ₅₀ of alpha-mangostin (F7F-3) in µg/mL and µmol/L.....	89



Chapter I

Introduction

Stingless bee is one of social insects in family Apidae like honeybee (*Apis mellifera*). In Thailand, *Tetragonula laeviceps* is one of native stingless bees that are widely dispersed and is one of the most meliniponiculture (stingless bee culturing) (2, 3). Since it has no sting, it is not aggressive like honeybee and easy to manage. In its hive, it is composed of many cells, called pots that are used to store larvae, pollen, honey, and other products. The main material used in the construction of these pots is cerumen which is a mixture of pure wax and propolis (4-6). It is dark brown and sticky material. Cerumen is not only the main material of storage pots and brood cells, but it is also the material for involucrum (Cerumen sheet that cover brood section for controlling temperature) to protect brood cells.

Previously, it was reported that products of bees including stingless bees such as honey, propolis, wax, pollen, and venom had many bioactivities and pharmaceutical benefits such as anti-viral (7), antimicrobial (8-11), anti-oxidant (12, 13), anti-inflammatory (14, 15), anti-cholesterol (16), and antiproliferative activities (17-19). Interestingly, a bioactivity of mixed bee products was more active than a single product (8, 16). Thus, cerumen, which is a kind of mixed products, should be interesting in searching for a better bioactivity. Due to a few research on cerumen, it was reported that pimaric acid, iso-pimaric acid, and gallic acid from crude ethanol extraction of *T. carbonaria*'s cerumen in Australia could inhibit 5-lipoxygenase which was one of inflammatory modulators (5). As known, a bioactivity and a chemical composition of bee products depends on species, biodiversity of food plants, climate, region, and separation technique (20). In this research, cerumen of *T. laeviceps* collected from Chantaburi province was the main target because it has a meliniponiculture and apiculture complex for orchard agricultural in this area. Also, it was focused on the antiproliferative activity against cancer cells, a disease causing by an abnormality in cell cycle which misled to the response in apoptosis process (21). As known, cancer is one of the most severe diseases causing the high rate of death nowadays. Since chemotherapy still gives many severe side effects to patients, it is important to find a new and better active chemical compound, especially from natural products. In this research, it was aimed to separate and analyse chemical compositions in cerumen of *T. laeviceps* by partition extraction with three different

organic solvents. All crude extracts were tested for the antiproliferative/ cytotoxic activity against five human cancer cell lines which were breast cancer cell line or BT474, lung cancer cell line or Chago, liver cancer cell line or Hep-G₂, stomach cancer cell line or KATO-III, and intestine cancer cell line or SW620. The most active crude extract of cerumen was further purified by column chromatography. The active fraction was obtained by MTT assay. The purity of separated chemical compositions was observed by thin layer chromatography (TLC). The most active and purest compound was analyzed for the structure by nuclear magnetic resonance (NMR) and molecular mass by mass spectroscopy (MS). Later, cancer cells treated with an active compound were observed for the morphology change. In addition, cell death type was investigated.

Objectives

- To determine whether *Tetragonula laeviceps* cerumen shows the antiproliferative activity
- To observe the change in cancer cells treated with *T. laeviceps* cerumen in term of morphology, cell death, and cytotoxicity
- To characterize a chemical structure of active compound in *T. laeviceps* cerumen

Chapter II

literature review

2.1 Biology of stingless bees *Tetragonula laeviceps*

It is one type of eusocial insects which has a main role in pollination of plants. The benefit to bee farmers is that it is stingless and not aggressive. It is similar to honeybee like *Apis mellifera*, *A. cerana* in many points. For example, both stingless bee and honeybee are in the same family of Apidae (22). They have a complete metamorphosis which is composed of egg, larva, pupa, and adult. They have a sex determination and share a lot of common behaviors. A queen and a worker are diploid female which was born by fertilization while a drone is haploid male which was born by parthenogenesis. For task assignment in a hive, a drone is in charge of mating only. Whenever, a drone is successfully mated to a queen, it will die. A worker has a lot of activities in a hive such as cleaning, constructing a hive, foraging, nursing broods, guarding an enemy. A queen controls and manages everything in a hive by using its pheromone. The most important role is that only a queen can lay eggs while workers are sterile (23).

Nowadays, stingless bees in Thailand are essential for orchard agriculture because they do not have floral preference like honeybees. Thus, they can forage nectar, pollen, and plant resin from various plant species. Besides, they are very good pollinators because they want pollen more than nectar. That helps to spread pollen better than honeybees. Farmers of some orchard agricultural areas prefer stingless bees than honeybees in order to increasing fruit product (24).

Tetragonula laeviceps is one type of stingless bees that is most widely dispersed in Thailand. It looks black (Figure 2.1). Due to Klakasikorn et al. (3), stingless bees were collected from 5 provinces in Thailand which were Chiang Mai, Mae Hongson, Nan, Kanchanaburi, and Chantaburi. After identified, it was reported that *T. laeviceps* could be dispersed in Chiang Mai, Nan, and Chantaburi. Its hive was host specific to *Havea brasiliensis* (Yang-pa-ra in Thai) trees.



Figure 2.1 *Tetragonula laeviceps* Smith 1857 (www.discoverlife.org)

Taxonomic key of *T. laeviceps* (2, 22, 25)

Kingdom Animalia

Phylum Arthropoda

Class Insecta

Order Hymenoptera

Family Apidae

Tribe Meliponini

Genus *Tetragonula*

Species *Tetragonula laeviceps*

A hive entrance of different stingless bee species has a different shape like cylindrical tube, no funnel. It is unique so it can be used for species identification. The tube is made from resin and mud. According to Figure 2.2, a hive in a dark hole is covered by batumen but on top and bottom of the hive is covered by a very thick batumen plate. Inside a hive, there are a lot of storage pots and brood cells which are made from cerumen as main material. Cerumen is a black-brown sticky mixture containing wax, propolis, and plant resin. These pots are used to keep honey and bee pollen (Figure 2.3). Brood cells are arranged in many rows and layers at the center of a hive. Both areas are separated by a laminate layer of cerumen called involucrum.

Involucrum is used to control the temperature within a hive. However, sometimes involucrum may not be needed (6, 26).

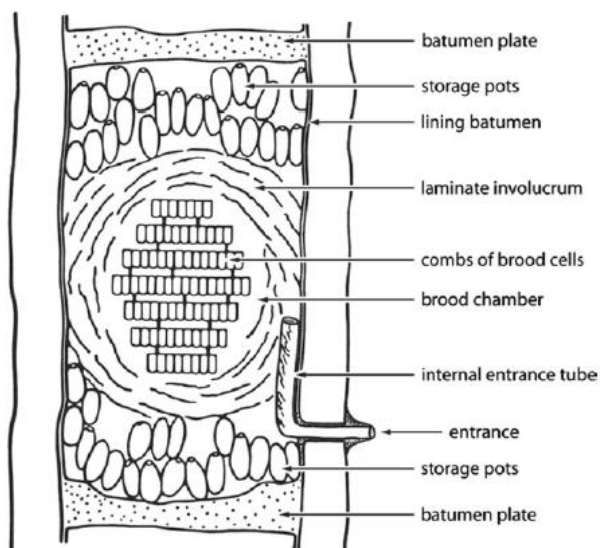


Figure 2.2 Overview of stingless bee's nest (27)

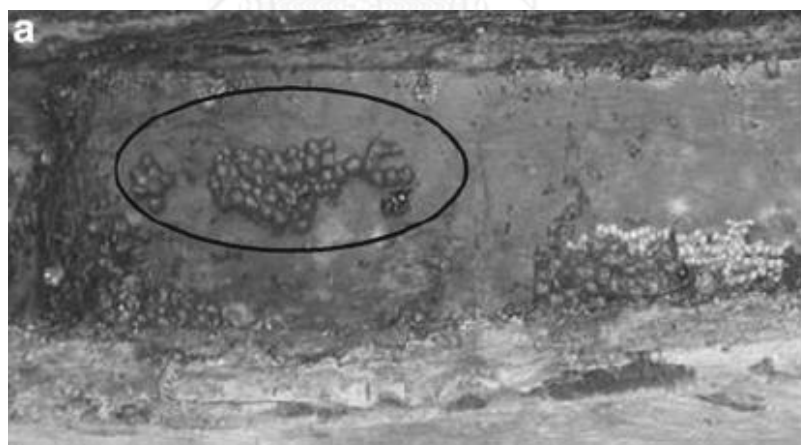


Figure 2.3 Honey pot of *T. laeviceps* (24)

In 1983, Sakagami and Inoue (26) reported *T. laeviceps* nesting in Indonesia. It could construct a nest in a bamboo shoot. On top of shoot cavity, it was coated with thick batumen that had a water layer surrounding with thin black resin. An entrance tube made from black resin was 9-10 cm in length. Inside the cavity, zones of honey pots, bee pollen pots, brood cells, and cocoon cells were separated (Figure 2.4).

Inner tunnel was located closely to brood cells. Honey and pollen pots were arranged in clump and were attached closely to cavity wall. Storage pots were made from cerumen and had an oval shape with the length of 5-11 mm and the width of 7-14 mm. Brood cells at the center of cavity were coated with involucrum layers. Worker cells had an oval shape with the 3.9 mm length and 3.0 mm width. A queen cell has a larger size ($6 \times 4 \text{ mm}^2$) than a worker cell.

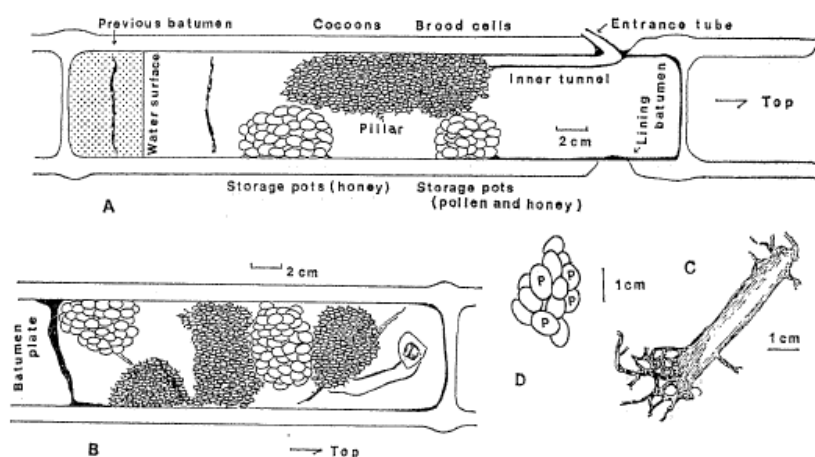


Figure 2.4 Overview of *T. laeviceps* nest in bamboo stem. A indicates large cavity. B indicates well occupied cavity. C indicates inner tunnel. D indicates honey pot and pollen pot which is labeled “p” (26).

In 2005, Chinx et al. (4) reported stingless bee nesting in the Cuc Phong national forest, northern Vietnam. They collected 35 hives of stingless bees which could be classified into 3 groups of *Lisotrigona carpentari*, *Lepidotrigona ventralis*, and *Tetragonula laeviceps*. *T. laeviceps*'s nest was found in a big tree trunk and between rocks. A hive entrance was not a tube but was a hole covered by black resin instead. The inner side of the nest was covered by thin black material (batumen plate). Brood cells were not arranged into layer but were in many clumps. New brood cells were brown. In contrast, cocoon cells looked yellow because wax was removed. These brood cells were covered by laminate involucrum. A storage pot had an oval shape with the 5-7 mm width and 12-15 mm height.

2.2 Bioactivity of bee and stingless bee products

For decades, honeybee and stingless bee products which are honey, bee pollen, beeswax, propolis, cerumen, royal jelly, and bee venom have had various bioactivities which are beneficial for medical and pharmaceutical applications. Since bioactivity of cerumen was hardly reported, in this chapter, bioactivity of other bee products were reported instead.

2.2.1 Antimicrobial activity

In 2011, Voidarou et al. (9) reported the antibacterial activity of 60 honey samples from *A. mellifera* collected from 4 different botanical sources in Greece. The antibacterial activity was against 16 bacterial strains belonging in 7 species of *Staphylococcus* spp., *Escherichia coli*, *Salmonella* sp., *Bacillus* sp., and *Shigella* sp. After agar well diffusion method with different concentrations of honey was done, the percentage of inhibition zone was calculated. The result showed that honey originated from coniferous botanical source had the best antimicrobial activity with the minimal dilution of 17.4% (w/v). The antimicrobial activity was followed by honey originated from thyme botanical source with the minimal dilution of 19.2% (w/v), honey originated from citrus and polyfloral botanical sources with the minimal dilutions of 20.8% (w/v) and 23.8% (w/v), respectively.

In 2012, Choudhari et al. (10) found that crude ethanol extract (CEE) of *Trigona* sp.'s propolis in India had the antibacterial and antifungal activity against 6 strains of multidrug resistant bacteria and *Candida glabrata* as fungi. The minimum inhibition concentration (MIC), minimum bactericidal concentration (MBC), and minimum fungicidal concentration (MFC) values were observed. It revealed that the MBC value was in the range of 2.43-19.50 µg/mL and the MFC value was 2.43 µg/mL. The killing curve for those microorganisms treated by CEE at its MIC value was in the period of 1.08 to 3.53 h. Later, active chemical compounds were analysed by gas chromatography-mass spectrophotometry (GC-MS), 15 out of 24 compounds were reported to be firstly found.

In 2014, Boonsai et al. (11) reported that cardanol from crude methanol extract (CME) of *A. mellifera*'s propolis in Thailand had the best antibacterial activity against *S. aureus* and *E. coli* with the IC₅₀ values of 0.175 µg/mL and 0.683 µg/mL, respectively. The change in morphology of *E. coli* was also observed after it was treated with cardol at its 3x IC₅₀ value

2.2.2 Antiviral activity

In 2010, Nolkemper et al. (7) reported that crude water extract (CWE) and CEE of *A. mellifera*'s propolis in Czech republic could inhibit plaques of herpes simplex virus in the IC_{50} range of $4-5 \times 10^{-4}$ % (w/v). Also, both CWE and CEE could reduce the risk on HSVII infected RC-37 cell lines at 99%. When both extracts were analysed by high performance liquid chromatography (HPLC), they revealed various types of polyphenolic compounds and phenylcarboxylic acids such as quercetin dihydrate, chrysin, pinocembrin, galanglin, benzoic acid, cinnamic acid, caffeic acid, and *p*-cumaric acid.

In 2012, Shahzad and Cohrs (28) reported that commercial Manuka honey and clover honey in Colorado, USA, could inhibit Varicella zoster virus that infected human malignant melanoma cells lines (MeWo). Both types of honey had half effective concentration (EC_{50}) at 4.5% (w/v). However, clover honey had cytotoxicity to uninfected MeWo cell lines. The viability of cells treated with 5% (w/v) clover honey was 60% while the viability of cells treated with 5% (w/v) Manuka honey was approximately 75%.

2.2.3 Anti-inflammatory activity

In 2010, Rached et al. (14) injected 1.5 mg/kg of bee venom from *A. mellifera* in Brazil to antigen-induced arthritic rabbits (n=7-9) every day for total 7 days. It could reduce leukocyte concentration to be $18,571 \pm 1,909$ cells/mL, comparing to the control rabbit which the leukocyte concentration was $40,968 \pm 5,248$ cells/mL. In addition, prostaglandin E_2 (PGE_2) concentration in the treated group decreased to be 0.49 ± 0.05 ng/mL, comparing to the control group which the PGE_2 concentration was 2.92 ± 0.68 ng/mL.

In 2010, Maruyama et al. (15) reported that CEE of *A. mellifera* bee pollen from *Cistus* sp. and *Brassica* sp. in China had the anti-inflammatory activity to carrageenan inducing edema at hind paw of mice. CEE at 100 mg/kg and 300 mg/kg could inhibit the percentage of swelling at 48.4 and 43.5, respectively. Both concentrations were significantly efficient, comparing to anti-inflammatory drugs. For example, indomethacin had the percentage of swelling at 27.3. Furthermore, CEE could inhibit cyclooxygenase-1 (COX-1) and cyclooxygenase-2 (COX-2), main inflammatory enzymes, with the IC_{50} values of > 150 μ g/mL and 10.3 μ g/mL, respectively.

2.2.4 Anti-cholesterol activity

In 2010, Nemoseck et al. (29) reported that clover honey from *A. mellifera* in USA could decrease the body weight, adiposity, and triglyceride in Sprague-Dawley rats. Total 36 rats were used. Eighteen rats had been fed with diet mixing with honey while other 18 rats had been fed with diet mixing with liquid sucrose for 33 days. For the first group, the body weight, food uptake, epididymal fat weight, serum triglyceride, and leptin were less than the second group by 14.7%, 13.3%, 20.1%, 29.6%, and 21.6%, respectively. However, non-high density lipoprotein (non-HDL) cholesterol in the first group was less than the second group by 16.8%.

In 2011, Kasianenko et al. (16) reported bee products such as honey, bee pollen, and bee bread from *Apis mellifera* in Russia could treat patients those had a problem of cholesterol level. Total cholesterol and low density lipoprotein (LDL) cholesterol were decreased in a patient treated with honey and bee pollen to 18.3% and 23.9%, respectively. Also, total cholesterol and LDL cholesterol were decreased in a patient treated with bee bread to 15.7% and 20.5%, respectively. Furthermore, body mass index (BMI) of overweight and obese patients treated with these bee products decreased, comparing to the untreated patients.

2.2.5 Anti-oxidant activity

In 2009, Saric et al. (12) studied bee pollen from *A. mellifera* collected in Dalmatia and surrounding island in Croatia. It was originated from *Cystus incanus* L. flower pollen. It was *in vivo* tested for the antioxidant activity on laboratory mice. The result showed that the level of antioxidant enzymes such as lipid peroxidation (LPO), superoxide dismutase (SOD), catalase (CAT), and glutathione peroxidase (gpX) in liver, brain, and erythrocyte was changed. Also, lipid peroxidation in liver decreased. When analyzing this bee pollen by HPLC, it revealed various phenolic compounds in the group of flavonol, flavones, and phenyl propanoid or caffeic acid.

In 2011, Morais et al. (13) studied *A. mellifera* bee pollen collected from 5 national parks in northern Portugal. The dominant flower pollens in bee pollen came from 8 families of plants. This bee pollen was tested for the antioxidant activity by di (phenyl)-(2,4,6-trinitrophenyl) iminoazanium (DPPH) and beta-carotene bleaching assay. The result revealed that bee pollen from Parque Natural de Montesinho had the best DPPH reduction with the EC₅₀ value of 2.60 µg/mL and the best beta-carotene bleaching efficiency with the EC₅₀ value of 3.11 µg/mL.

2.2.6 Antiproliferative activity

In 2010, Jo et al. (17) determined the antiproliferative activity against ovarian cancer cell lines (SKOV3 and PA-1 cell lines) and apoptosis relating protein from bee venom and mellitin (major protein in bee venom) of *A. mellifera*. The result showed that bee venom and mellitin had the antiproliferative activity against SKOV3 cell line with the IC_{50} values of 3.8 $\mu\text{g/mL}$ and 1.5 $\mu\text{g/mL}$, respectively. In addition, bee venom and mellitin had the antiproliferative activity against PA-1 cell line with the IC_{50} values of 2.6 $\mu\text{g/mL}$ and 1.2 $\mu\text{g/mL}$, respectively. The expression and translation modification of apoptotic proteins increased in treated cell lines. However, the expression and modification of cancer proteins such as JAK2, STAT3, Bcl-2 decreased.

In 2011, Umthong et al. (18) found that 30DCM, a partial purified composition from *T. laeviceps*'s propolis from Samut Songkram province had the antiproliferative activity against 5 cancer cell lines with the IC_{50} range of 4.09-14.67 $\mu\text{g/mL}$. Also, the partial purified sample had no effect on CH-liver cell line as normal cells.

In 2012, Teerasripreecha et al. (19) found that cardol and cardonal purified from *Apis mellifera*'s propolis in Nan province had the antiproliferative activity against 5 cancer cell lines with the IC_{50} range of 3.13–5.97 $\mu\text{g/mL}$ and 10.80–29.30 $\mu\text{g/mL}$, respectively. Also, both compounds had no cytotoxicity and DNA damaging to normal fibroblast (Hs27 cell line).

2.3 Xanthone derivatives

Xanthone is an organic compound firstly used as ovicide and larvicide of *Carpocapsa pomonella* which was pest of apple trees (30). This compound could be synthesized by shikimate and acetate pathway with phenylalanine and *meta*-hydroxybenzoic acid. The result showed the product of 1,3,5-trihydroxyxanthone that was the origin of compounds in xanthone group or genistein derivatives (31).

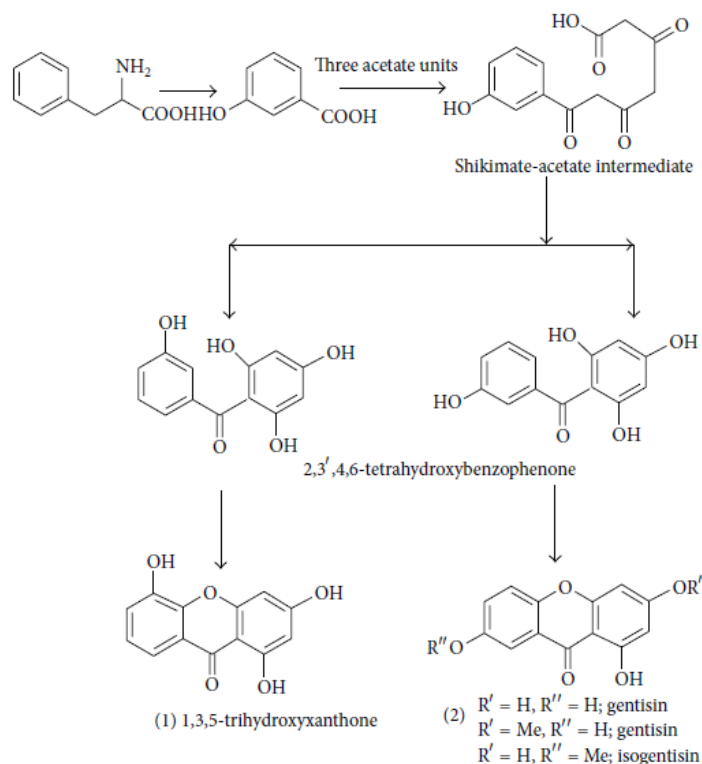


Figure 2.5 A pathway of xanthone biosynthesis (30)

The nucleus structure of xanthenes is dibenzo- γ -pyrone ring. The chemical structure is shown in Figure 2.5 and the main formula is $C_{13}H_8O_2$. The difference of xanthenes are from various functional groups and alkyl groups.

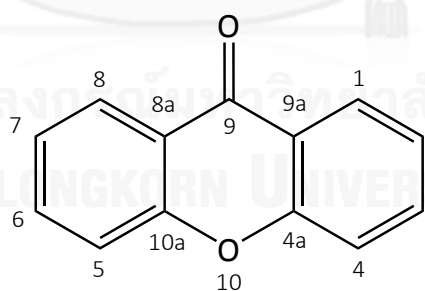


Figure 2.6 Nucleus structure of xanthone group.

Xanthone was mostly found in *Garcinia mangostana* or mangosteen, a tropical fruit found in Southeast Asia including Thailand. This fruit was renowned to be “queen of fruit” because its pericarp contained chemical compounds having various interesting bioactivities which were valuable for pharmaceutical and medicinal applications (32).

Xanthone compositions were found in many parts of mangosteen like fruit, bark, root (1, 33, 34). It was reported that 50 types of xanthenes were found in pericarp. In addition, xanthenes were still found in other plants. For example, 6 pruniflorone and 19 known xanthenes were found in stem of *Cratoxylum formosum*.

Mangostin group was one of mostly found xanthenes in mangosteen. Compounds in this mangostin group were alpha-mangosteen, beta-mangostin, and gamma-mangostin (Figure 2.7). The last one was the one found in this research.

Alpha-mangostin is the most important composition in these derivatives. There are three positions of hydroxy group at carbon position 1, 3, and 6. Methoxy group is at position 7 of nucleus ring. At position 2 and 8, there are terpene alkyl groups.

Beta-mangostin has a structure like alpha mangostin but there are 2 positions of methoxy group at carbon position 3 and 7, instead.

Gamma-mangostin has no methoxy group in a nucleus ring.

Mangostin group had a lot of bioactivities. Examples were below.

In 1983, Sundaram et al. (35) found that alpha mangostin from mangosteen had the antibacterial and antifungal activities with the MIC values of 12-50 $\mu\text{g}/\text{mL}$ and 1-5 $\mu\text{g}/\text{mL}$, respectively.

In 2003, Suksamran et al. (36) reported the anti-tuberculosis activity of mangostins from mangosteen. Alpha and beta mangostin could inhibit *Mycobacterium tuberculosis* at the similar MIC value of 6.25 $\mu\text{g}/\text{mL}$ while gamma mangostin could inhibit *M. tuberculosis* at the MIC value of 25 $\mu\text{g}/\text{mL}$.

In 2007, Chen et al. (37) reported alpha and gamma mangostin from mangosteen had the anti-inflammatory effect. Both could inhibit nitric oxide production from lipopolysaccharide stimulated murine macrophaged RAW 264.7 cell line with the IC_{50} values of 12.4 and 10.1 μM , respectively. In addition, both mangostins could decrease production of prostaglandin E2 which was the inflammatory modulator with the IC_{50} values of 11.08 and 4.50 μM , respectively. Also, they could decrease the transcription of *iNOS* and *COX-2* genes.

In 2005, Matsumoto et al. (38) found that alpha, beta, and gamma mangostins from mangosteen had the antiproliferative activity against colon cancer DLD-1 cell line with the IC_{50} value of 20 μM . In addition, cell cycle arrest was observed. It presented that the cell cycle of DLD-1 cell line treated by alpha and beta

mangostins was arrested at G₁ subphase while the cell cycle of the same cell line treated by gamma mangostin was arrested at S subphase.

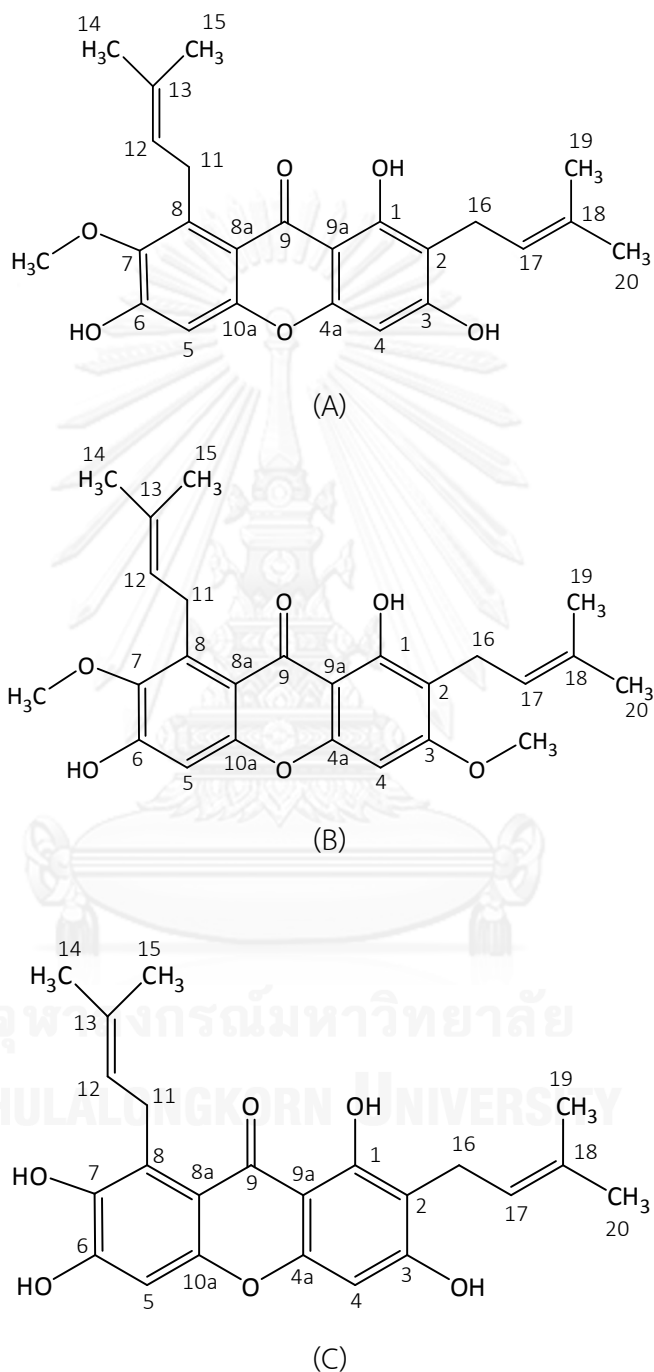


Figure 2.7 Chemical structure of mangostin group. Alpha mangostin was in (A). Beta mangostin was in (B) and gamma mangostin was in (C). Carbon positions were from Ghazali .(1)

Relative xanthenes like garcinone, gartanin groups also had interesting bioactivities.

In 2002, Ho et al. (39) reported that garcinone E (Figure 2.8) from crude ethyl acetate extract (CEAcE) from mangosteen had the antiproliferative activity against many types of cancer cell lines such as 6 hepatoma cell lines, 4 lung carcinoma cell lines, and 4 gastric carcinoma cell lines in the IC_{50} range of $0.4 \pm 0.01 \mu\text{g/mL}$ to $>10 \mu\text{g/mL}$.

In 2013, Liu et al. (40) reported that gartanin (Figure 2.9) and alpha mangostin from mangosteen had the antiproliferative activity against 6 bladder cancer cell lines. The result showed that gartanin had the antiproliferative activity against those 6 cell lines in the IC_{50} range of 4.1-18.1 $\mu\text{g/mL}$. In addition, gartanin also increased the expression of p53 protein but decreased the expression of Bcl-2 protein that was an anti-apoptosis protein.

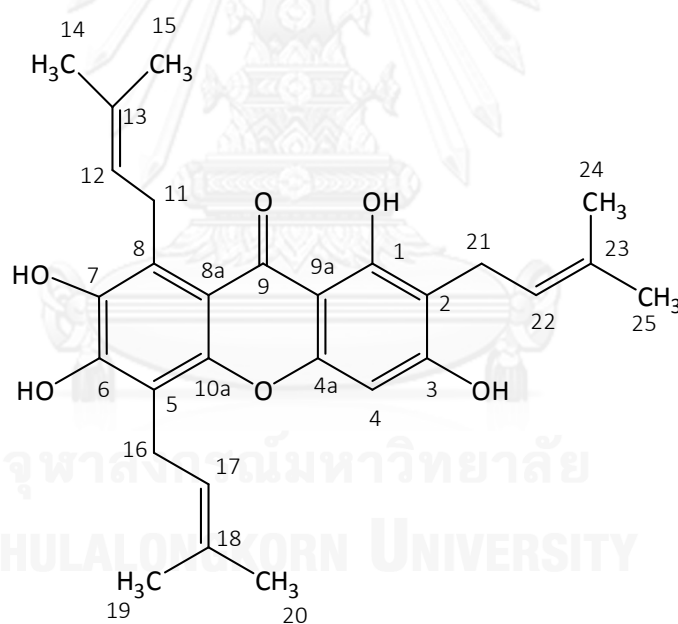


Figure 2.8 Garcinone E (Carbon position from Sakai (41)).

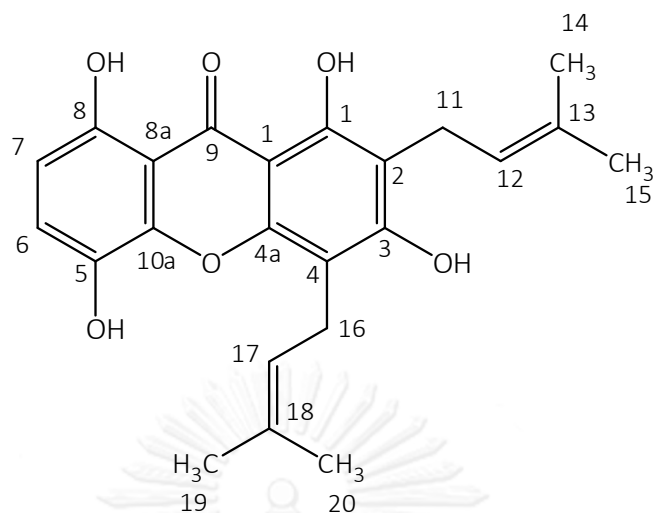


Figure 2.9 Gartanin (Carbon position from Ghazali (1)).

2.4 Cancer disease

Cancer is one of the most severe diseases. It occurs from the disorder of cell cycle. Cell division cannot be controlled. It is caused by too up-regulated or down-regulated expression of cell cycle genes. Also, it is caused by DNA damage and DNA mutation from radiation ray such as UV or gamma ray, microorganism, oncogenic virus, polluted environment, and chemical carcinogen such as tobacco, liquor, poison, heavy metal, radioactive element.

2.4.1 Overview of cancer patients (42, 43)

In 2012, World Health Organization (WHO) reported that 8.2 million patients from all over the world were dead by cancer and 14.1 million patients were still suffered by cancer. Top five of cancers were found to be lung cancer, breast cancer, liver cancer, stomach cancer, and colorectum cancer.

In 2011, National Cancer Institute of Thailand reported that the top three of cancer in male patients were colorectum cancer (16.2%), respiratory system cancer, especially lung cancer (15.5%), and liver together with bile ducts cancer (15.3%). Furthermore, the top three of cancer in female patients were breast cancer (37.5%), cervix cancer (14.4%), and colorectum cancer (9.6%).

2.4.2 Apoptosis and cancer

Apoptosis or program cell death is one of cell physiology processes or biochemistry processes (44). The change of morphology within a cell such as cell shrinkage, chromatin condensation, organelle shrinking, DNA fragmentation can be observed. This process is essential in animal development. For example, during metamorphosis, a tadpole's tail will be degraded when it grows to be a frog. Also, during the development of paw, fingers between hand plate and toes between foot plate can be separated from each other's (45). There are two types of apoptosis pathways called an intrinsic and an extrinsic pathway (Figure 2.10).

Extrinsic apoptosis pathway is directly related to environment such as radiation, toxin, over-oxidation or irreversible DNA damage. When a cell is in this environment, its nucleus will release p53 protein as transcription factor to cytoplasm. This protein can activate p21 protein so the cell cycle will be arrested in order for repairing DNA. If it cannot be repaired, p53 protein will activate Bax protein. Bax protein with Bcl-2 protein can activate the outer membrane of mitochondria to release cytochrome C which will have an interaction with APAF protein. That will result in activating procaspase-9 to be caspase-9 and formation of apoptosome (46-48).

Intrinsic apoptosis pathway is related to tumor necrosis factor-alpha from T lymphocyte. This necrosis factor will bind to a death receptor or Fas located at cell membrane with the help of FADD as adapter. This form will, later, be able to activate procaspase-8 to be caspase-8 (49, 50).

Both caspase-8 and apoptosome will have an interaction to caspase-3. This enzyme will activate DFFA to be DFF. This DFF will enter into nucleus and cause DNA fragmentation and chromatin condensation. Caspase-3 also digests cytoskeleton protein resulting in cell shrinkage, blebbing, and lysate. Later, apoptotic cells will be removed by macrophage cells (51, 52).

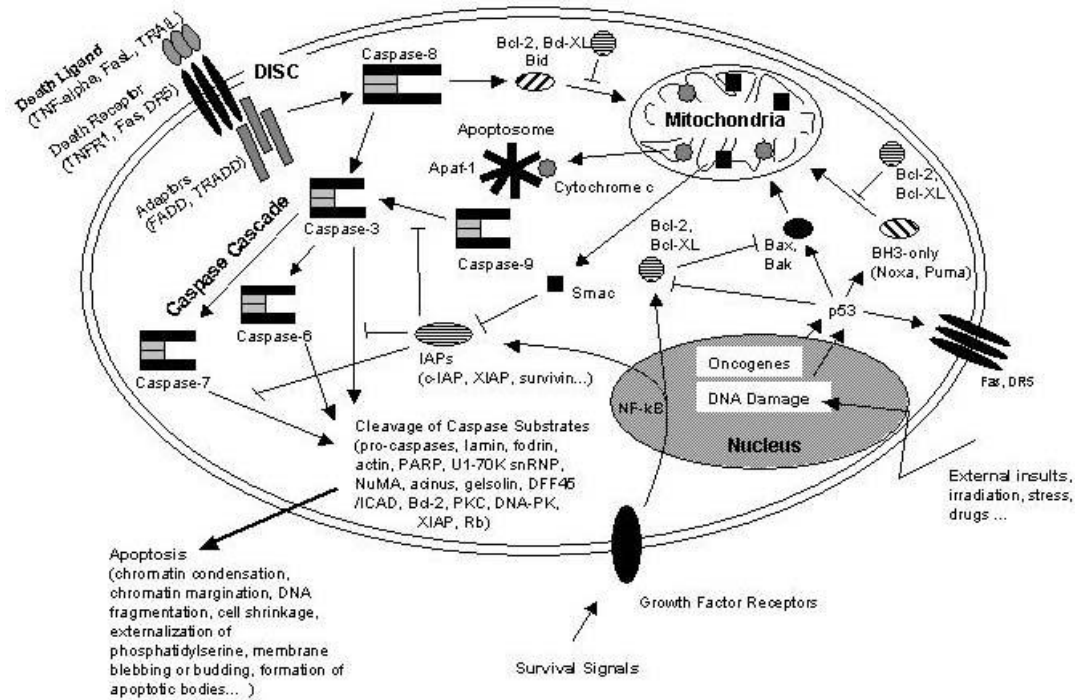


Figure 2.10 Extrinsic and intrinsic apoptosis pathway (52).

2.4.3 Angiogenesis

Angiogenesis is one of reasons why cancer cells can survive, develop, and easily spread to other tissue and organs (Figure 2.11). New blood vessel can be created or formed by this process. Vascular endothelial growth factor (VEGF) is a main protein or transcription factor controlling this process. It can induce endothelial cells to form a new blood vessel which will connect to the main vessel finally.

In cancer cells, VEGF is over expressed. Thus, new blood vessels are more created within clumped cancer cells so they can have sufficient nutrients and oxygen. (21, 53)

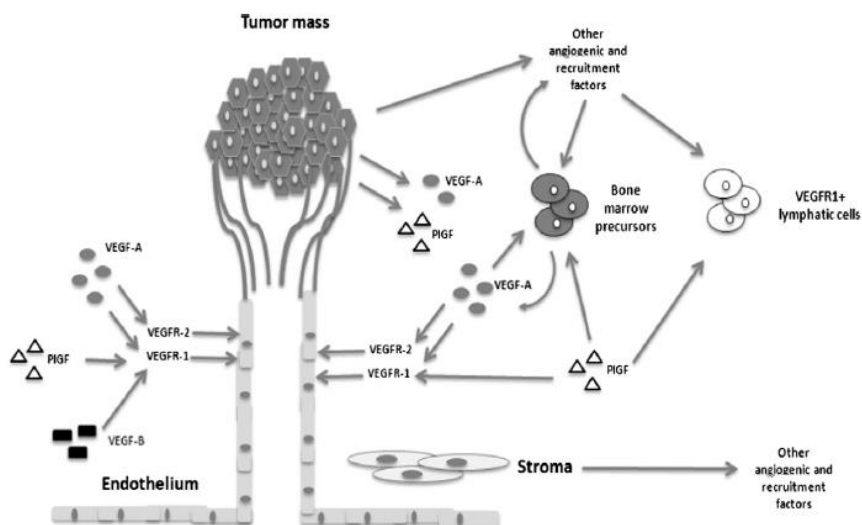


Figure 2.11 Angiogenesis overview (53).

2.4.4 Treatment of cancer

There are many ways to treat cancer like surgery, radiotherapy, chemotherapy, and immunotherapy. At present, chemotherapy is very efficient for cancer treatment. A lot of chemotherapeutic drugs were successfully developed as below.

Paclitaxel or Taxol (Figure 2.12) was the secondary metabolite of plants classified in *Taxol* spp. like a yew tree. It was the first anticancer drug and could be effective to many types of cancer. It could inhibit microtubule synthesis in cancer cells so spindle fiber which was important in cell division could not be formed (54). After the chemical structure of Taxol was revealed, it could be successfully synthesized in a laboratory (55-57).

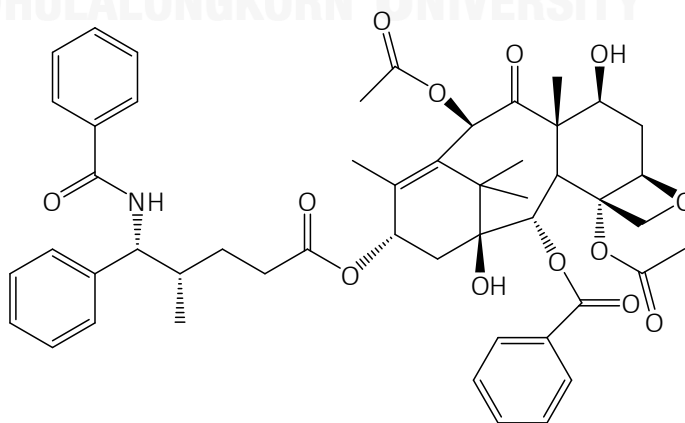


Figure 2.12 Paclitaxel (Taxol).

5-Fluorouracil (Figure 2.13) could induce apoptosis of cancer cells by pyrimidine nucleic acid substitution. Thus, DNA replication and transcription could not occur. That led to cell cycle arrest and apoptosis eventually (58).

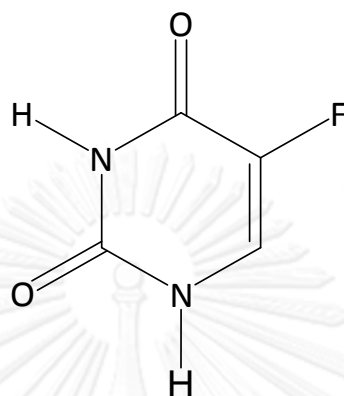


Figure 2.13 5-fluorouracil.

Doxorubicin or Adriamycin (Figure 2.14) could treat various types of cancer. This drug played a main role in DNA intercalation and inhibited the function of topoisomerase II. Thus, DNA replication could not be continued (59).

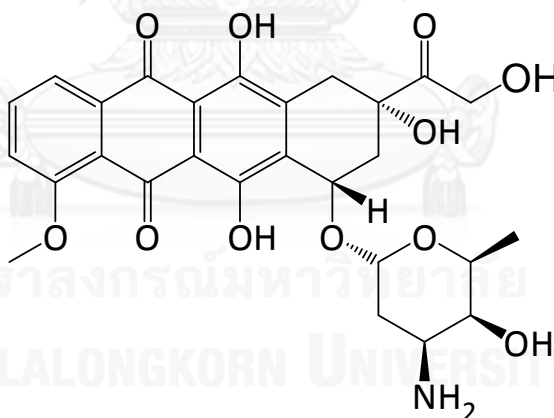


Figure 2.14 Doxorubicin.

At present, searching for new anticancer drugs is still challenging because of chemotherapeutic resistant cancer. In addition, new types of cancer can still be reported such as cancer causing by infection of new virus or new oncovirus (60). Besides, new innovation or technology has been developing in order for the better treatment like RNAi technology (61). The most interesting innovation was nanoparticle application. It helped an anticancer drug to be specifically delivered into cancer cells. Thus, there was no harm to normal cells (62). Furthermore, nano-

encapsulated drug containing both anticancer compound and anti-angiogenesis compound was successfully developed (63). A drug containing plasmid of *p53* gene or various DNA repairing genes was also developed for cancer therapy (64) Briefly about nano-encapsulated drug, the outer surface was made from various materials such as nanosilver, chitosan, liposome. It had a specific ligand to bind to a receptor presenting at cancer cell membrane only. Thus, after the binding, a drug could enter into the cancer cell immediately (21). In overall, it seems to be that cancer patients may hope to be cured.



Chapter III

Materials and Methods

3.1 Equipments & Supplies

- Laminar flow (ISSCO)
- Carbon dioxide incubator (Thermo Electron Cooperation)
- Autoclave (Udono-RII)
- UV light (Wilber Lourmat)
- Nuclear magnetic resonance (NMR) spectroscopy
 - Varian Model Mercury⁺ 400 spectrometer
 - Bruker Model ADVANCE (400 MHz) spectrometer
- Shaker (Bioer technology)
- Centrifuge (Hettich)
- Rotary evaporator
 - for crude extract (Heidolph)
 - for fraction (Eyela)
- Hot plate stirrer (Clifton cerastir)
- Distillator (Labquip)
- Cooler (AT 901)
- Pump
 - Vacuum pump for column chromatography (Hailea®)
 - Water pump for evaporator (Eyela)
- Microplate reader (Biotek synergy HT)
- Inverted light Microscope (Nikon)
- Inverted light Microscope and camera (Zeiss and Canon EOS 7D)
- Vortex (Genie)

- Multichannel micropipette
 - 2-20 μL (Arise)
 - 5-50 μL (Thermo scientific)
 - 20-200 μL (Socorex)
 - 50-300 μL (Discovery comfort)
- Single micropipette
 - 0.5-10 μL (Biohit)
 - 20-200 μL (Biohit)
 - 50-200 μL (Biohit)
 - 200-1,000 μL (Biohit)
- Cultured flask (Nunclon™)
- 96 well plate (Costar®)
- Autopipette (Swiftpet+)
- 50 ml plastic centrifugal tube (Biologix)
- Pipette tip
 - 10 μL (Axygen)
 - 300 μL (Axygen)
 - 1,000 μL (Axygen)
 - 1.5 mL microcentrifuge tube (Axygen)
- Cryotube (Nunc)
- Silica gel 60 F254 coating thin layer chromatography plate (Merck)
- Silica gel 60G (0.004-0.063 μm) (Merck)
- Filter paper(Whatman®)
- Buchner funnel (M.T.)
- Aluminum foil (Diamond)

- Glassware

- Round bottom flask
 - 25 mL (NK)
 - 100 mL (Schott duran, Pyrex)
 - 250 mL (Favorit®)
 - 500 mL (Witeg)
 - 1,000 mL (Schott duran, Pyrex)
 - 2,000 mL (Schott duran, Pyrex)
- Beaker
 - 100 mL (Schott duran, Pyrex)
 - 250 mL (Schott duran, Pyrex)
 - 500 mL (Schott duran, Pyrex)
- Flask
 - 50 mL (Schott duran, Pyrex)
 - 100 mL (Schott duran, Pyrex)
 - 200 mL (Schott duran, Pyrex)
 - 250 mL (Schott duran, Pyrex)
 - 1,000 mL (Schott duran, Pyrex)
- Volumetric cylinder
 - 10 mL (Witeg)
 - 100 mL (Witeg)
 - 250 mL (Simax)
 - 1,000 mL (Witeg)
- Glass column with bulb
 - 1,500 mL (Schott duran)
 - 350 mL (Schott duran)
 - 250 mL (Schott duran)
- Adaptor for evaporator (NK)

- NMR tube 2.5 ml(Duran®)
- Funnel distillatory collection (Schott duran)

3.2 Chemicals

- Solvent, commercial grade
 - Methanol (TSL chemical)
 - Dichloromethane or methylene chloride (TSL chemical)
 - Ethyl acetate (TSL chemical)
 - Hexane (TSL chemical)
- Solvent, analytical grade
 - Methanol (Burdick and Jackson)
 - Dichloromethane or methylene chloride (Burdick and Jackson)
 - Hexane (Burdick and Jackson)
- Dimethyl sulfoxide (DMSO)
 - For cryomedium preparation (Analytical grade) (Sigma)
 - For general use (RCl labscan)
- Deuterated chloroform contained with TMS (Cambridge)
- Ceric ammonium molybdate powder (Sigma)
- RPMI 1640 medium (Gibco, Invitrogen)
- Basal iscove medium (Gibco, Invitrogen)
- Fetal calf serum (Biochrom AG)
- Trypsin (Biochrom AG)
- 3-(4,5-dimethylthiazol-2-yl)-2,5-diphenyltetrazolium bromide (MTT) powder (Biobasic Inc)
- Doxorubicin (Sigma)
- 5-fluorouracil (Sigma)

3.3 Cerumen collection

Cerumen of *Tetragonula laeviceps* was collected from mangosteen and rambutan orchard and meliniponiculture complex in Makham district, Chantaburi province, Thailand in May 8, 2012. This cerumen was from honeypot after honey was squeezed (Figure 3.1). It was wrapped by aluminium foil and kept in dark at $-20\text{ }^{\circ}\text{C}$ until used.



Figure 3.1 *T. laeviceps*'s honeypot cerumen as raw material.

3.4 Bioassay guided partition extraction

Method 1

It was adapted from Umthong *et al.* (18) and Teerasripreecha *et al.* (19). Two hundred grams of small pieces of cerumen were dissolved in 900 mL of 80% methanol (MeOH) and shaken at $15\text{ }^{\circ}\text{C}$, 100 rpm for 18 h. Next, the mixture was centrifuged at 5,862 g, $20\text{ }^{\circ}\text{C}$ for 15 min. Supernatant were collected. The obtained sample would be crude methanol extract (CME). Remaining pellet from CME was further dissolved in 900 mL of dichloromethane (DCM) which the ratio between pellet and solvent was 1: 4.4. The mixture was again centrifuged at 5,862 g, $20\text{ }^{\circ}\text{C}$ for 15 min. Supernatant were collected. The obtained sample would be crude DCM extract (CDE). Remaining pellet from CDE was further dissolved in 900 mL of hexane. The mixture was again centrifuged at 5,862 g, $20\text{ }^{\circ}\text{C}$ for 15 min. Supernatant were collected. The obtained sample would be crude hexane extract (CHE).

Method 2

In addition, 70 g of small pieces of cerumen were used for the extraction but the first used solvent was hexane. Then, it was followed by DCM and 80% MeOH.

The volume used for each extraction was 310 mL. The process and the condition used in this method were similar to those used in method 1 (18, 19).

All of six crude extracts were evaporated with rotary evaporator in order to remove the solvent. All crudes were then weighed and kept in the dark at 4 °C until used.

3.5 The Isolation and Identification of bioactive compounds

All commercial grade solvents in this step were distilled prior to used. First, 1,000 mL of commercial grade solvent was added in a round flask (2,000 mL in size). Four to 5 small ceramic pieces were added and solvent was then heated at its boiling point. After it was evaporated, it would be condensed by a condenser connecting with a cooler. Later, distilled solvent was dropped into a funnel distillatory collector and was collected in a container.

3.5.1 The Isolation of bioactive crude extracted from cerumen of *T.*

laeviceps

A glass column (5 cm diameter x 50 cm height with 500 ml bulb) was packed with 300 g of silica gel 60G (0.040-0.063 µm) as stationary phase and 1,000 mL of hexane was used as initial mobile phase. Next, 6 g of active crude was mixed with 12 g of silica gel 60G (0.040-0.063 µm) and the mixture was left at RT until dry. Then, it was grinded in a mortar until it was like sandy powder. It was added onto the top of packed silica gel in the column. Then, it was eluted by the stepwise gradient of organic solvents such as hexane, ethyl acetate, MeOH. While eluting, a fraction of 100 mL was collected. Total number of collected fractions was mentioned in Table 3.1. Vacuum pump was also used in order to increase the speed of elution.

Table 3.1 The stepwise gradient of mobile phase used in the column chromatography for active crude extracts

Serial step of mobile phase	Mobile phase system (Hexane: Ethyl acetate: Methanol)	Eluted fraction number
1	100: 0: 0	1-10
2	95: 5: 0	11-18
3	90: 10: 0	19-28
4	85: 15: 0	29-33
5	80: 20: 0	34-38
6	70: 30: 0	39-43
7	60: 40: 0	44-48
8	50: 50: 0	49-53
9	40: 60: 0	54-63
10	30: 70: 0	64-73
11	25: 75: 0	74-78
12	20: 80: 0	79-88
13	10: 90: 0	89-98
14	0: 100: 0	99-108
15	0: 75: 25	109-118
16	0: 50: 50	119-128
17	0: 25: 75	129-138
18	0: 0: 100	139-160

All fractions were analyzed by thin layer chromatography (TLC) as described in 3.5.4. Any fractions those showed the same pattern would be merged and evaporated to remove the solvent. The merged fraction was weighed and tested for the antiproliferative activity against 5 cancer cell lines.

3.5.2 The Isolation of bioactive fractions

A glass column (3 cm diameter and 60 cm height with 140 ml bulb) was packed by silica gel 60G at 3/5 of the column height for stationary phase and DCM were used as initial mobile phase. Fraction from Table 4.4 with antiproliferative activity (see the examination procedure 3.6.1) were mixed by silica gel 60 G (0.040-0.063 μm) and left at RT to dry the sample. Then, it was grinded into sandy powder and was added on top of the column. It was eluted by the stepwise gradient of organic solvents DCM- MeOH as mentioned in Tables 3.2 and 3.3. A fraction of 5 ml was collected.

Table 3.2 The stepwise gradient of mobile phase used in the column chromatography for the bioactive fraction (the combined fraction VII).

Serial step of mobile phase	Mobile phase system (Dichloromethane: Methanol)	Eluted fraction number
1	100: 0	1-17
2	99.5: 0.5	18-32
3	99: 1	33-47
4	98.5: 1.5	48-62
5	98: 2	63-77
6	97.5: 2.5	78-92
7	97: 3	93-107
8	96.5: 3.5	108-122
9	96: 4	123-137
10	95.5: 4.5	138-152
11	95: 5	153-167
12	94.5: 5.5	168-187
13	94: 6	188-203
14	93.5: 6.5	204-218
15	93: 0	219-233
16	92.5: 7.5	234-248
17	90: 10	249-263
18	85: 15	264-283
19	80: 20	284-298
20	75: 25	299-313
21	70: 30	314-328
22	65: 35	329-343
23	60: 40	344-363

Table 3.3 The stepwise gradient of mobile phase used in the column chromatography for bioactive fraction (the combined fraction VIII).

Serial step of mobile phase	Mobile phase system (Dichloromethane: Methanol)	Eluted fraction number
1	100: 0	1-20
2	99.5: 0.5	21-35
3	99: 1	36-50
4	98.5: 1.5	51-65
5	98: 2	66-80
6	97.5: 2.5	81-95
7	97: 3	96-110
8	96.5: 3.5	111-125
9	96: 4	126-140
10	95.5: 4.5	141-155
11	95: 5	156-175
12	94.5: 5.5	176-190
13	94: 6	191-205
14	93.5: 6.5	206-220
15	93: 0	221-235
16	92.5: 7.5	236-250
17	92: 8	251-265
18	90: 0	266-280
19	85: 15	281-300
20	80: 20	301-315
21	75: 25	316-330
22	70: 30	331-345
23	60: 40	346-360

All fractions were analyzed by TLC. Any fractions those showed the same pattern would be merged and evaporated to remove the solvent. All merged subfractions were tested for the antiproliferative activity or further step.

3.5.3 The Isolation of subfractions that originated from bioactive fractions

A glass column (2.5 cm diameter and 50 cm height with 100 ml bulb) was packed with silica gel 60G at 1/2 of the height for stationary phase and DCM was used as initial mobile phase. Active subfractions from 3.6.2 were mixed by 0.5 g of silica gel 60 G (0.040-0.063 μm) and was left at RT until dry. Then, it was grinded to be sandy powder and added on the top of the column. It was eluted by the stepwise gradient of organic solvent such as DCM, MeOH as recorded in Tables 3.4 and 3.5. A fraction of 2.5 mL was collected.



Table 3.4 The stepwise gradient of mobile phase used in the column chromatography for bioactive subfraction (combined subfraction F7F).

Serial step of mobile phase	Mobile phase system (Dichloromethane: Methanol)	Eluted fraction number
1	100: 0	1-30
2	99.5: 0.5	31-60
3	99: 1	61-90
4	98.5: 1.5	91-120
5	98: 2	121-150
6	97.5: 2.5	151-180
7	97: 3	181-210
8	96.5: 3.5	211-240
9	96: 4	241-270
10	95: 5	271-300
11	94: 6	301-330
12	93: 7	331-360
13	92: 8	361-390
14	91: 9	391-420
15	90: 10	421-450
16	85: 15	451-480
17	80: 20	481-510
18	75: 25	511-540
19	70: 30	541-570
20	65: 35	571-600
21	60: 40	601-630
22	50: 50	631-660

Table 3.5 The stepwise gradient of mobile phase used in the column chromatography for bioactive subfraction (combined subfraction F8E).

Serial step of mobile phase	Mobile phase system (Dichloromethane: Methanol)	Eluted fraction number
1	100: 0	1-40
2	99.5: 0.5	41-65
3	99: 1	66-90
4	98.5: 1.5	91-120
5	98: 2	121-150
6	97.5: 2.5	151-180
7	97: 3	181-210
8	96.5: 3.5	211-240
9	96: 4	241-270
10	95: 5	271-300
11	94: 6	301-330
12	93: 7	331-360
13	92: 8	361-390
14	91: 9	391-420
15	90: 10	421-450
16	85: 15	451-480
17	80: 20	481-510
18	75: 25	511-540
19	70: 30	541-570
20	65: 35	571-600
21	60: 40	600-630

All fractions were analyzed by TLC. Any fractions those showed the same pattern would be merged. All merged subfractions will be tested for the antiproliferative activity or further experiment step.

3.5.4 Thin layer chromatography (TLC) identification

Solvents in this step were analytical grade. An aluminum silica gel coated TLC plate (Merck) was cut into small pieces at the size of 5 x 5 cm². The baseline was drawn at 0.7 cm higher from the bottom of the plate. Also, the solvent front line was drawn at 0.5 cm lower from the top of the plate. Each sample was spotted on a TLC plate by using a small glass capillary tube. The mobile phases were 100% of CH₂Cl₂, 97: 3 (v/ v) of CH₂Cl₂-MeOH, 95: 5 (v/ v) of CH₂Cl₂-MeOH, and 90: 10 (v/ v) of CH₂Cl₂-MeOH. The mobile phase (5 mL) was added in a glass TLC tank. Then, a spotted TLC plate had been dipped into the TLC tank until the solvent level reached the solvent front line. The TLC plate was left at RT until dry. A composition in sample could be observed by 2 ways. The first one, an overview of composition could be screened under the ultraviolet light. The second one, it was observed by using ceric ammonium molybdate dipping reagent (Detail in appendix C and D). A TLC plate was dipped in the reagent and hot blow until dry. Then, it was heated by a hot plate stirrer until compositions were appeared.

3.5.5 Identification of chemical structure

Evaporated, purified, and active chemical composition (5-10 mg) was dissolved in 600 µL of deuterated chloroform mixed with TMS (Tetramethylsilane) for reference. Then, it was transferred to a glass NMR tube. All samples were analyzed and recorded for the ¹H NMR spectrum with Variance NMR (Nuclear magnetic resonance) spectroscopy and ¹³C NMR and 2-dimensional NMR spectrum such as COSY (Correlation Spectroscopy), HSQC (Heteronuclear Single Quantum Coherence Spectroscopy), and HMBC (Heteronuclear Multiple Bond Correlation) with Bruker NMR spectroscopy for analyzed chemical structure of that active compound (Figure 3.6). Then, all spectrums were analyzed by NMR program, Mest Renova, for peak reference calibration, phase and baseline correction, integration calculation, J coupling calculation, peak analysis, multiplets analysis, and correlation of peak in ¹H spectrum and ¹³C spectrum in 2-dimensional NMR. Reference peak of ¹H NMR is 7.260 ppm and ¹³C NMR is 77.160 ppm. The chemical structure was designed by chemdraw ultra version 10.0.



Figure 3.2 NMR spectroscopy. Variance for ^1H NMR is in (A) and Bruker for ^{13}C and 2D NMR is in (B).

3.6 The antiproliferative activity

It was modified step of antiproliferative activity assay from Santos *et al.* (65), Hernandez *et al.* (66), Najafi *et al.* (67), Umthong *et al.* (18) and Teerasripreecha *et al.* (19).

3.6.1 Cancer cell lines

Five cancer cell lines in this research were human ductal carcinoma or breast cancer cell line (BT 474), human undifferentiated lung or lung cancer cell line (Chago), human hepatoblastoma or liver cancer cell line (Hep-G₂), human gastric carcinoma or stomach cancer cell line (KATO-III), and human colon adenocarcinoma (SW620). Human skin fibroblast cell (CRL-1947) was used as control (Figure 3.2). All cell lines were maintained, cultured, and tested for cytotoxicity at the Institute of Biotechnology and Genetic engineering, Chulalongkorn University. All cancer cell lines were cultured in RPMI 1640 medium with 5% (v/v) fetal bovine serum while CRL-1947 cell line was cultured in Basal Iscove medium. All cell lines were subcultured at every 3-4 days until use.

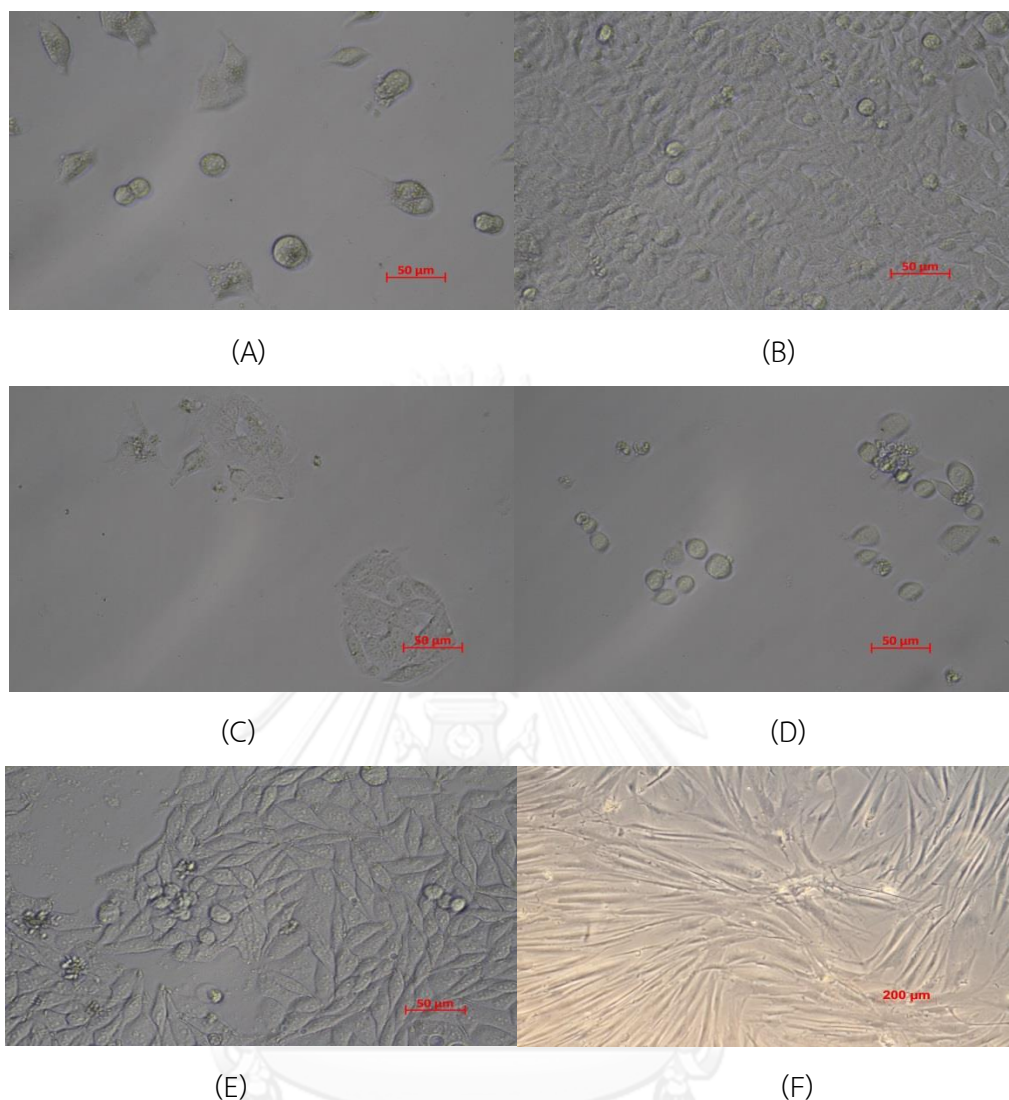


Figure 3.3 Image from microscope (20X magnification) showing morphology of five cancer cell lines: BT474 was in (A). Chago was in (B). Hep-G2 was in (C). KATO-III was in (D). SW620 was in (E) and CRL-1947 (normal cell line) was in (F).

3.6.2 Cancer cell line preparation

By trypsinisation, the medium in cell culturing flask was aspirated out. One mL of trypsin – EDTA [0.05 % (w/v) in phosphate buffer saline at pH 7.4] was added to the cells. They were then incubated at RT until cells began to detach from the surface of flask. Next, trypsin was aspirated out and 3 mL of new fresh RPMI 1640 medium or Basal Isscove medium were added to the detached cells. The cell suspension was transferred into a tube (15 mL in size). In order to count the number of cells, 10 μL of cell suspension were ten-fold diluted (10 μL of cell suspension per 90 μL of fresh RPMI media). Ten μL of diluted cell suspension was next transferred to

haematocytometer. Cells positioned at four large corner squares of haematocytometer were counted. The concentration of cells could be calculated by the following formula:

$$\text{Concentration of cells (cells/mL)} = (\text{total cells from four corners}/4) \times 10 \text{ (dilution factor)} \times 10^4 \text{ cells/mL}$$

The suspension of cells was transferred to a centrifugal tube (50 mL in size) or larger container. RPMI 1640 medium or Basal Iscove medium with 5% (v/v) FCS was added in order to adjust the required concentration (Appendix C). Then, the required cells with the required volume were transferred to each well of a 96 well plate.

3.6.3 Antiproliferative activity assay

For each cell line, cancer cells [5×10^3 cells/mL in 200 μL of RPMI 1640 medium with 5% (v/v) FCS] were transferred into each well of a 96 well plate. Similar condition was applied to CRC-1947 cell lines as well. All cell lines were incubated in an incubator at 37°C with 5% CO_2 for overnight. Later, each culture well was treated with 2 μL of a targeted chemical composition (crude or fraction) at different concentrations which were diluted by pure DMSO. In addition, 2 μL of pure DMSO in each well was used as control.

Positive control used in this research was anti-cancer drugs which were doxorubicin or doxil and 5- fluorouracil or 5-FU (Figure 3.3). Doxorubicin was prepared in various concentrations by diluted in sterile normal saline. Two μL at any concentration was treated to cells in each well and solely 2 μL of sterile normal saline was used as control. In the case of 5-FU, it was prepared in various concentrations by diluted in DMSO. Two μL at any concentration was treated to cells in each well and solely 2 μL of pure DMSO was used as control.

All treated cell lines were incubated at 37°C with 5% CO_2 for 72 h. These experiments were in triplication.

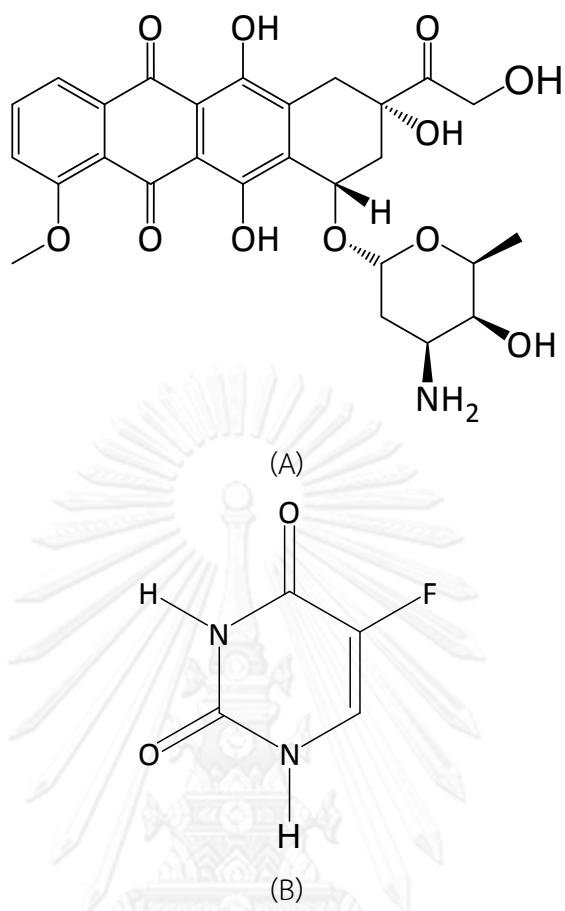


Figure 3.4 The chemical structure of anti-cancer drugs. Doxorubicin (A) and 5-FU (B) were used as positive control.

3.6.4 [3-(4,5-dimethyl-thiazol-2-yl)2,5-diphenyl-tetrazolium bromide]

(MTT) assay

This step was a continued process from 3.7.3. After 72 h of incubation, 10 μL of MTT solution (5 mg/mL in sterile normal saline) was added into each well. Then, it was further incubated at 37 $^{\circ}\text{C}$ with 5% CO_2 for another 4 h. After that, the medium was aspirated supernatant out. Thus, purple-blue formazan crystal was clearly visible (Figure 3.4). The mixture containing 150 μL of DMSO and 25 μL of 0.1 M glycine was used to dissolve the crystal. The absorbance was measured at 540 nm by a microplate reader.

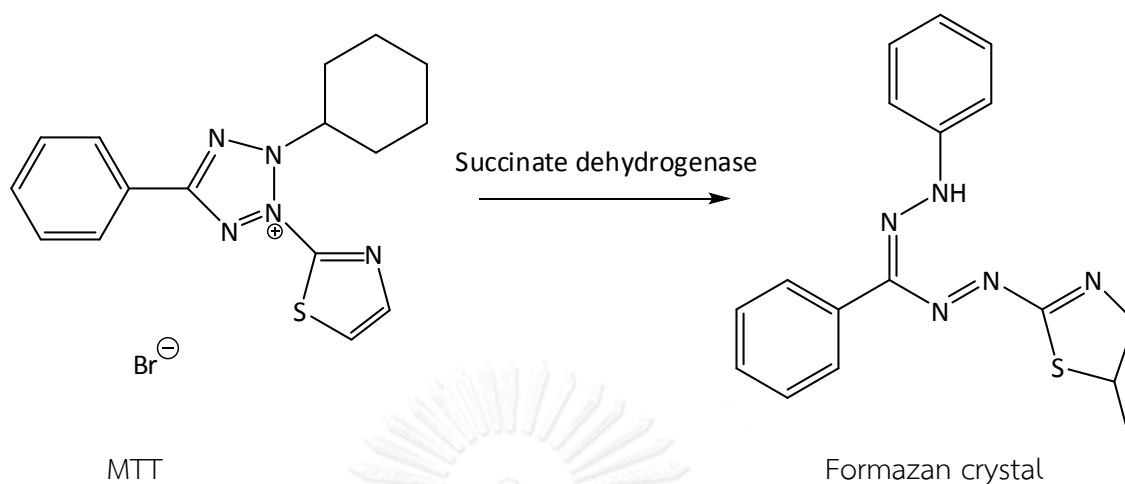


Figure 3.5 Overview of [3-(4, 5-dimethyl-thiazol-2-yl) 2, 5-diphenyl-tetrazolium bromide] (MTT) assay. For viable cells, succinate dehydrogenase from mitochondria can use MTT as substrate and later formazan crystal as reaction product will be formed.

3.6.5 Calculation for 50% inhibition concentration (IC₅₀) value

According to the absorbance at 540 nm, the relative percentage of viable cells could be calculated by the following formula.

$$\text{Percentage of viable cell} = \frac{(\text{Absorbance at 540 nm of sample})}{(\text{Absorbance at 540 nm of control})} \times 100$$

Percentage of viable cell of control is set to be 100%. All data were plotted in a graph. Percentage of viable cell was on Y axis while concentration of crude, fraction or active compound ($\mu\text{g/mL}$) was on X axis. The line was horizontally drawn from the 50% point until it reached the curve line. Then, the line was drawn vertically until it reached the X axis where indicated the concentration of IC₅₀ value.

3.6.6 Statistical analysis

According to IC_{50} value, all data were analysed by SPSS version 17. The mean and standard deviation (S.D.) was calculated. Mean and S.D. values were compared by one way analysis of variance or ANOVA with Tukey HSD.

3.7 Cell morphology analysis

Five cancer cell lines were cultured in a 96 well plate as same as mentioned in MTT cytotoxicity assay. They were treated with a purified compound at its IC_{50} value and pure DMSO was used as control. All cell lines were observed and photographed by an inverted light microscope and camera at 0, 24, 48, and 72 h (Figure 3.5). These experiments were in triplication. All pictures will be measured of scale with Axio vision 4.8.2.



Figure 3.6 An inverted light microscope connecting to a camera.

Chapter IV

Results

4.1 Crude extract of cerumen

By successive extraction with MeOH, DCM and Hexane (method 1 in 3.4) crude methanol extract (CME), crude dichloromethane extract (CDE), and crude hexane extract (CHE) were obtained in 4.86, 52.00 and 23.55% respectively (Table 4.1) while the reverse polarity of the solvents for the extraction (method 2 in 3.4) gave reCME (9.28%), reCDE (30.10%) and reCHE (43.37%). Six crude extracts had a difference in yield, weight, appearance as recorded in Table 4.1 and 4.2, respectively.

Table 4.1 Mass, yield, and appearance of crude extracts.

Crude extract	Mass (g)	Yield percentage (200 g)	Appearance
CME	9.715	4.858	Brown liquid
CDE	103.994	51.997	Sticky, red-brown, resinous rubber
CHE	47.010	23.549	Sticky, yellow-brown wax

Table 4.2 Mass, yield, and appearance of crude reverse polarity extracts.

Crude reverse polarity extract	Mass (g)	Yield percentage (70 g)	Appearance
ReCME	5.850	9.280	Brown liquid
ReCDE	19.020	30.100	Sticky, red-brown, resinous rubber
ReCHE	27.410	43.370	Sticky, yellow-brown wax

4.2 Antiproliferative activity of crude extracts

The concentrations of all 6 crude extracts were prepared to be 0, 1, 10, and 100 $\mu\text{g/mL}$ in order to test for the antiproliferative activity against 5 cancer cell lines. The results revealed that all crude extracts had the antiproliferative activity against 5 cancer cell lines (Table 4.3).

For CME, it had the antiproliferative activity against 5 cancer cell lines. The IC_{50} values were $6.95 \pm 0.46 \mu\text{g/mL}$ for BT474, $2.20 \pm 1.10 \mu\text{g/mL}$ for Chago, $2.11 \pm 0.97 \mu\text{g/mL}$ for KATO-III, $0.87 \pm 0.08 \mu\text{g/mL}$ for Hep-G₂, and $0.57 \pm 0.02 \mu\text{g/mL}$ for SW620.

For reCME, it had the antiproliferative activity against 5 cancer cell lines. The IC_{50} values of reCDE were $56.57 \pm 9.15 \mu\text{g/mL}$ for BT474, $2.38 \pm 1.51 \mu\text{g/mL}$ for Chago, $0.89 \pm 0.05 \mu\text{g/mL}$ for KATO-III, $0.84 \pm 0.08 \mu\text{g/mL}$ for Hep-G₂, and $0.57 \pm 0.00 \mu\text{g/mL}$ for SW620.

CDE also had the antiproliferative activity against 5 cancer cell lines. The IC_{50} values of CDE were $5.04 \pm 0.22 \mu\text{g/mL}$ for BT474, $3.63 \pm 0.02 \mu\text{g/mL}$ for KATO-III, $0.95 \pm 3.75 \mu\text{g/mL}$ for Chago, $0.74 \pm 0.05 \mu\text{g/mL}$ for Hep-G₂, and $0.56 \pm 0.00 \mu\text{g/mL}$ for SW620.

In overview, reCDE had the best antiproliferative activity against 5 cancer cell lines. The IC_{50} values of ReCDE were $5.25 \pm 0.27 \mu\text{g/mL}$ for BT474, $1.53 \pm 0.56 \mu\text{g/mL}$ for Chago, $0.78 \pm 0.05 \mu\text{g/mL}$ for KATO-III, $0.75 \pm 0.04 \mu\text{g/mL}$ for Hep-G₂, and $0.56 \pm 0.02 \mu\text{g/mL}$ for SW620.

Furthermore, CHE had the weak antiproliferative activity against 5 cancer cell lines. The IC_{50} values were $6.95 \pm 0.46 \mu\text{g/mL}$ for BT474, $2.20 \pm 1.10 \mu\text{g/mL}$ for Chago, $2.11 \pm 0.97 \mu\text{g/mL}$ for KATO-III, $0.87 \pm 0.08 \mu\text{g/mL}$ for Hep-G₂, and $0.57 \pm 0.02 \mu\text{g/mL}$ for SW620.

Lastly, reCHE had the antiproliferative activity against 5 cancer cell lines. The IC_{50} values were $36.42 \pm 4.92 \mu\text{g/mL}$ for BT474, $4.89 \pm 2.39 \mu\text{g/mL}$ for Chago, $5.21 \pm 1.69 \mu\text{g/mL}$ for KATO-III, $0.92 \pm 0.03 \mu\text{g/mL}$ for Hep-G₂, and $0.56 \pm 0.00 \mu\text{g/mL}$ for SW620.

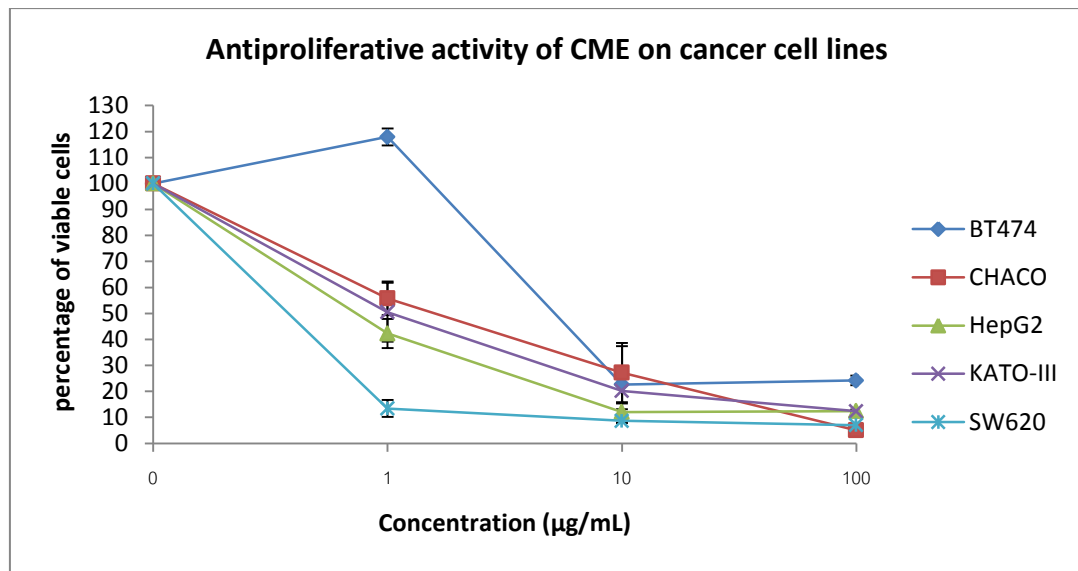
All of IC_{50} values were from graphs described in Figure 4.1(A), (B), (C), (D), (E), and (F), respectively.

Table 4.3 The IC₅₀ values of 6 crude extracts on the cancer cell lines.

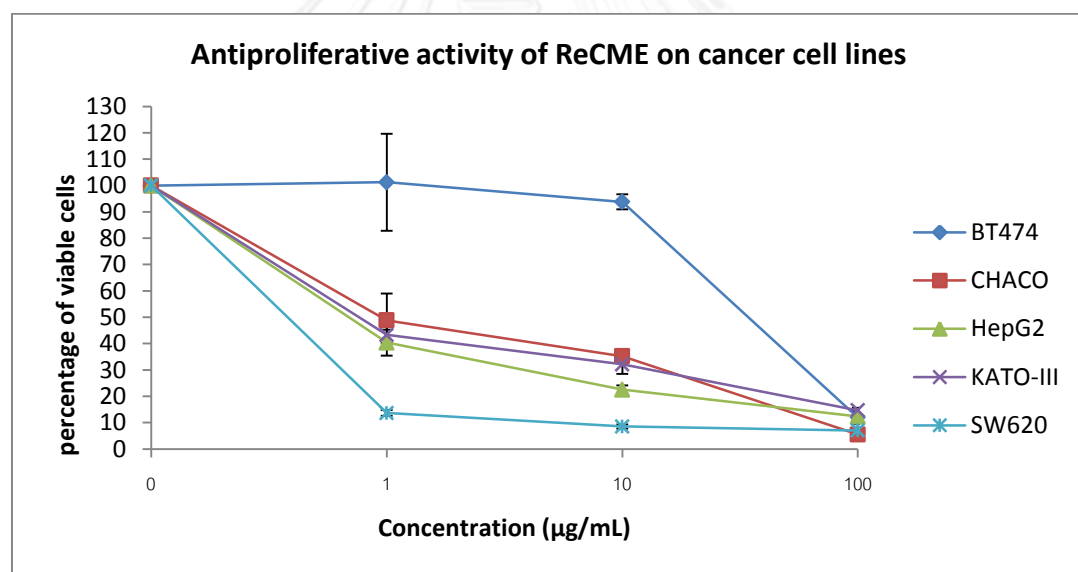
Cancer cell lines	IC ₅₀ (µg/mL)				
	BT474	Chago	Hep-G ₂	KATO-III	SW620
CME	6.95 ± 0.46 ^a	2.20 ± 1.10 ^a	0.87 ± 0.08 ^a	2.11 ± 0.97 ^{ab}	0.57 ± 0.02 ^a
CDE	5.04 ± 0.22 ^a	0.95 ± 0.04 ^a	0.74 ± 0.05 ^a	3.63 ± 1.95 ^{ab}	0.55 ± 0.00 ^a
CHE	37.57 ± 3.60 ^b	6.97 ± 0.69 ^b	0.29 ± 1.48 ^a	2.42 ± 1.08 ^{ab}	0.57 ± 0.01 ^a
reCME	56.57 ± 9.15 ^c	2.38 ± 1.51 ^a	0.84 ± 0.08 ^a	0.89 ± 0.05 ^a	0.57 ± 0.00 ^a
reCDE	5.24 ± 0.27 ^a	1.53 ± 0.56 ^a	0.75 ± 0.04 ^a	0.78 ± 0.05 ^a	0.56 ± 0.01 ^a
reCHE	36.42 ± 4.92 ^b	4.89 ± 2.39 ^{ab}	0.92 ± 0.03 ^{ab}	5.21 ± 1.69 ^b	0.56 ± 0.00 ^a

Remark (1): These experiments were in triplication.

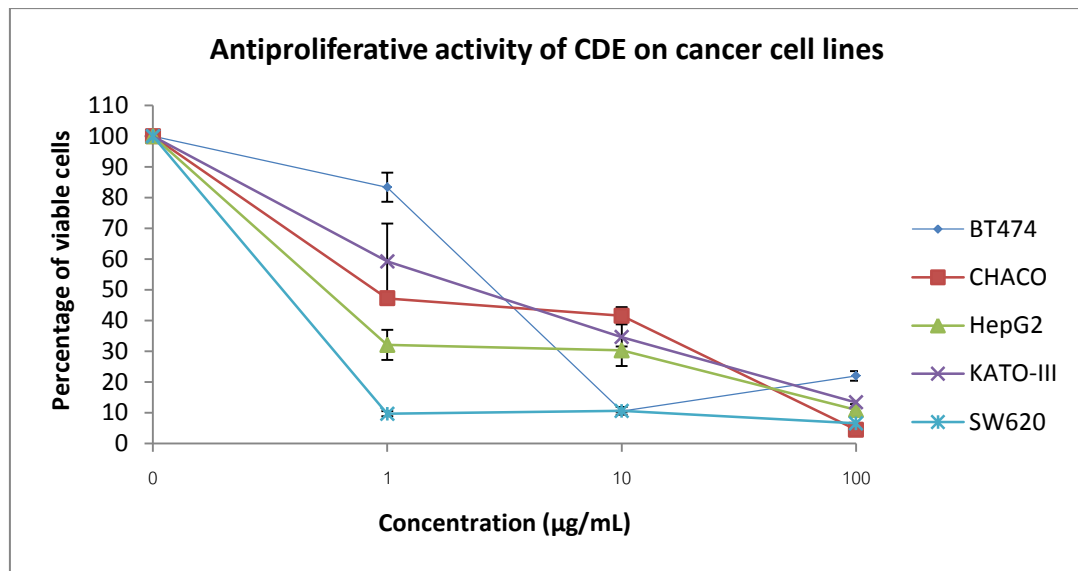
Remark (2): The different uppercase letter showed the significant difference of IC₅₀ values when p- value was equal or less than 0.05. The mean was compared by Tukey HSD in SPSS V.17. (Example: Group (a) has a statistic significant difference of mean from group (b) or (c). In case of group (a) and (b) not have a statistic significant difference, the letter of this case is showed as (ab)).



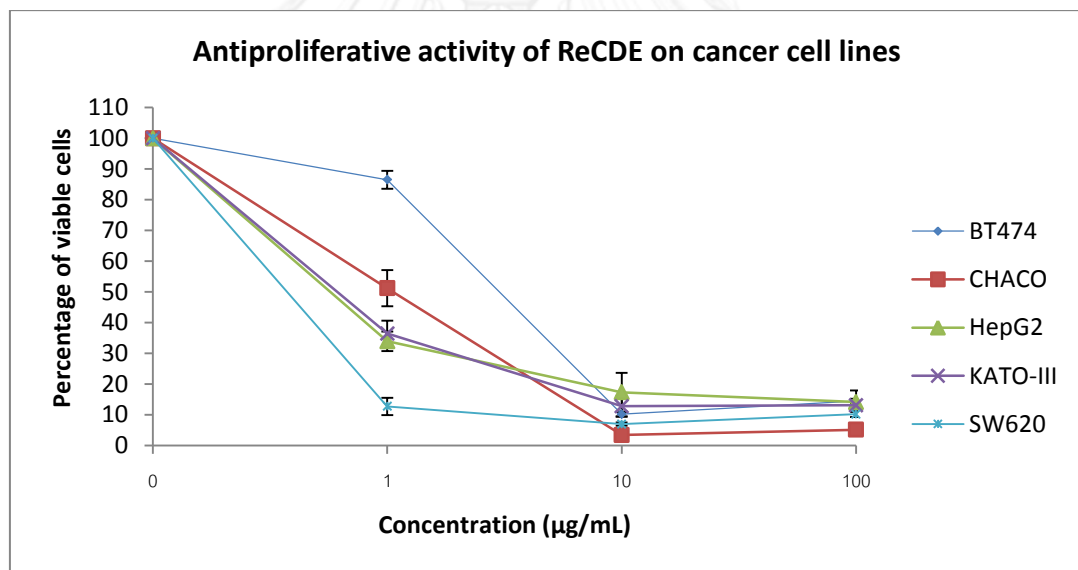
(A)



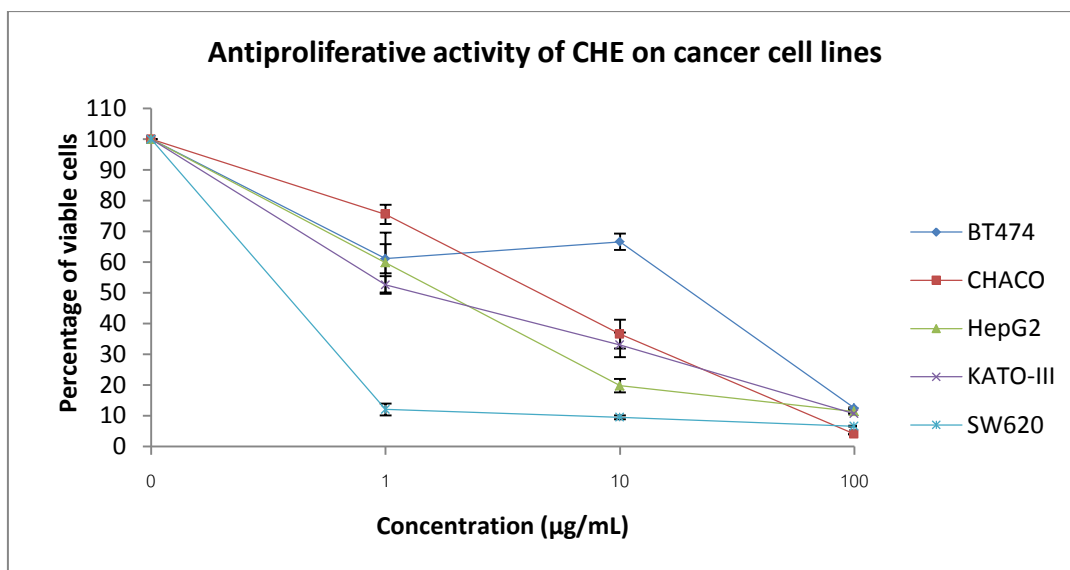
(B)



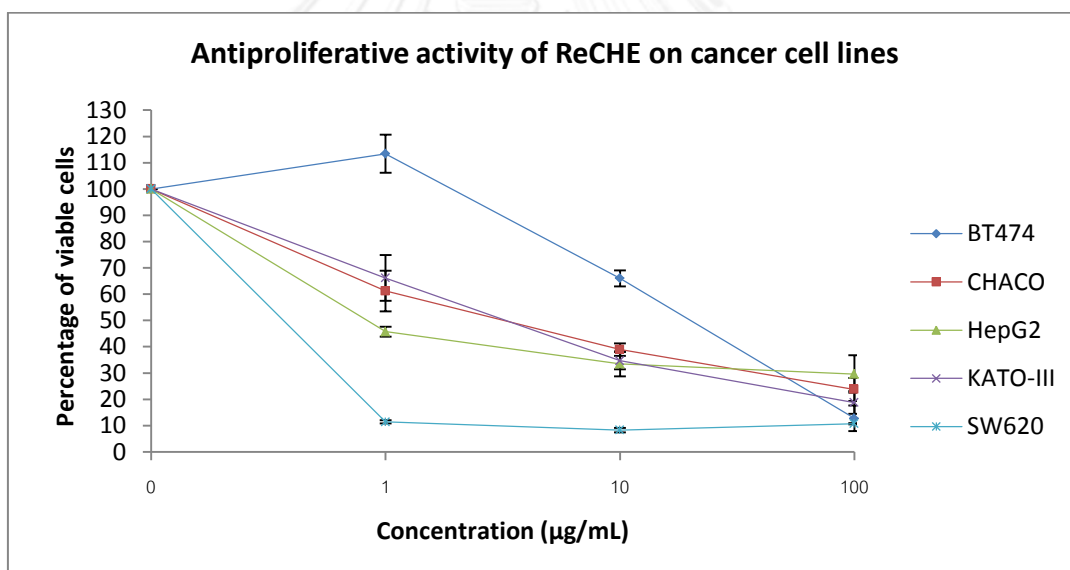
(C)



(D)



(E)



(F)

Figure 4.1 Percentage of viable cells presenting graph of 6 crude extracts against 5 different cancer cell lines. The antiproliferative activity of CME was in (A). The activity of reCME was in (B). The activity of CDE was in (C). The activity of reCDE was in (D). The activity of CHE in (E) and the activity of reCHE was in (F). The percentage of viable cells was shown as mean of triplication of percentage \pm S.D. in $\mu\text{g/mL}$ unit.

4.3 Chemical composition of the reverse crude dichloromethane extract

ReCDE had the best overview antiproliferative activity against 5 cancer cell lines. So this crude extract was further purified by silica gel 60G column chromatography (large column, 1,500 mL in size). One hundred and sixty fractions were obtained. According to TLC, fractions presenting the same pattern were merged. Thus, 16 various fractions were obtained. The mass, yield, and character were recorded as in Table 4.4.

Table 4.4 Mass, yield, and appearance of merged fractions from reCDE extract after isolation with column chromatography.

Merged fraction number	Mass (mg)	Yield (% of ReCDE, 6,000 mg)	Eluted fraction number	Appearance
I	1,879	31.31	21-26	Yellow wax
II	179	2.98	27	Yellow wax
III	662	11.03	28-35	Yellow-white wax
IV	58	0.96	36-37	Yellow-white wax
V	301	5.02	38-41	Yellow, oily
VI	329	5.48	42-47	Yellow, oily
VII	379	6.32	48-51	Brown, oily
VIII	304	5.07	52-56	Brown, oily
IX	151	2.52	57-60	Red-brown, oily
X	147	2.45	57-60	Red-brown, oily
XI	62	1.03	61-72	Red-brown, oily
XII	140	2.33	73-100	Red solid
XIII	100	1.67	101-112	Red-brown solid
XIV	329	5.48	113-121	Red-brown solid
XV	120	2.00	122-135	Brown solid
XVI	112	1.87	136-150	Brown solid

4.4 Antiproliferative activity of merged fractions from reCDE

Sixteen merged fractions were used to determine the antiproliferative activity against 5 cancer cell lines. The same concentrations (0, 1, 10, and 100 $\mu\text{g}/\text{mL}$) of each fraction were prepared. The result revealed that only fraction I, II, XV, and XVI did not have the activity against any cancer cell lines.

Fraction III had the low antiproliferative activity against KATO-III and SW620 cell lines with the IC_{50} values of $81.57 \pm 2.09 \mu\text{g}/\text{mL}$ and $76.43 \pm 2.78 \mu\text{g}/\text{mL}$, respectively.

Fraction XIV had the antiproliferative activity against BT474 with the IC_{50} value of $59.57 \pm 4.07 \mu\text{g}/\text{mL}$, Chago with the IC_{50} value of $57.50 \pm 1.85 \mu\text{g}/\text{mL}$, Hep-G₂ with the IC_{50} value of $55.15 \pm 5.31 \mu\text{g}/\text{mL}$, KATO-III with the IC_{50} value of $60.15 \pm 6.57 \mu\text{g}/\text{mL}$, and SW620 with the IC_{50} value of $68.97 \pm 1.16 \mu\text{g}/\text{mL}$.

Remaining fraction had the antiproliferative activity against all cancer cell lines.

Fraction VII, VIII, and IX were the most active against 5 cancer cell lines according to the IC_{50} values and statistical analysis.

Fraction VII had the best antiproliferative activity against 5 cancer cell lines. The IC_{50} value of Hep-G₂ was $3.38 \pm 2.18 \mu\text{g}/\text{mL}$. The IC_{50} value of Chago was $5.44 \pm 0.33 \mu\text{g}/\text{mL}$. The IC_{50} value of BT474 was $5.84 \pm 0.38 \mu\text{g}/\text{mL}$. The IC_{50} value of KATO-III was $6.07 \pm 0.36 \mu\text{g}/\text{mL}$ and the IC_{50} value of SW620 was $6.46 \pm 0.17 \mu\text{g}/\text{mL}$.

Next, fraction VIII had the antiproliferative activity against Hep-G₂ with the IC_{50} value of $5.37 \pm 0.57 \mu\text{g}/\text{mL}$, BT474 with the IC_{50} value of $5.81 \pm 0.24 \mu\text{g}/\text{mL}$, Chago with the IC_{50} value of $5.98 \pm 0.73 \mu\text{g}/\text{mL}$, KATO-III with the IC_{50} value of $6.33 \pm 0.48 \mu\text{g}/\text{mL}$, and SW620 with the IC_{50} value of $6.60 \pm 0.29 \mu\text{g}/\text{mL}$.

Lastly, fraction IX had the antiproliferative activity against Hep-G₂ with the IC_{50} value of $4.05 \pm 0.49 \mu\text{g}/\text{mL}$, SW620 with the IC_{50} value of $6.34 \pm 0.08 \mu\text{g}/\text{mL}$, Chago with the IC_{50} value of $7.33 \pm 0.31 \mu\text{g}/\text{mL}$, BT474 with the IC_{50} value of $7.74 \pm 0.49 \mu\text{g}/\text{mL}$, and KATO-III with the IC_{50} value of $7.96 \pm 0.46 \mu\text{g}/\text{mL}$.

Fraction V, X, XII, and XIII had the medium activity against 5 cancer cell lines according to the IC_{50} value and statistical analysis.

Fraction XII had the antiproliferative activity against Chago, BT474, SW620, KATO-III, and Hep-G₂ with the IC₅₀ value of 6.56 ± 0.28 , 7.58 ± 0.54 , 9.47 ± 0.13 , 23.66 ± 12.36 , and 29.14 ± 31.85 $\mu\text{g/mL}$, respectively.

Next, fraction V had the antiproliferative activity against BT474, SW620, Chago, Hep-G₂, and KATO-III with the IC₅₀ value of 6.94 ± 0.74 , 8.65 ± 0.19 , 13.97 ± 4.26 , 18.39 ± 10.73 , and 33.52 ± 5.49 $\mu\text{g/mL}$, respectively.

Then, fraction X had the antiproliferative activity against Hep-G₂, SW620, KATO-III, Chago, and BT474 with the IC₅₀ value of 8.03 ± 1.40 , 12.08 ± 5.34 , 23.80 ± 20.30 , 24.28 ± 14.32 , and 47.17 ± 26.67 $\mu\text{g/mL}$, respectively.

Lastly, fraction XIII had the antiproliferative activity against Chago, BT474, Hep-G₂, SW620, and KATO-III with the IC₅₀ value of 20.02 ± 7.63 , 21.03 ± 17.34 , 21.07 ± 20.54 , 27.74 ± 4.34 , and 53.38 ± 12.73 $\mu\text{g/mL}$, respectively.

Fraction IV, VI, and XI had the low activity against 5 cancer cell lines according to the IC₅₀ values and statistical analysis.

Fraction XI had the antiproliferative activity against SW620, Chago, Hep-G₂, BT474, and KATO-III with the IC₅₀ value of 34.25 ± 14.98 , 47.64 ± 2.43 , 54.87 ± 3.92 , 55.31 ± 10.40 , and 59.71 ± 5.72 $\mu\text{g/mL}$, respectively.

Next, fraction VI had the antiproliferative activity against Hep-G₂, Chago, KATO-III, SW620, and BT474 with the IC₅₀ value of 28.76 ± 26.83 , 47.26 ± 6.54 , 60.62 ± 3.05 , 65.25 ± 3.93 , and 74.41 ± 6.87 $\mu\text{g/mL}$, respectively.

Lastly, fraction IV had the antiproliferative activity against KATO-III, SW620, BT474, Chago, and Hep-G₂ with the IC₅₀ value of 51.84 ± 2.93 , 56.77 ± 0.65 , 59.57 ± 4.07 , 60.73 ± 4.95 , and 61.35 ± 9.11 $\mu\text{g/mL}$, respectively.

All of IC₅₀ values were compared by using Tukey HSD one way analysis of variance at 95% significant level ($p \leq 0.05$). All fractions except fraction I, II, XV, and XVI had no activity. The result showed that the best to the least antiproliferative activity was from fraction VII, VIII, IX, XII, V, X, XIII, XI, VI, and IV, respectively.

The IC₅₀ values (mean \pm S.D.) were shown in Table 4.5. The percentage of cell viability was shown in the form of graph as in Figure 4.2.

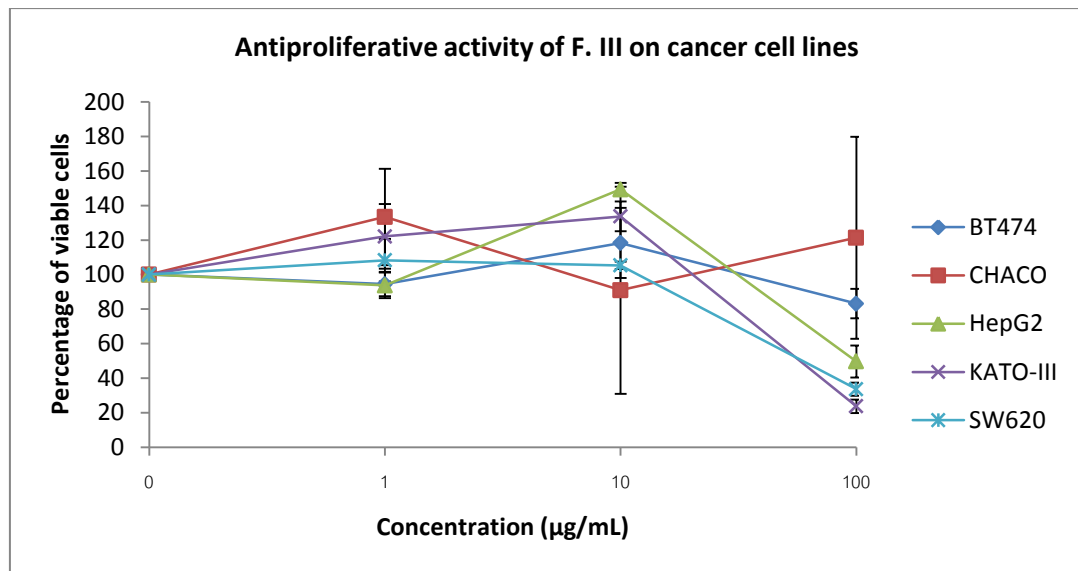
Table 4.5 The IC₅₀ values of merged fractions from reverse crude dichloromethane extract.

Fraction/Cancer cell lines	IC ₅₀ (µg/mL)				
	BT474	Chago	HepG-2	KATO-III	SW620
I	> 100	> 100	> 100	> 100	> 100
II	> 100	> 100	> 100	> 100	> 100
III	> 100	> 100	> 100	81.57 ± 2.09 ^d	76.43 ± 2.78 ^e
IV	59.57 ± 4.07 ^{bc}	60.73 ± 4.95 ^b	61.35 ± 9.11 ^c	51.84 ± 2.93 ^{bcd}	56.77 ± 0.65 ^d
V	6.94 ± 0.74 ^{ab}	13.97 ± 4.26 ^a	18.39 ± 10.73 ^{abc}	33.52 ± 5.49 ^{abc}	8.65 ± 0.19 ^a
VI	74.41 ± 6.87 ^c	47.26 ± 6.54 ^b	28.76 ± 26.83 ^{abc}	60.62 ± 3.05 ^{cd}	65.25 ± 3.93 ^{de}
VII	5.84 ± 0.38 ^a	5.44 ± 0.33 ^a	3.38 ± 2.18 ^a	6.07 ± 0.36 ^a	6.46 ± 0.17 ^a
VIII	5.81 ± 0.24 ^a	5.98 ± 0.74 ^a	5.37 ± 0.57 ^{ab}	6.33 ± 0.48 ^a	6.60 ± 0.30 ^a
IX	7.74 ± 0.49 ^{ab}	7.32 ± 0.31 ^a	4.05 ± 0.49 ^{ab}	7.96 ± 0.46 ^a	6.34 ± 0.08 ^a
X	47.17 ± 26.67 ^{abc}	24.28 ± 14.32 ^a	8.02 ± 1.40 ^{ab}	23.80 ± 20.30 ^{ab}	12.08 ± 5.34 ^{ab}
XI	55.31 ± 10.40 ^{abc}	47.64 ± 2.43 ^b	54.87 ± 3.92 ^{bc}	59.71 ± 5.71 ^{cd}	34.25 ± 14.98 ^c
XII	7.58 ± 0.54 ^{abc}	6.56 ± 0.28 ^a	29.24 ± 31.85 ^{abc}	23.66 ± 12.36 ^{ab}	9.47 ± 0.13 ^a
XIII	21.03 ± 17.34 ^{abc}	20.02 ± 7.63 ^a	21.06 ± 20.54 ^{abc}	53.38 ± 12.53 ^{bcd}	27.74 ± 4.34 ^{bc}
XIV	> 100	57.50 ± 1.85 ^b	55.15 ± 5.31 ^{abc}	60.15 ± 6.57 ^{cd}	68.97 ± 1.16 ^{de}
XV	> 100	> 100	> 100	> 100	> 100
XVI	> 100	> 100	> 100	> 100	> 100

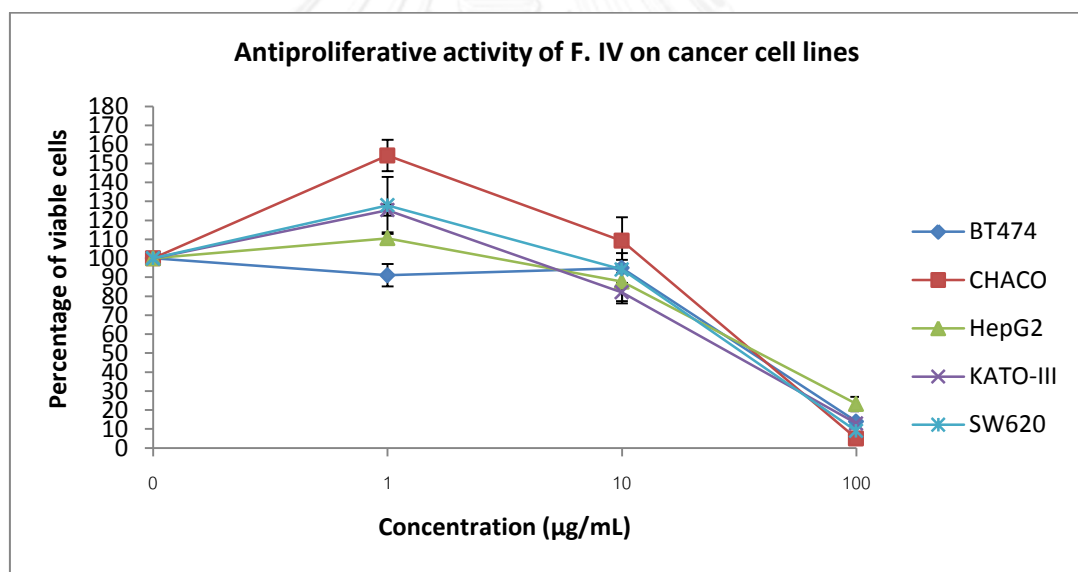
Remark (1): These experiments were in triplication.

Remark (2): The mean of IC₅₀ values were compared by one-way ANOVA, followed by Tukey HSD in SPSS V.17. The different uppercase letter showed the significant difference when p- value was equal or less than 0.05. (Example : Group (a) has a statistic significantly difference of mean from group (b) or (c). In case of group (a) and (b) not have a statistic significantly difference, the letter of this case is showed as (ab). In case of group (a), (b) and (c) not have a statistic significantly difference, the letter of this case is showed as (abc)).

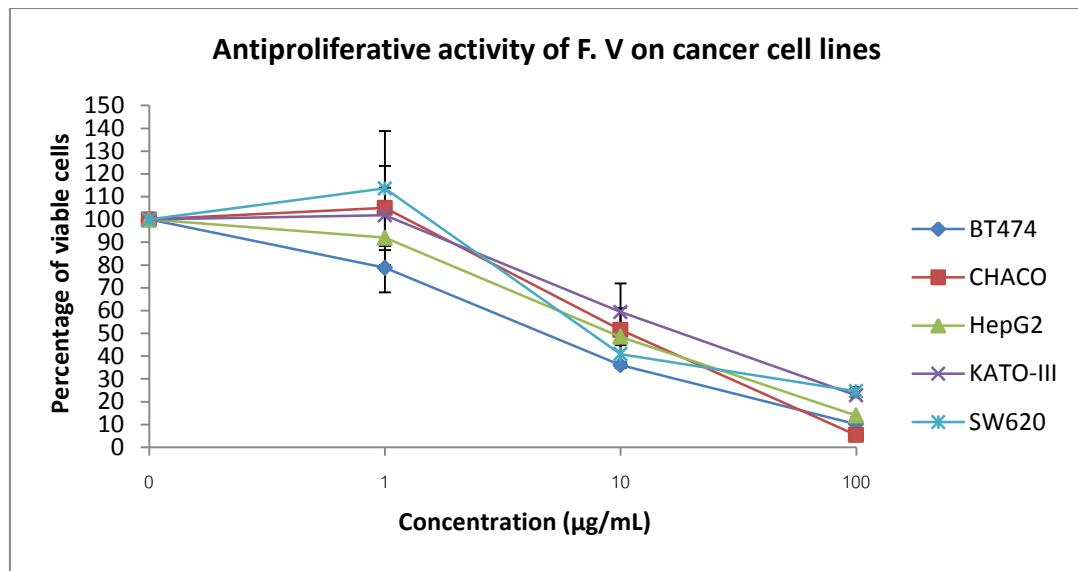
Remark (3): IC₅₀ value at > 100 showed no antiproliferative activity against cancer cell lines in this concentration range.



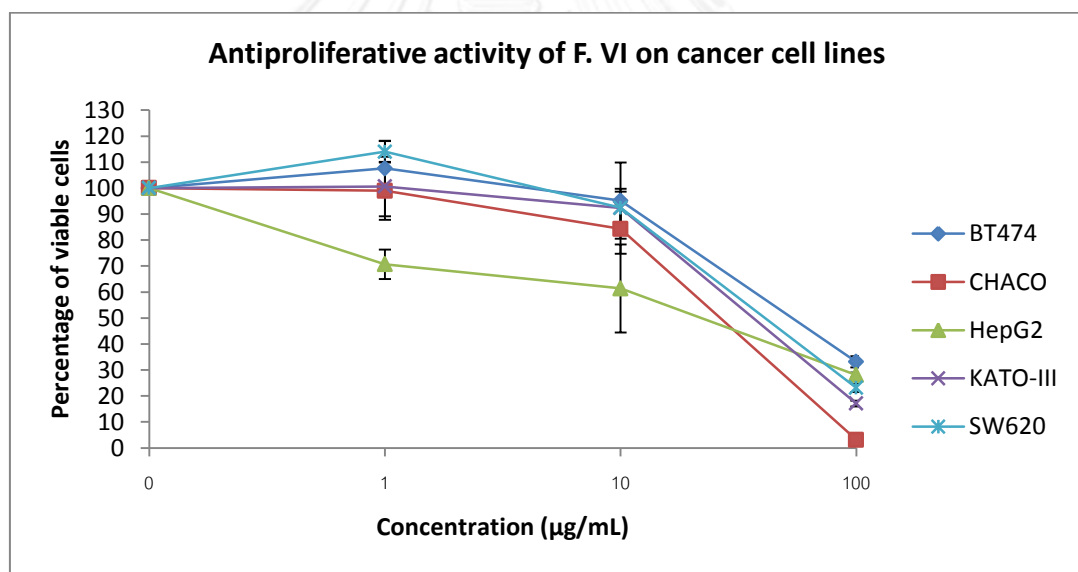
(A)



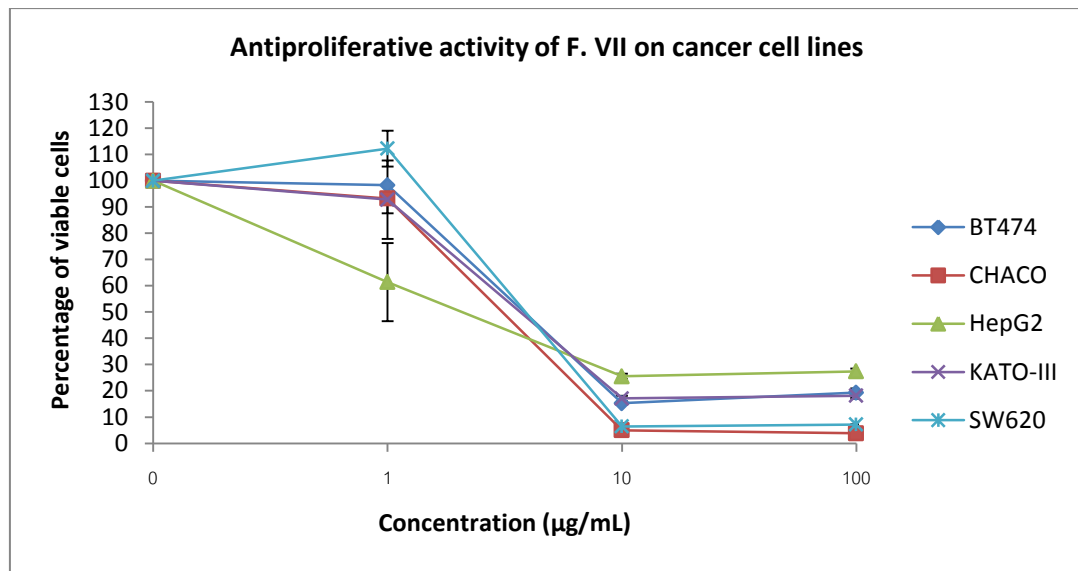
(B)



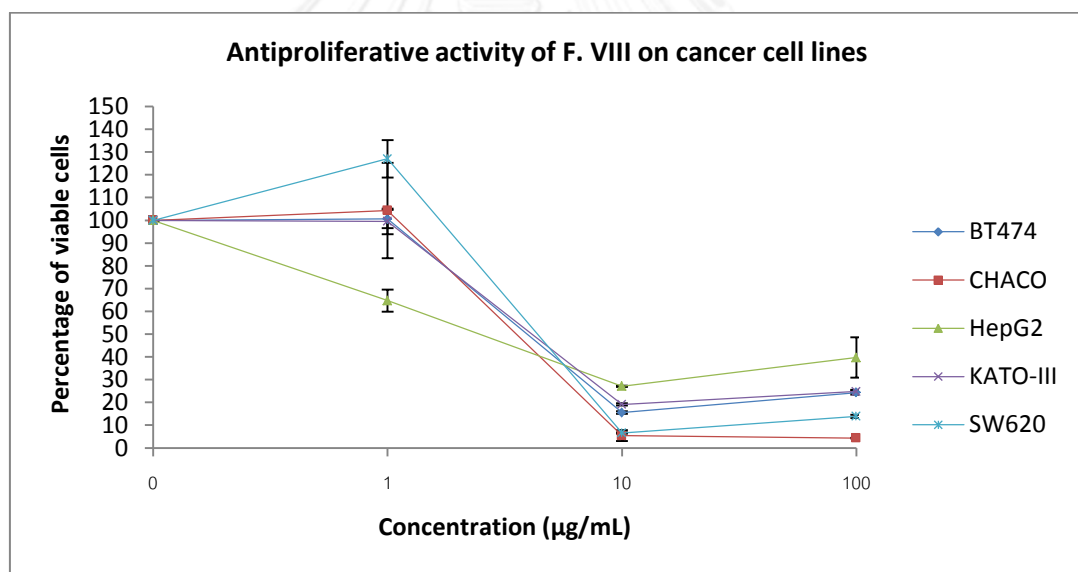
(C)



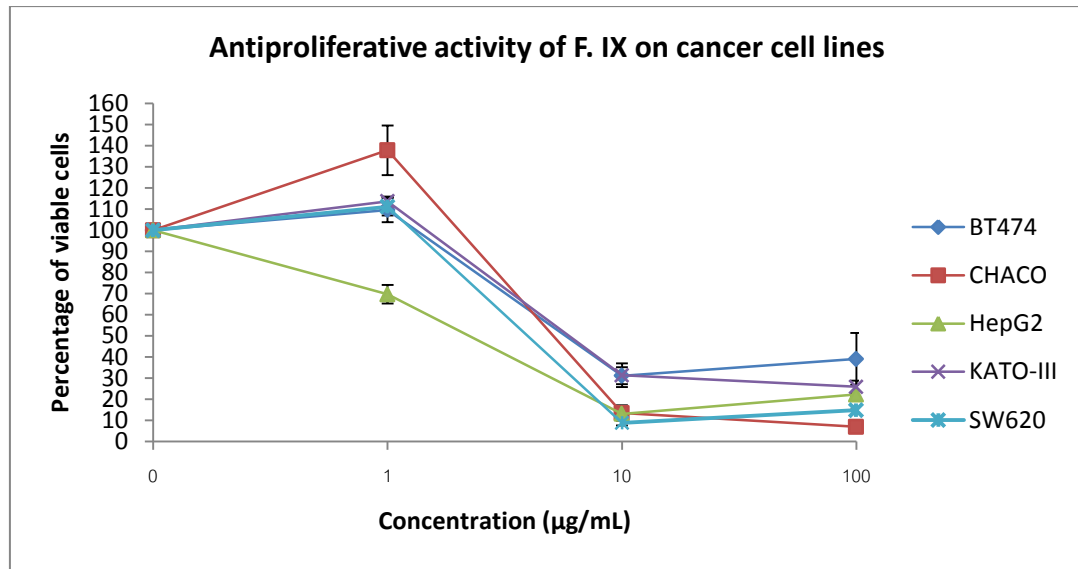
(D)



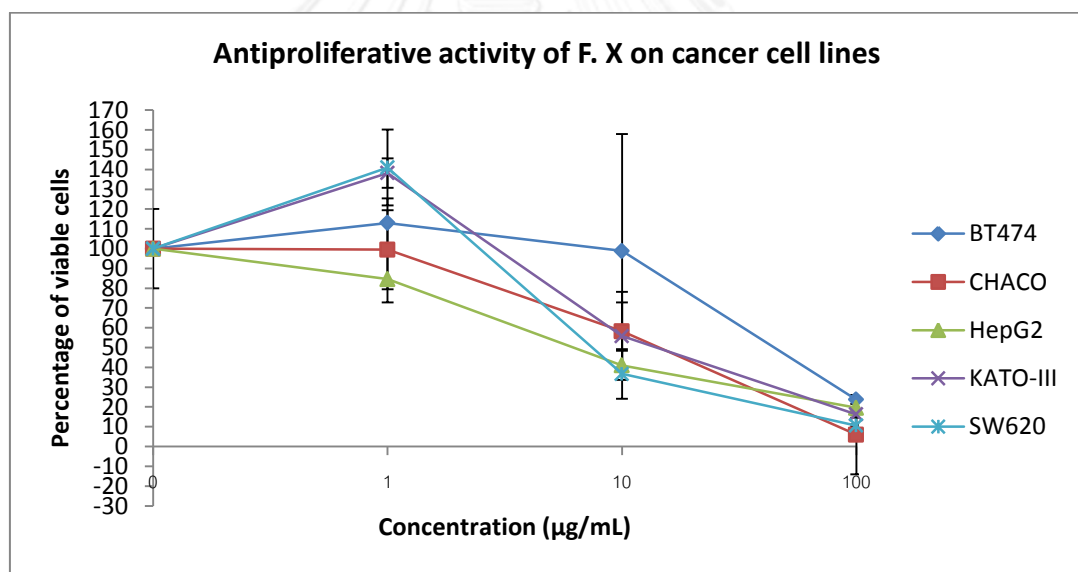
(E)



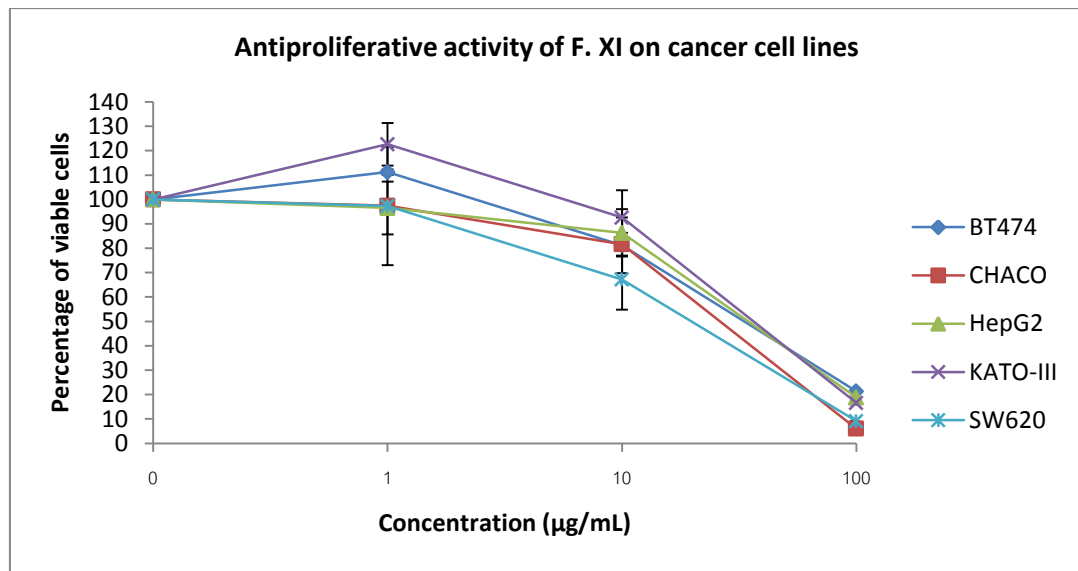
(F)



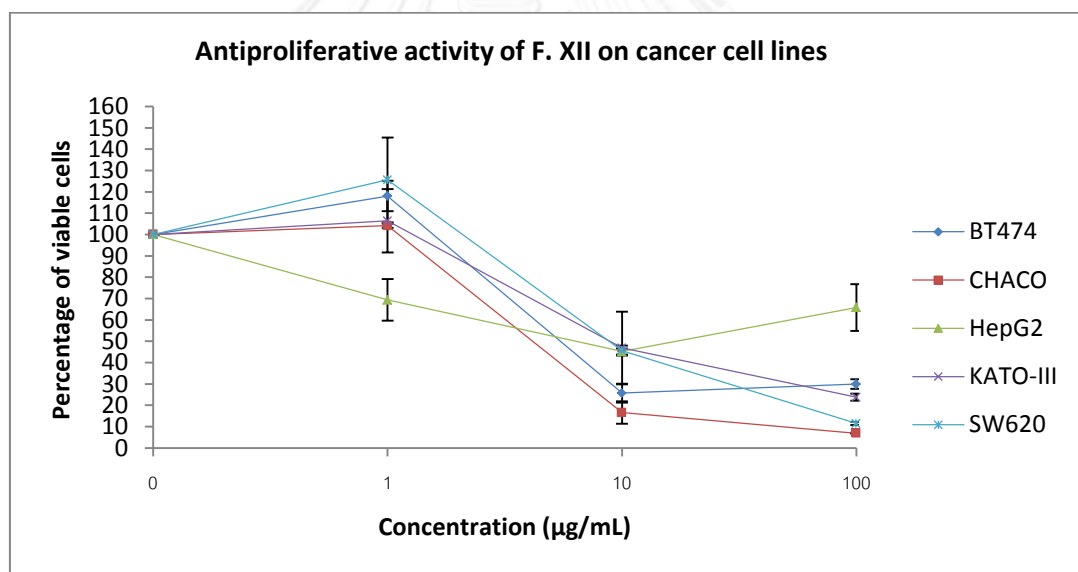
(G)



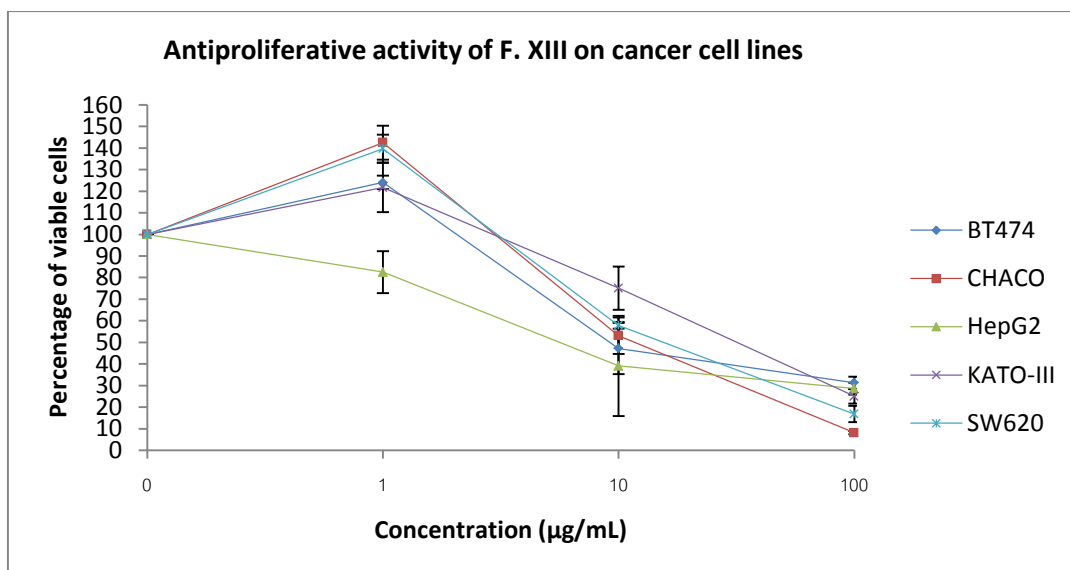
(H)



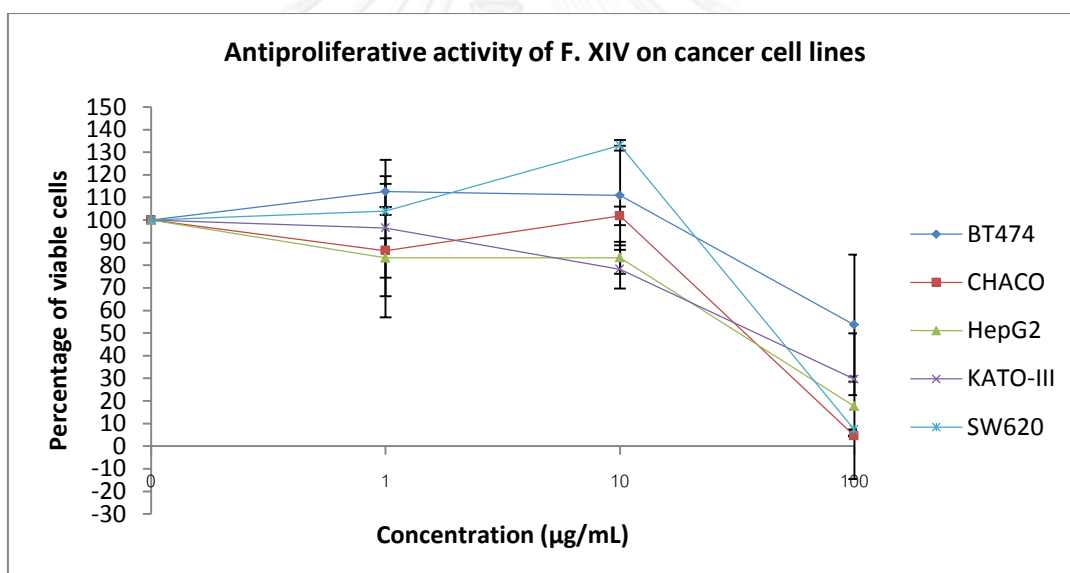
(I)



(J)



(K)



(L)

Figure 4.2 Percentage of viable cells presenting graph of 12 fractions of reverse crude dichloromethane extract against 5 cancer cell lines. The antiproliferative activity of fractions III, IV, V, VI, VII, VIII, IX, X, XI, XII, XIII, and XIV was in (A), (B), (C), (D), (E), (F), (G), (H), (I), (J), (K) and (L) respectively. The percentage shown as mean \pm S.D. in $\mu\text{g/mL}$ unit.

4.5 Chemical composition from fraction VII and VIII

From the first step chromatography, fraction VII and VIII had the best antiproliferative activity against 5 cancer cell lines. Both fractions would be purified in the next step by silica gel 60G column chromatography (medium column, 350 mL in size). Total of 363 fractions were obtained when fraction VII was used as starting materials. Total of 370 fractions were obtained when fraction VIII was used as starting materials. By TLC, fractions presenting the same pattern would be merged. Finally, ten combined fraction would be obtained from the original fraction VII. Nine combined fraction would be obtained from the original fraction VIII. Again, mass yield, and character of those merged fractions were recorded as in Tables 4.6 and 4.7.

Table 4.6 Mass, yield, and appearance of 10 subfractions (fraction VII as origin).

subfractions	Mass (mg)	Yield (% of F. VII, 330 mg)	Eluted fraction number	Appearance
F7A	3.40	1.03	55-77	Yellow brown solid
F7C	2.30	0.70	78-107	Yellow brown powder
F7D	4.80	1.45	108-170	Yellow brown powder
F7E	22.90	6.94	171-187	Yellow powder
F7F	216.60	65.64	188-194	Yellow brown, oily
F7G	19.40	5.88	195-243	Brown powder
F7H	9.30	2.82	244-275	Brown solid
F7I	4.10	1.24	276-300	Red brown solid
F7J	13.90	4.21	300-334	Red brown solid
F7K	26.40	8.00	335-363	Yellow green solid

Table 4.7 Mass, yield, and appearance of 9 compositions (fraction VIII as origin).

subfraction	Mass (mg)	Yield (% of F. VII, 300 mg)	Eluted fraction number	Appearance
F8A	2.10	0.70	55-90	Yellow brown solid
F8B	6.40	2.13	90-120	Yellow powder
F8C	1.90	0.63	121-130	Yellow powder
F8D	11.50	3.83	131-158	Yellow, oily
F8E	220.50	73.5	159-165	Yellow brown, oily
F8F	27.60	9.20	166-195	Yellow brown, oily
F8G	19.00	6.30	196-300	Red brown, solid
F8H	10.00	3.33	301-350	Red brown, solid
F8I	14.50	4.83	351-370	Yellow brown green solid

4.6 The antiproliferative activity of the combined fraction from fractions VII and VIII

After silica gel 60G chromatography (medium column, 350 mL in size), fraction VII (original from the first step chromatography) gave 10 subfractions and fraction VIII (original from the first step chromatography) gave 9 subfractions. All subfractions were tested for the antiproliferative activity against 5 cancer cell lines. Active subfractions were further searched for the IC_{50} value. The result revealed that subfractions F7E, F7F, and F8E had the antiproliferative activity. The additional concentration range (10, 5, 2.5, 1.25, and 0.625 $\mu\text{g/mL}$) of these 3 compositions were prepared to treat cancer cell line, except subfraction F7E which more concentration range of 0.3125 – 0.15625 $\mu\text{g/mL}$ was prepared.

The result revealed that 3 subfractions had the different activity.

Subfraction F7E had the strong antiproliferative activity against 5 cancer cell lines. This composition had the activity against KATO-III with the IC_{50} value of 0.88 ± 0.06 $\mu\text{g/mL}$. The IC_{50} value of HepG₂ was 0.32 ± 0.08 $\mu\text{g/mL}$. The IC_{50} value of Chago was 0.35 ± 0.08 $\mu\text{g/mL}$. The IC_{50} value of HepG₂ was 0.42 ± 0.11 $\mu\text{g/mL}$. And the IC_{50}

value of KATO-III was $0.56 \pm 0.09 \mu\text{g/mL}$. This subfraction was examined by TLC and ^1H NMR spectroscopy as a pure compound. Thus, this compound was subjected to a structural analysis.

Subfraction F7F also had the antiproliferative activity against SW620 with the IC_{50} of $0.95 \pm 0.06 \mu\text{g/mL}$, KATO-III with the IC_{50} of $1.10 \pm 0.06 \mu\text{g/mL}$, BT474 with the IC_{50} of $1.61 \pm 0.18 \mu\text{g/mL}$, Chago with the IC_{50} of $1.62 \pm 0.15 \mu\text{g/mL}$, and Hep-G₂ with the IC_{50} of $1.71 \pm 0.27 \mu\text{g/mL}$.

Subfraction F8E had the weak antiproliferative activity against Hep-G₂ with the IC_{50} value of $3.96 \pm 1.93 \mu\text{g/mL}$, KATO-III with the IC_{50} of $4.16 \pm 0.91 \mu\text{g/mL}$, Chago with the IC_{50} of $4.30 \pm 1.81 \mu\text{g/mL}$, SW620 with the IC_{50} of $4.67 \pm 0.20 \mu\text{g/mL}$, and BT474 with the IC_{50} of $6.28 \pm 1.18 \mu\text{g/mL}$.

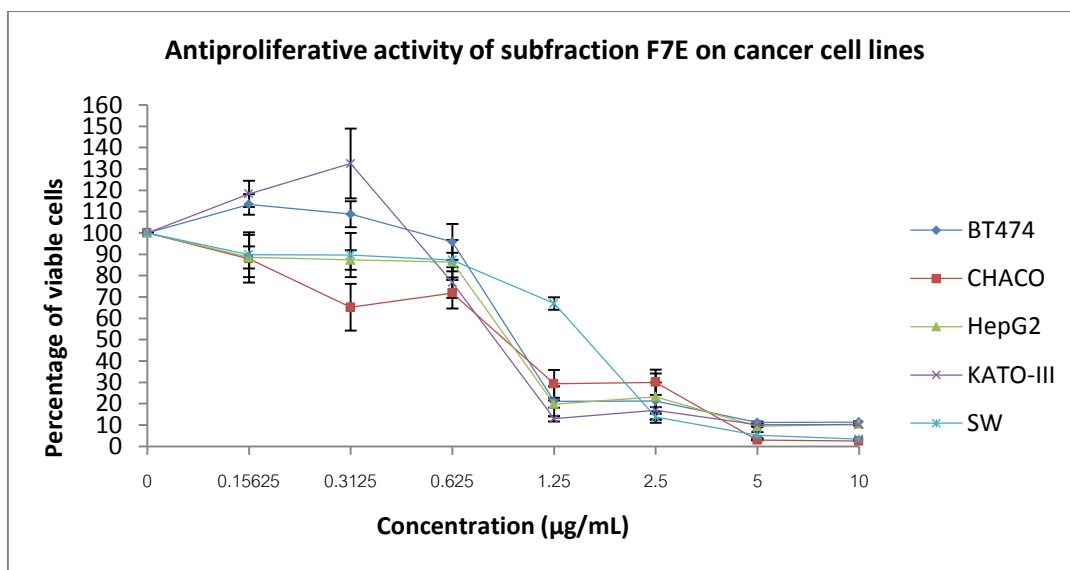
Subfraction F7E had the very strong activity so, this subfraction was used to analyse the chemical structure which would be mentioned later in the section of 4.12. Since subfraction F7F and F8E still had the activity, they were continued purity in the next step.

Data of the IC_{50} values were shown in Tables 4.8 and 4.9 as mean \pm S.D. The activity graphs were shown in Figures 4.3 and 4.4.

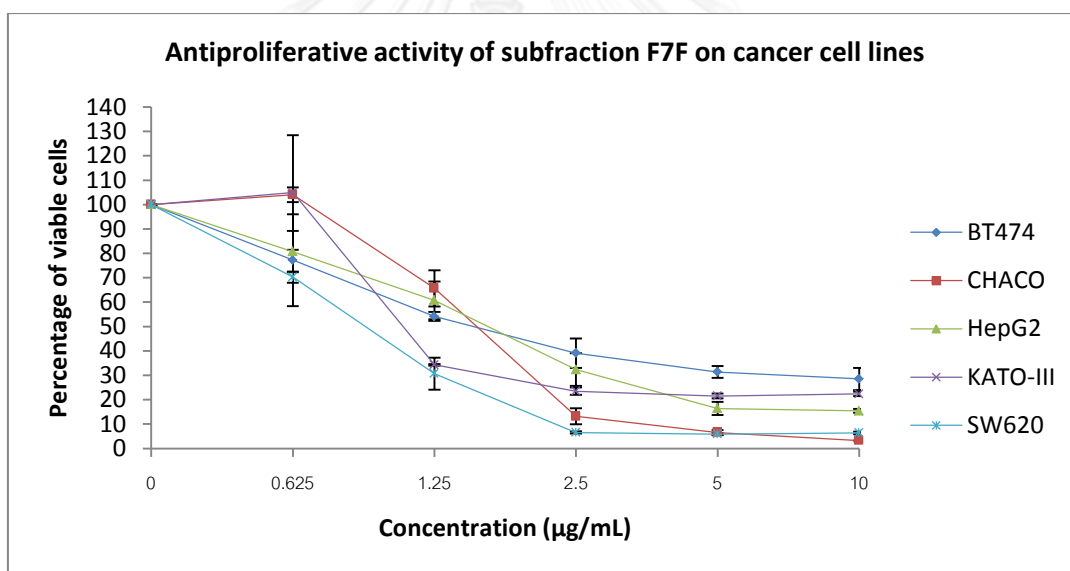
Table 4.8 The IC_{50} values of subfraction F7E and F7F originated from fraction VII.

Cancer cell lines	IC_{50} ($\mu\text{g/mL}$)	
	Subfraction F7E	Subfraction F7F
BT474	1.01 ± 0.03	1.61 ± 0.02
Chago	0.94 ± 0.08	1.62 ± 0.01
Hep-G ₂	0.97 ± 0.02	1.71 ± 0.03
KATO-III	0.88 ± 0.03	1.10 ± 0.06
SW620	1.64 ± 0.06	0.95 ± 0.06

Remark: Each experiment was in triplication.



(A)



(B)

Figure 4.3 The percentage of viable cells of subfractions F7E and F7F against different 5 cancer cell lines. The activity with concentrations at 0, 0.15625, 0.3125, 0.625, 1.25, 2.50, 5, and 10 µg/mL of subfraction F7E was in (A). The activity with concentration at 62.5, 125, 250, 500 and 1000 µg/mL of subfraction F7F was in (B). The percentage of viable cells was shown as mean of triplication of percentage \pm S.D. in µg/mL unit.

Table 4.9 The IC₅₀ values of subfraction F8E originated from fraction VIII.

Cancer cell lines	IC ₅₀ (µg/mL)
	Subfraction F8E
BT474	6.28 ± 1.18
Chago	4.30 ± 1.81
HepG ₂	3.96 ± 1.93
KATO-III	4.16 ± 0.91
SW620	4.67 ± 0.20

Remark: Each experiment was in triplication.

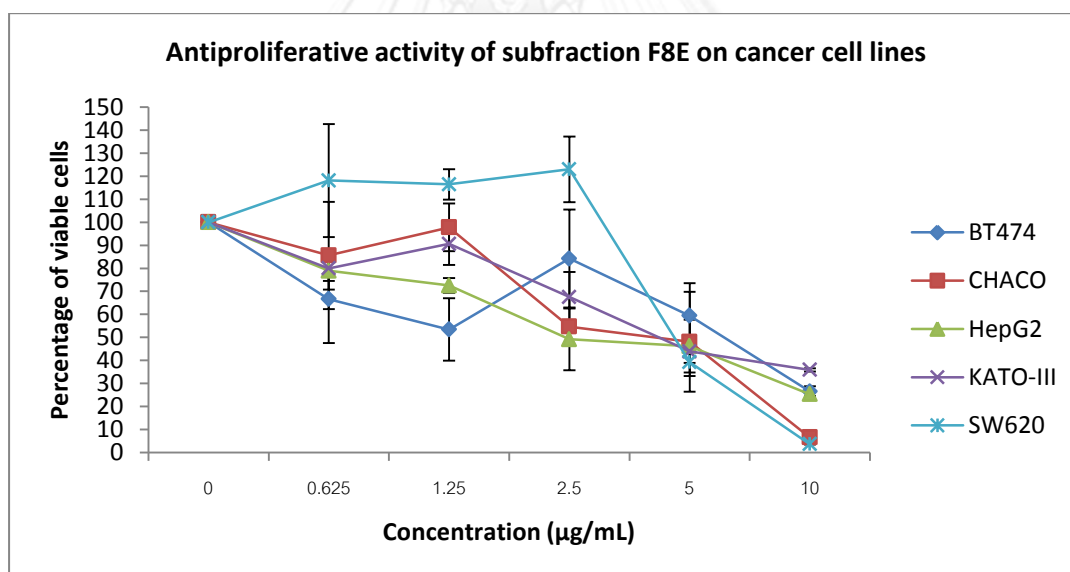


Figure 4.4 The percentage of viable cells of subfraction F8E against different 5 cancer cell lines with concentrations at 0.625, 1.25, 2.5, 5 and 10 µg/mL. The percentage of viable cells was shown as mean of triplication of percentage ± S.D. in µg/mL unit

4.7 Chemical composition from F7F and F8E subfractions

Since subfractions F7F and F8E still had the antiproliferative activity and TLC analysis showed many chemical compositions, both subfractions were purified by silica gel 60G chromatography (small column, 250 mL in size). To obtain 660 fractions from subfraction F7F and 600 fractions from subfraction F8E. The fraction with similar pattern on TLC were combined. Finally, Thirteen combined fraction would be obtained from the original subfraction F7F. Thirteen combined fraction would be obtained from the original subfraction F8E. Again, mass yield, and character of those merged fractions were recorded as in Tables 4.6 and 4.7 respectively.

Table 4.10 Mass, yield, and appearance of 13 combined fractions originated from subfraction F7F.

Fraction	Mass (mg)	Yield (% of F7F, 205 mg)	Eluted fraction number	Appearance
F7F-1	7.3	3.56	51-120	Brown, oily
F7F-2	1.9	0.93	121-140	Brown, oily
F7F-3	31.4	15.32	141-170	Yellow crystal
F7F-4	13.1	6.39	171-172	Yellow, oily
F7F-5	39.8	19.41	173-177	Yellow, oily
F7F-6	34.2	16.68	178-183	Yellow, oily
F7F-7	25.8	12.59	184-210	Orange, oily
F7F-8	12.0	5.85	211-230	Red, oily
F7F-9	8.6	4.20	231-261	Orange, oily
F7F-10	9.5	4.63	262-303	Yellow, oily
F7F-11	1.7	0.83	304-308	Yellow solid
F7F-12	6.4	3.12	339-335	Yellow powder
F7F-13	34.2*	16.68*	336-660	Red-brown solid

* This fraction may not be completely evaporated.

Table 4.11 Mass, yield, and appearance of 13 combined fractions originated from subfraction F8E.

Fraction	Mass (mg)	Yield (% of F8E, 200 mg)	Eluted fraction number	Appearance
F8E-1	5.4	2.70	61-120	Yellow soild
F8E-2	1.0	0.50	121-140	Yellow soild
F8E-3	1.6	0.80	141-155	Orange solid
F8E-4	0.6	0.30	156-160	Yellow powder
F8E-5	10.2	5.10	161-190	Yellow, oily
F8E-6	5.6	2.80	191-200	Red-brown solid
F8E-7	33.5	16.75	201-210	Red-brown solid
F8E-8	15.1	7.55	201-218	Red, oily
F8E-9	43.5	21.75	219-234	Yellow, oily
F8E-10	16.9	8.45	235-242	Yellow, oily
F8E-11	36.0	18.00	243-337	Yellow solid
F8E-12	9.1	4.55	338-388	Yellow solid
F8E-13	28.3*	14.15*	389-600	Red solid

* This fraction may not be completely evaporated.

4.8 Antiproliferative activity of combined fractions from F7F and F8E

Twenty six combined fractions positions from subfractions F7F and F8E were tested for the antiproliferative activity against 5 cancer cell lines. The result revealed that the combined fractions F7F-3, F7F-4, F7F-5, F7F-6, F8E-5, F8E-6, and F8E-7 showed the antiproliferative activity with IC_{50} values in Tables 4.12 and 4.13. Later, more concentrations of these 7 compositions were prepared to treat cancer cell lines. For composition F8E-6 and F8E-7, more concentrations at 10, 5, 2.5, 1.25, 0.625 $\mu\text{g/mL}$ were prepared. Also, for composition F7F-4, F7F-5, and F7F-6, more concentration of 0.3125 $\mu\text{g/mL}$ was prepared. For composition F7F-3 and F8E-5, more concentration of 0.15625 $\mu\text{g/mL}$ was prepared.

Nonetheless, only composition F7F-3, F7F-4, F7F-5, and F7F-6 originated from subfraction F7F had the antiproliferative activity with the IC_{50} values below.

Composition F7F-3 had the strong antiproliferative activity against 5 cancer cell lines. This combined fraction was active against KATO-III cell line with the IC_{50} value of $0.36 \pm 0.06 \mu\text{g/mL}$, Hep-G₂ cell line with the IC_{50} value of $0.39 \pm 0.00 \mu\text{g/mL}$, BT474 cell line with the IC_{50} value of $0.50 \pm 0.01 \mu\text{g/mL}$, SW620 cell line with the IC_{50} value of $0.62 \pm 0.16 \mu\text{g/mL}$, and Chago cell line with IC_{50} value of $0.92 \pm 0.08 \mu\text{g/mL}$. Since this combined fraction was pure compound by using TLC and ¹H NMR analysis. It was further determined for the structure analysis.

The rest of 3 compositions also had the antiproliferative activity but not as strong as composition F7F-3.

Composition F7F-4 was active against Hep-G₂ cell line with the IC_{50} value of $3.16 \pm 0.81 \mu\text{g/mL}$, BT474 cell line with the IC_{50} value of $4.55 \pm 0.21 \mu\text{g/mL}$, KATO-III cell line with the IC_{50} value of $7.24 \pm 0.62 \mu\text{g/mL}$, Chago with the IC_{50} value of $8.13 \pm 0.63 \mu\text{g/mL}$, and SW620 cell line with the IC_{50} value of $8.47 \pm 0.84 \mu\text{g/mL}$.

Composition F7F-5 was active against BT474 cell line with the IC_{50} value of $3.32 \pm 0.77 \mu\text{g/mL}$, Hep-G₂ cell line with the IC_{50} value of $6.36 \pm 0.38 \mu\text{g/mL}$, KATO-III cell line with the IC_{50} value of $6.48 \pm 0.78 \mu\text{g/mL}$, SW620 cell line with the IC_{50} value of $8.13 \pm 0.63 \mu\text{g/mL}$, and Chago cell line with the IC_{50} value of $6.67 \pm 1.58 \mu\text{g/mL}$.

Composition F7F-6 was active against SW620 cell line with the IC_{50} value of $3.07 \pm 0.14 \mu\text{g/mL}$, BT474 cell line with the IC_{50} value of $4.06 \pm 0.62 \mu\text{g/mL}$, KATO-III cell line with the IC_{50} value of $4.41 \pm 0.19 \mu\text{g/mL}$, Hep-G₂ cell line with the IC_{50} value of $4.60 \pm 0.14 \mu\text{g/mL}$, and Chago cell line with the IC_{50} value of $8.46 \pm 0.76 \mu\text{g/mL}$.

Next, for subfraction F8E, composition F8E-5, F8E-6, and F8E-7 had the antiproliferative activity with the IC_{50} values below.

Composition F8E-7 was active in some cancer cell lines. Chago and Hep-G₂ cell lines were not sensitive to this composition. It was active against BT474 cell line with the IC_{50} value of $3.77 \pm 0.73 \mu\text{g/mL}$, KATO-III cell line with the IC_{50} value of $7.07 \pm 0.34 \mu\text{g/mL}$ and SW620 cell line with the IC_{50} value of $2.17 \pm 0.05 \mu\text{g/mL}$.

Besides, composition F8E-5 and F8E-6 had antiproliferative activity against all 5 cancer cell lines.

The combined fraction F8E-5 had the antiproliferative activity against KATO-III cell line with the IC_{50} value of $1.69 \pm 0.06 \mu\text{g/mL}$, SW620 cell line with the IC_{50} value of $1.74 \pm 0.26 \mu\text{g/mL}$, Hep-G₂ cell line with the IC_{50} value of $1.93 \pm 0.04 \mu\text{g/mL}$, BT474 cell line with the IC_{50} value of $1.94 \pm 0.15 \mu\text{g/mL}$, and Chago cell line with the IC_{50} value of $3.88 \pm 0.10 \mu\text{g/mL}$. This fraction was similar to the fractions F7E and F7F-

3 in term of TLC plate. Thus, this combined fraction was further determined for the structure analysis.

The combined fraction F8E-6 was active against BT474 cell line with the IC_{50} value of $2.32 \pm 0.49 \mu\text{g/mL}$, Hep-G₂ cell line with the IC_{50} value of $5.37 \pm 1.14 \mu\text{g/mL}$, Chago cell line with the IC_{50} value of $5.86 \pm 0.89 \mu\text{g/mL}$, KATO-III cell line with the IC_{50} value of $5.93 \pm 1.54 \mu\text{g/mL}$, and SW620 cell line with the IC_{50} value of $7.07 \pm 0.34 \mu\text{g/mL}$.

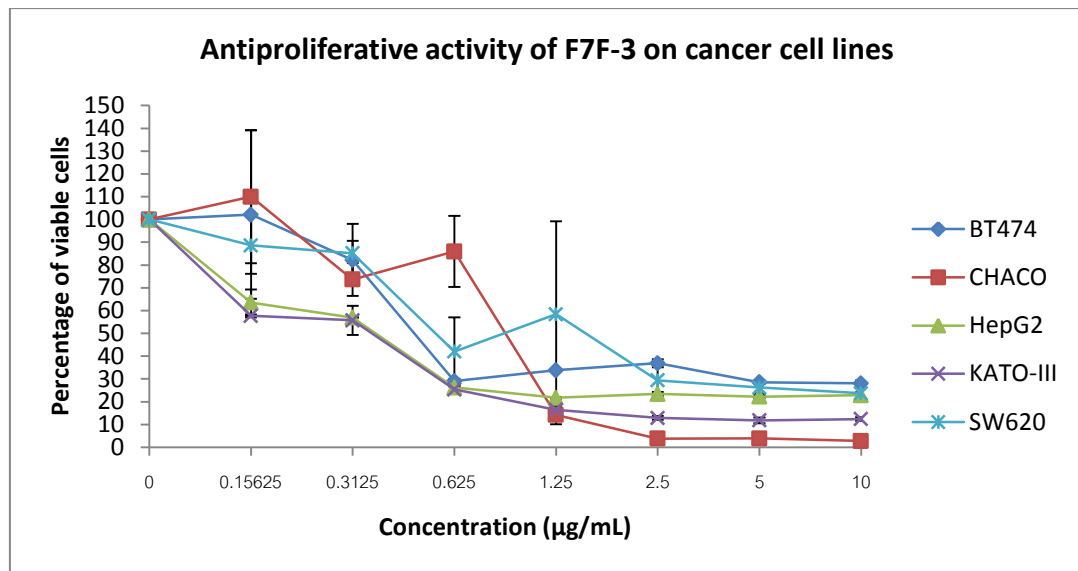
Data of the IC_{50} values were shown in Tables 4.12 and 4.13 as mean \pm S.D. Activity graphs were shown in Figures 4.5 and 4.6.

Table 4.12 The IC_{50} values of the F7F-3, F7F-4, F7F-5, and F7F-6 originated from subfraction F7F.

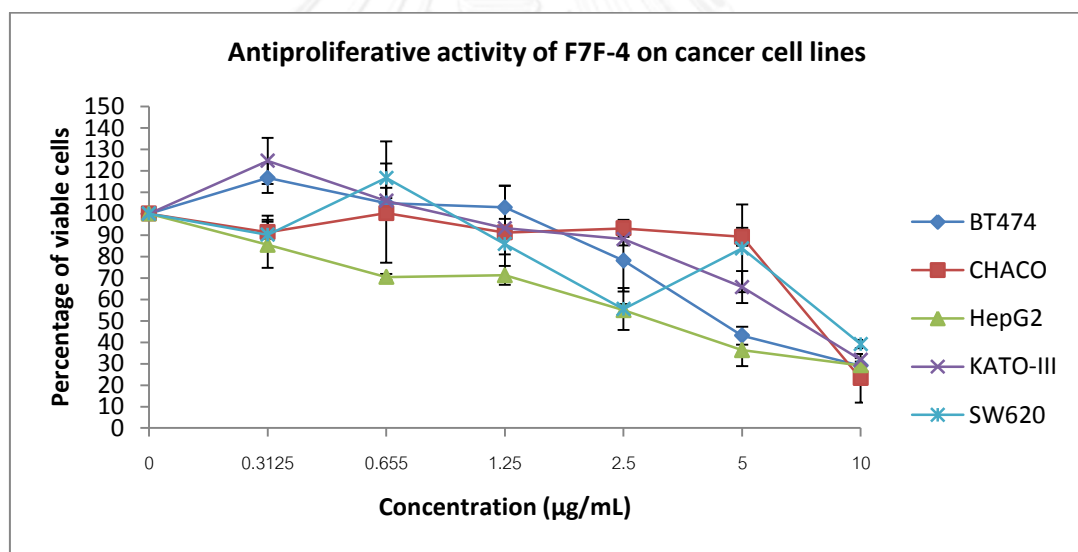
Cancer cell lines	IC_{50} ($\mu\text{g/mL}$)			
	F7F-3	F7F-4	F7F-5	F7F-6
BT474	0.50 ± 0.01^a	4.55 ± 0.21^b	3.31 ± 0.77^b	4.06 ± 0.62^b
Chaco	0.92 ± 0.08^a	8.13 ± 0.63^b	6.67 ± 1.58^b	8.46 ± 0.76^b
HepG ₂	0.39 ± 0.04^a	3.16 ± 0.81^b	6.36 ± 0.38^c	4.60 ± 0.14^b
KATO-III	0.36 ± 0.06^a	7.24 ± 0.62^c	6.48 ± 0.78^c	4.41 ± 0.19^b
SW620	0.62 ± 0.16^a	8.47 ± 0.83^c	6.48 ± 1.00^c	3.07 ± 0.14^b

Remark (1): These experiments were in triplication.

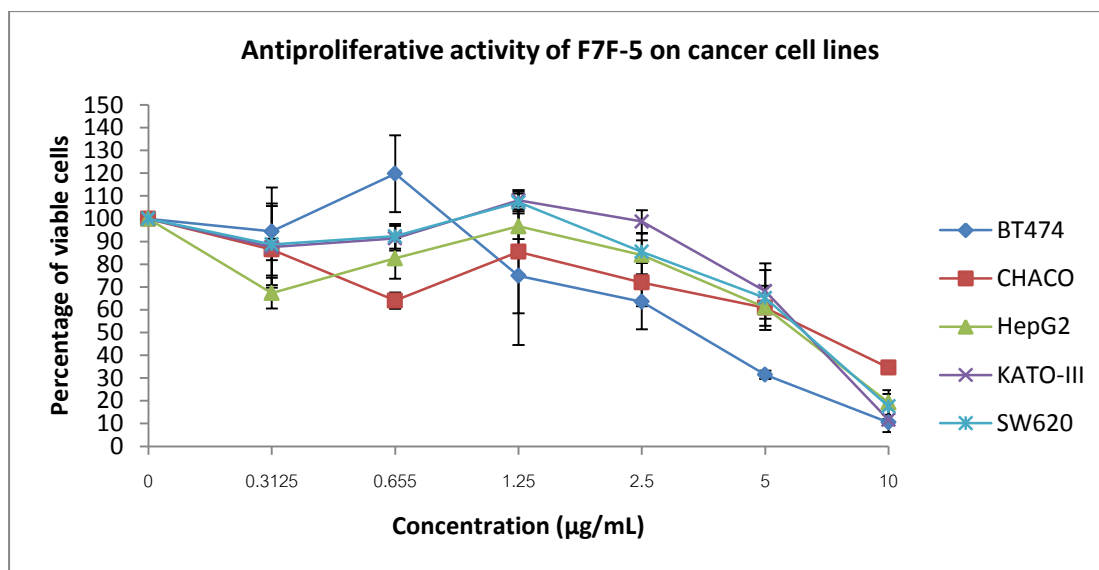
Remark (2): The different uppercase letter showed the significant difference when p - value was equal or less than 0.05. The data of mean was compared by Tukey HSD in SPSS V.17. (Example: Group (a) has a statistic significantly difference of mean from group (b) or (c).)



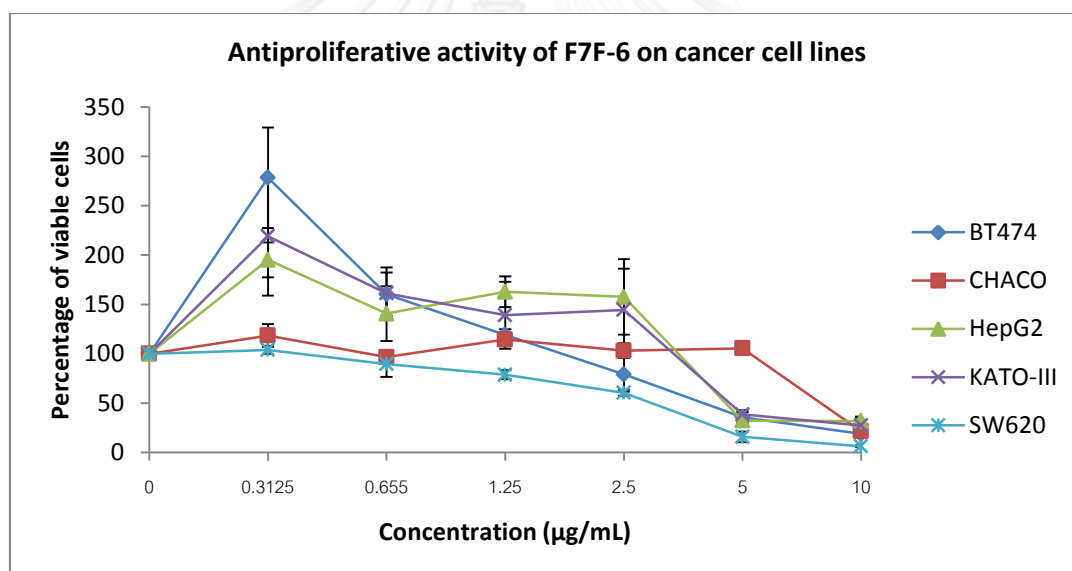
(A)



(B)



(C)



(D)

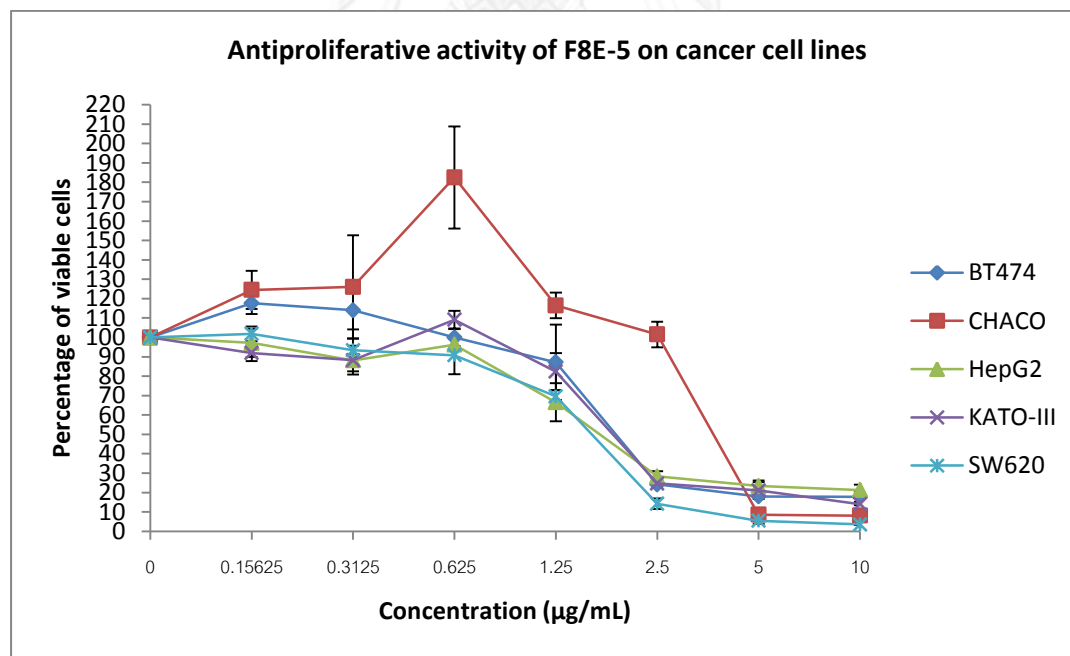
Figure 4.5 The graphs presenting the percentage of viable cells of the combined fractions from subfraction F7F against different 5 cancer cell lines. Concentrations at 0, 0.15625, 0.3125, 0.625, 1.25, 2.5, 5, and 10 µg/mL of F7F-3 were used. For F7F-4, F7F-5 and F7F-6, concentrations at 0.3125, 0.625, 1.25, 2.5, 5, and 10 µg/mL were prepared. The percentage of viable cell by composition F7F-3 was in (A), by composition F7F-4 was in (B) by composition F7F-5 was in (C) by composition F7F-6 was in (D). The data was shown as mean \pm S.D. in µg/mL unit.

Table 4.13 The IC₅₀ values of F8E-5, F8E-6, and F8E-7 originated from subfraction F8E.

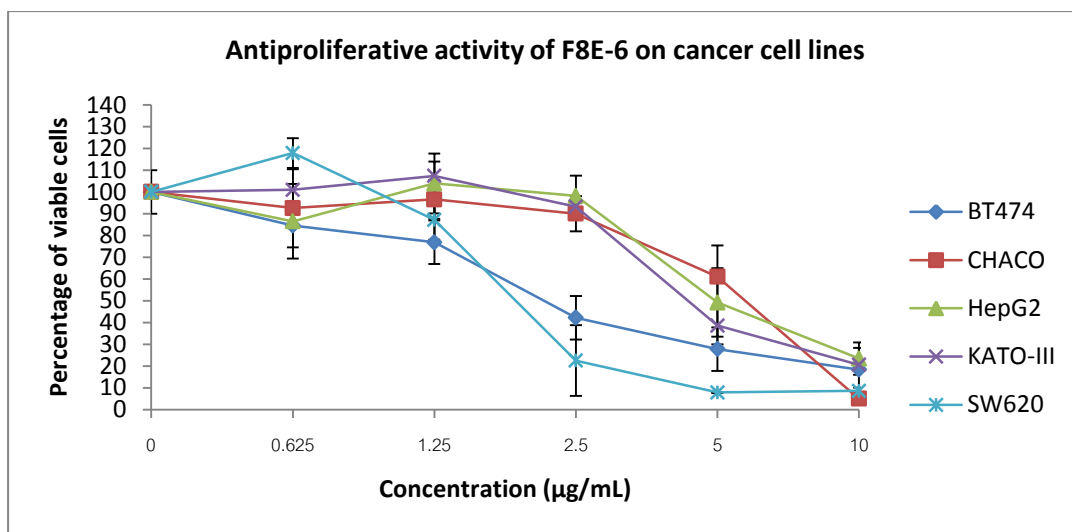
Cancer cell lines	IC ₅₀ (µg/mL)		
	F8E-5	F8E-6	F8E-7
BT474	1.94 ± 0.15 ^a	2.32 ± 0.49 ^{ab}	3.77 ± 0.73 ^b
Chago	3.88 ± 0.10	5.86 ± 0.89	> 10
HepG ₂	1.93 ± 0.04	5.37 ± 1.14	> 10
KATO-III	1.73 ± 0.26 ^a	5.93 ± 1.54 ^b	7.07 ± 0.34 ^b
SW620	1.68 ± 0.06 ^a	7.07 ± 0.34 ^a	2.17 ± 0.05 ^a

Remark (1): These experiments were in triplication.

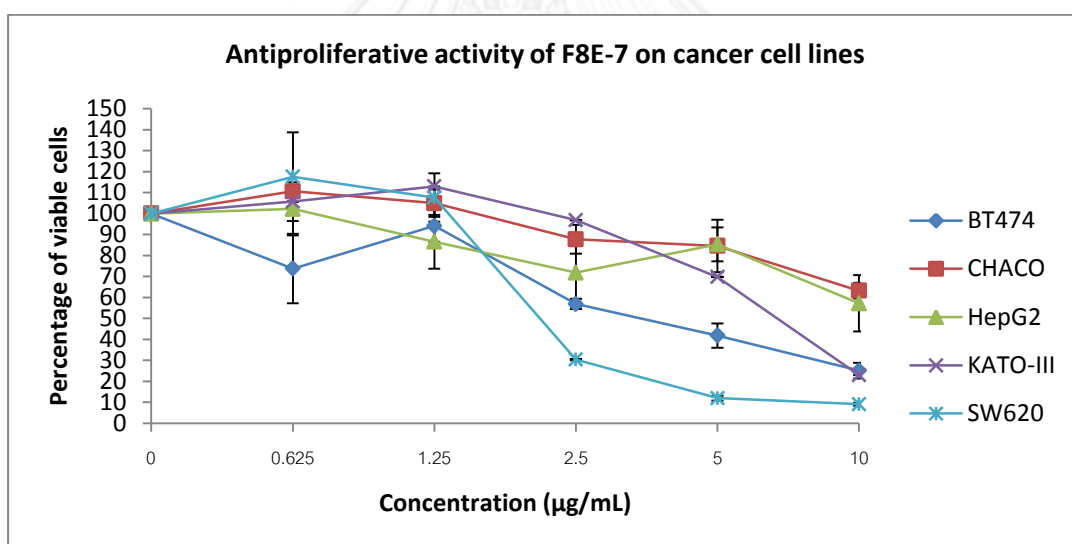
Remark (2): The different uppercase letter showed the significant difference when p - value was equal or less than 0.05. The data was compared by Tukey HSD in SPSS V.17.



(A)



(B)



(C)

Figure 4.6 The graphs presenting the percentage of viable cells of combined fraction from subfraction F8E against different 5 cancer cell lines. Concentrations of F8E-5 at 0, 0.15625, 0.3125, 0.625, 1.25, 2.5, 5, and 10 µg/mL were prepared. Concentrations of F8E-6 and F8E-7 at 0.625, 1.25, 2.5, 5, and 10 µg/mL were prepared. The activity of F8E-5, F8E-6 and F8E-7 was in (A), (B) and (C), respectively. The percentage of viable cells was shown as mean \pm S.D. in µg/mL unit.

4.9 The antiproliferative activity of chemotherapeutic drugs

All cancer cell lines were treated by 2 chemotherapeutic drugs which were doxorubicin and 5-fluorouracil. They were used as positive control. The antiproliferative activity was compared to the activity of active compounds of cerumen.

5-fluorouracil had the antiproliferative activity against Chago cell line with the IC_{50} value of $0.38 \pm 0.08 \mu\text{g/mL}$ and SW620 cell line with the IC_{50} value of $5.9 \pm 0.79 \mu\text{g/mL}$. However, BT474, HepG₂, and KATO-III cell lines were not sensitive to 5-fluorouracil.

Doxorubicin also had the antiproliferative activity against SW620 cell line with the IC_{50} value of $0.07 \pm 0.00 \mu\text{g/mL}$. The IC_{50} value of HepG₂ was $0.32 \pm 0.08 \mu\text{g/mL}$. The IC_{50} value of Chago was $0.35 \pm 0.08 \mu\text{g/mL}$. The IC_{50} value of BT474 was $0.42 \pm 0.11 \mu\text{g/mL}$. Also, the IC_{50} value of KATO-III was $0.56 \pm 0.08 \mu\text{g/mL}$.

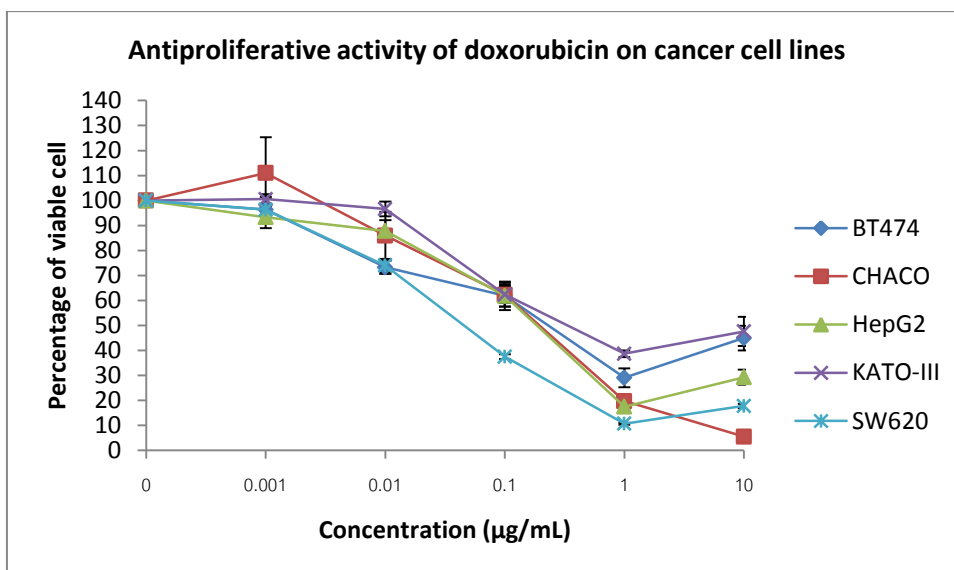
The data of both drugs were showed in Table 4.14 and Figure 4.7. In addition IC_{50} of doxorubicin and 5-fluorouracil would be calculated from $\mu\text{g/mL}$ to $\mu\text{mol/L}$.

Table 4.14 The IC_{50} values of doxorubicin and 5-fluorouracil in $\mu\text{g/mL}$ and $\mu\text{mol/mL}$.

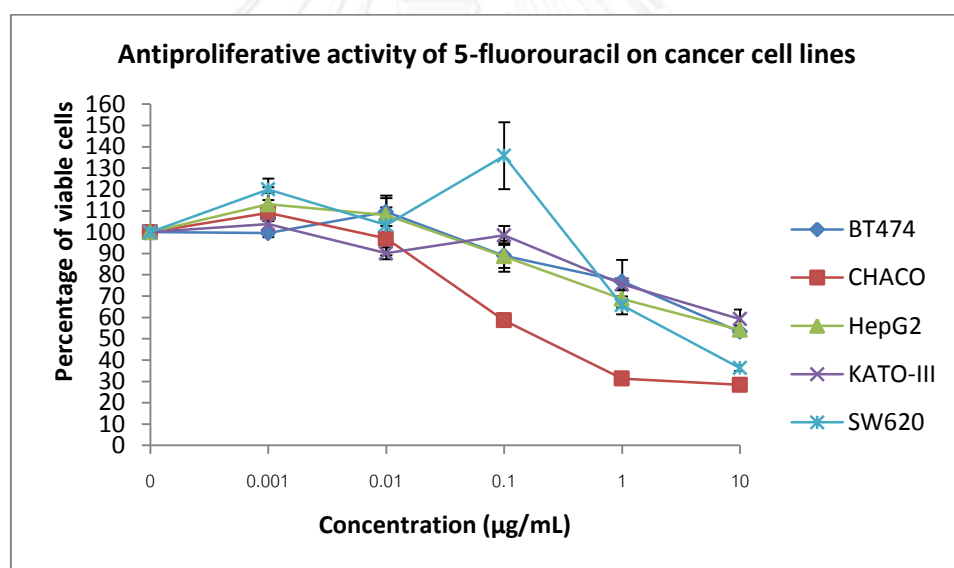
Cell lines\Drug	IC_{50} ($\mu\text{g/mL}$)		IC_{50} ($\mu\text{mol/L}$)	
	Doxorubicin	5-fluorouracil	Doxorubicin	5-fluorouracil
BT474	0.42 ± 0.12	> 10	0.77 ± 0.21	> 76.5
CHACO	0.35 ± 0.07	0.38 ± 0.08	0.65 ± 0.14	2.91 ± 0.64
HepG ₂	0.32 ± 0.08	> 10	0.59 ± 0.15	> 76.5
KATO-III	0.56 ± 0.09	> 10	1.03 ± 0.16	> 76.5
SW620	0.07 ± 0.00	5.69 ± 0.79	0.12 ± 0.00	43.53 ± 5.60

Remark (1): These experiments were in triplication.

Remark (2): Structure of both chemotherapeutic drugs was in page 19 and 38. Doxorubicin and 5-fluorouracil have a molecular weight at 543.52 and 130.77 g/mol, respectively (Atomic weight of carbon, hydrogen, oxygen, nitrogen and fluorine are 12.010, 1.008, 15.999, 14.007 and 18.998 g/mol, respectively). 10 $\mu\text{g/mL}$ of 5-fluorouracil is equal of 76.5 in $\mu\text{mol/L}$ unit.



(A)



(B)

Figure 4.7 The graphs presenting the percentage of viable cells from chemotherapeutic drugs against 5 different cancer cell lines. Concentrations of doxorubicin and 5-fluorouracil at 0, 0.001, 0.01, 0.1, 1, and 10 µg/mL were prepared. The activity of doxorubicin was in (A) and the activity of 5-fluorouracil was in (B). The percentage of viable cells was shown as mean \pm S.D. in µg/mL unit.

4.10 CRL-1947 fibroblast cytotoxicity

CRL-1947 fibroblast as a representative of normal cells was treated with 3 bioactive compounds including subfraction F7E, F7F-3, and F8E-5. Also, 2 chemotherapeutic drugs, doxorubicin and 5-fluorouracil were used as positive control. The F7F-3 had the cytotoxicity with the IC_{50} value of $4.56 \pm 0.31 \mu\text{g/mL}$ and composition F7E had the cytotoxicity with the IC_{50} value of $9.01 \pm 0.48 \mu\text{g/mL}$. In contrast, F8E-5 had no cytotoxicity to fibroblast. Also, both doxorubicin and 5-fluorouracil had no cytotoxicity to fibroblast. In overall, the result showed that purified compounds had low cytotoxicity to fibroblast (Table 4.15) and Figure 4.8.

Table 4.15 Cytotoxicity of the isolated compounds and drugs to fibroblast.

Purified compound/ drug	The IC_{50} value ($\mu\text{g/mL}$) of fibroblast
F7E	9.01 ± 0.48
F7F-3	4.56 ± 0.31
F8E-5	> 10
Doxorubicin	> 10
5-Fluorouracil	> 10

Remark: These experiments were in triplication.

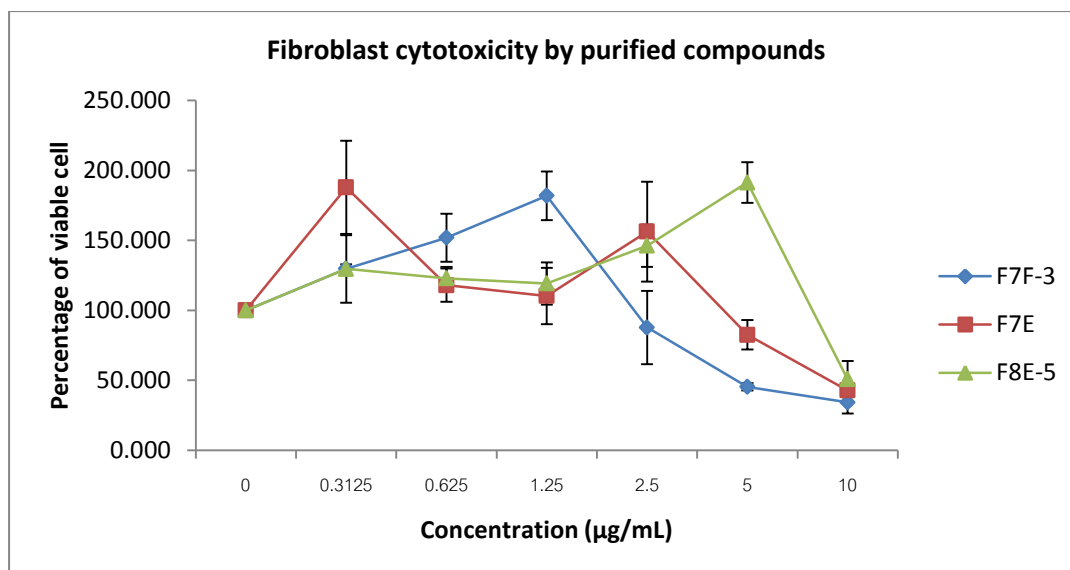


Figure 4.8 Fibroblast cytotoxicity by purified compounds. Concentrations of the isolated compounds at 0, 0.3125, 0.625, 1.25, 2.5, 5, and 10 µg/mL were prepared. The percentage of viable cells was shown as mean \pm S.D. in µg/mL unit.

4.11 Morphology of untreated cancer cell lines

Cancer cell lines were separately treated with F7E, F7F-3 and F8E-5 subfractions at their IC_{50} values. The change in morphology was observed under a light microscope at 0, 24, 48, 72 h of incubation. A picture was captured with a photograph device that was connected directly to a microscope and a computer.

Among those 3 samples, subfraction F7F-3 had the best antiproliferative activity against 5 cancer cell lines. The IC_{50} values of those 3 samples were shown in Table 4.16.

Table 4.16 The IC₅₀ value of F7E, F7F-3 and F8E-5.

Cancer cell lines	IC ₅₀ (µg/mL)		
	F7E	F7F-3	F8E-5
BT474	1.01 ± 0.03	0.50 ± 0.01	1.94 ± 0.15
Chago	0.94 ± 0.08	0.92 ± 0.08	3.88 ± 0.10
HepG ₂	0.97 ± 0.02	0.39 ± 0.04	1.93 ± 0.04
KATO-III	0.88 ± 0.03	0.36 ± 0.06	1.73 ± 0.26
SW620	1.64 ± 0.06	0.62 ± 0.16	1.68 ± 0.06

After 5 cancer cell lines were treated with subfraction F7F-3 at its IC₅₀ value, the morphology change of 5 cancer cell lines were observed and compared to the morphology change of cancer cell lines treated with 100% DMSO as control (Figures 4.9-4.13

4.11.1 Untreated BT474 cell line

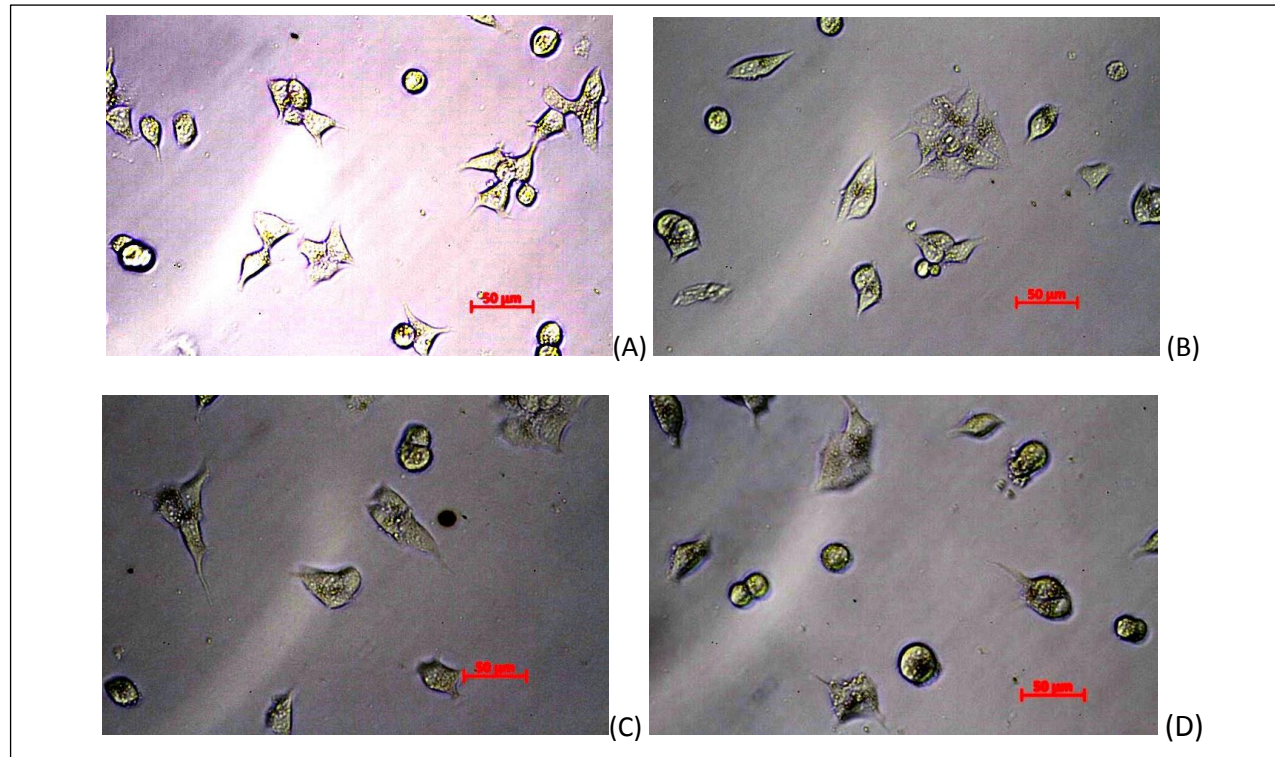


Figure 4.9 The morphology of untreated BT474 cell line at 0 h (A), 24 h (B), 48 h (C), and 72 h (D). All images were magnified at 20X and the drawn scale bar was 50 µm.

4.11.2 Untreated Chago cell line

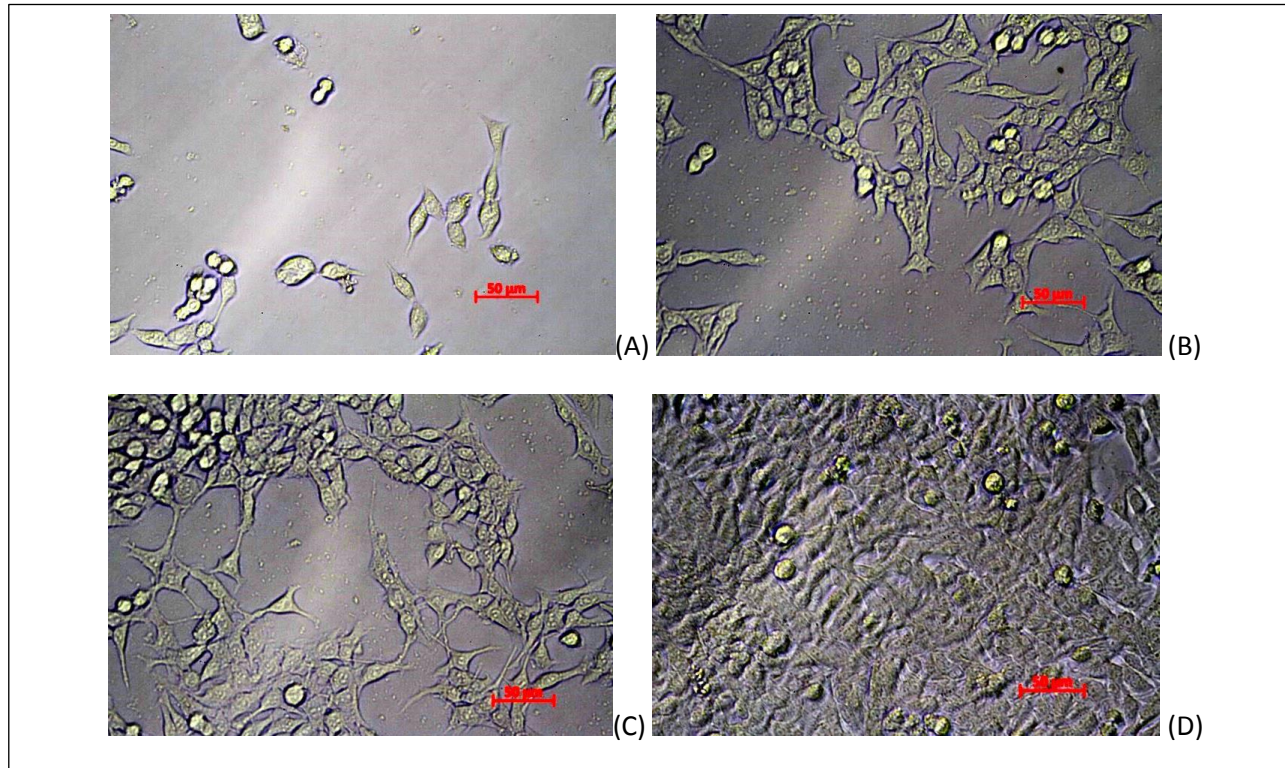


Figure 4.10 The morphology of untreated Chago cell line at 0 h (A), 24 h (B), 48 h (C), and 72 h (D). All images were magnified at 20X and the drawn scale bar was 50 µm.

4.11.3 Untreated Hep-G₂ cell lines

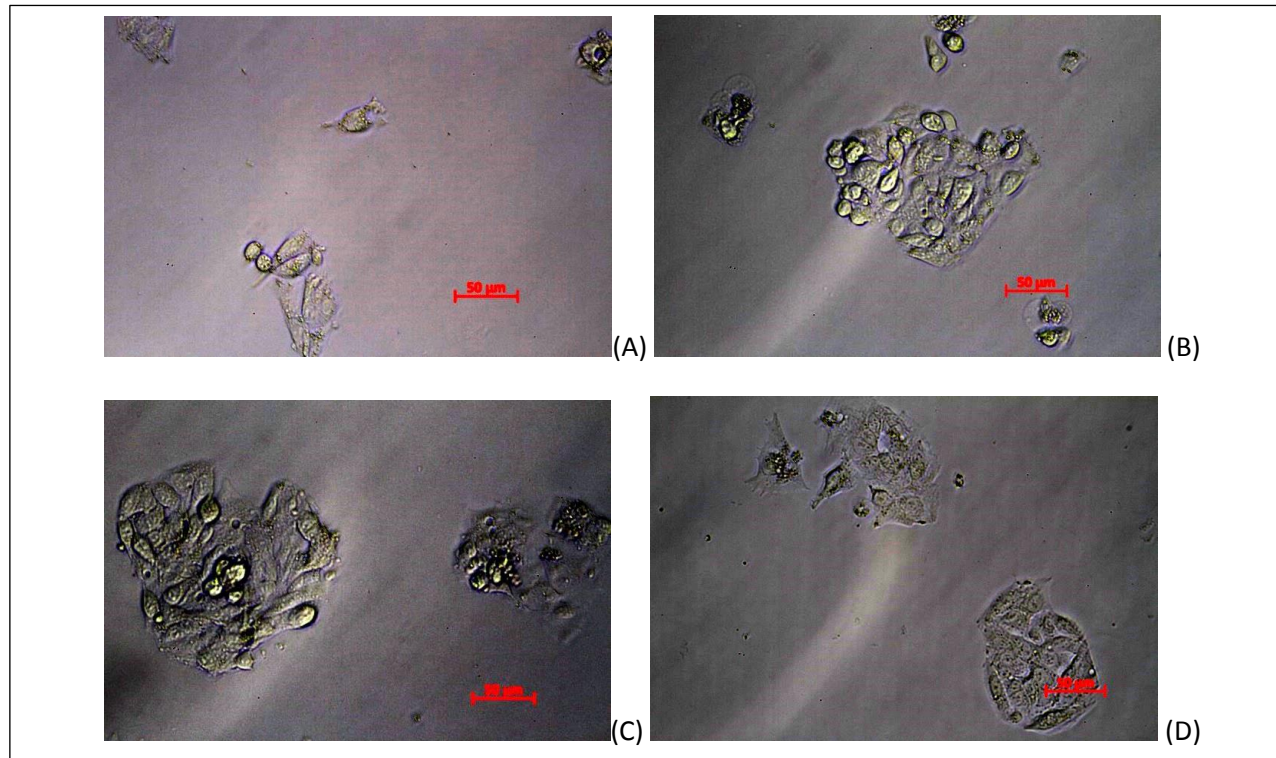


Figure 4.11 The morphology of untreated Hep-G₂ cell line at 0 h (A), 24 h (B), 48 h (C), and 72 h (D). All images were magnified at 20X and the drawn scale bar was 50 µm.

4.11.4 Untreated KATO-III cell line

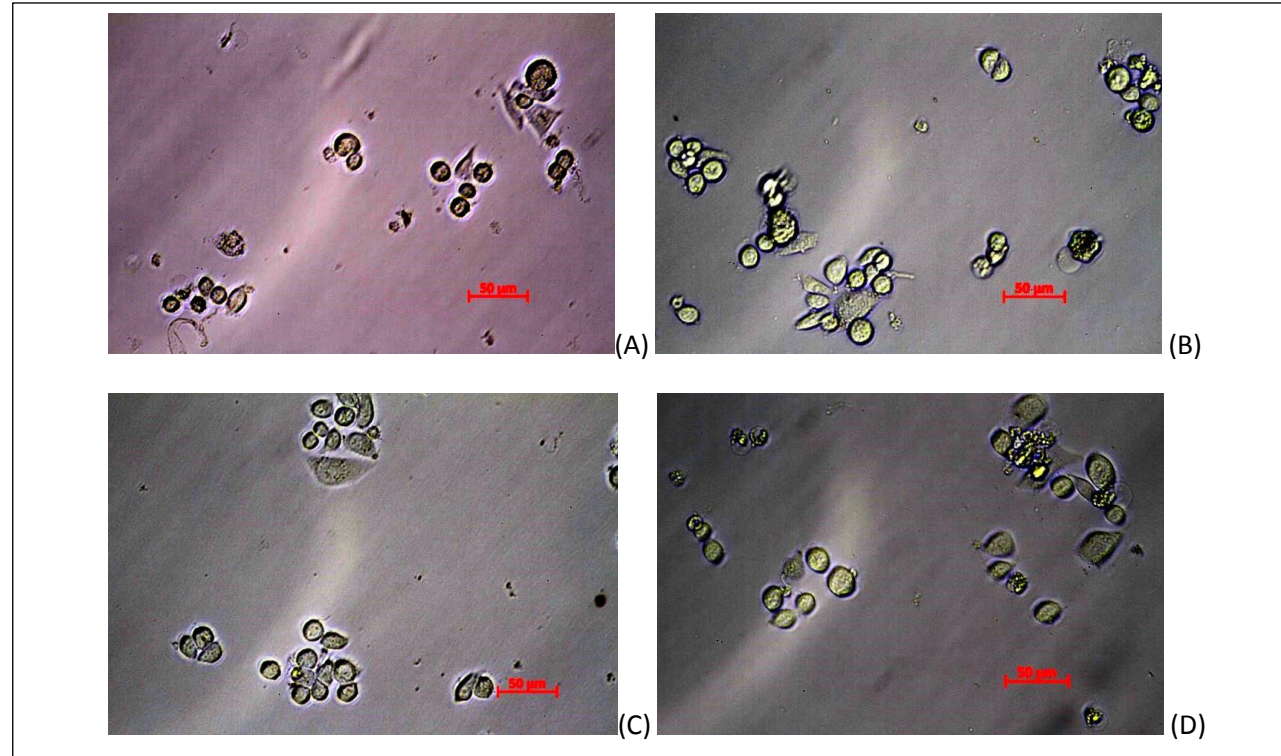


Figure 4.12 The morphology of untreated KATO-III cell line at 0 h (A), 24 h (B), 48 h (C), and 72 h (D). All images were magnified at 20X and the drawn scale bar was 50 µm.

4.11.5 Untreated SW 620 cell line

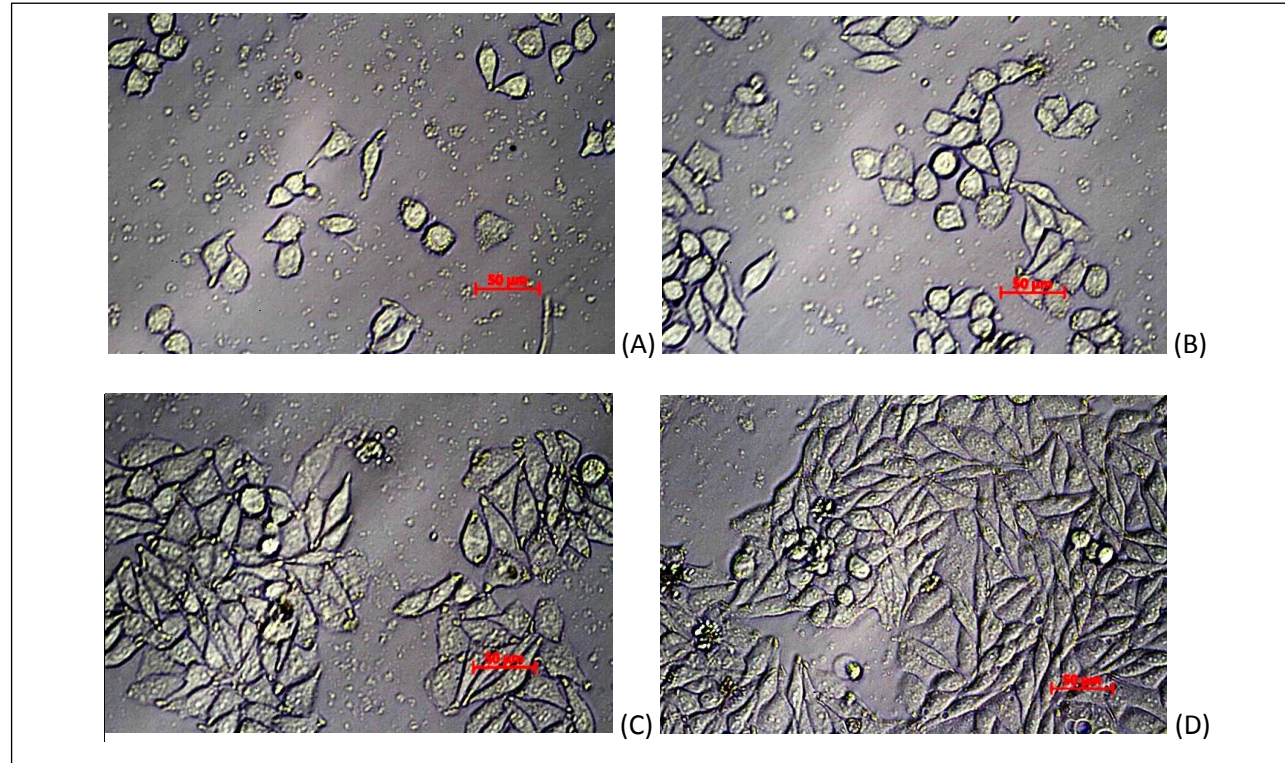


Figure 4.13 The morphology of untreated SW620 cell line at 0 h (A), 24 h (B), 48 h (C), and 72 h (D). All images were magnified at 20X and the drawn scale bar was 50 µm.

For an overview of untreated cell line morphology, all untreated cancer cell lines were mixed with 100% DMSO as control only. The cell density of all cell lines was similar. The cell number of cell lines tended to increase. Each cell line had an identity of shapes.

In Figure 4.9, BT474 cells looked round in shape and had various types of shape. Some cell lines are attached together to form a clump. The density of cells is low or the cells were not spread all over the area of a well plate.

In Figure 4.10, Chago cells looked round, stellate, and spindle oval in shape. This cell line had a very fast growth rate. At 72 h of incubation (Figure 4.10D), the density of cells was high and cells were spread all over the area of a well plate.

In Figure 4.11, Hep-G₂ cells had a spindle oval shape. Cell lines were tightly attached to each other so many small clumps were observed. This cell line had the medium rate of growth. The density of cells was moderate and cells were not spread all over the area of a well plate.

In Figure 4.12, KATO-III cells had a round and oval shape. Cells were mostly separated but, in some area, small clumps of cells could be noticed. The density of cells was low and cells were not spread all over the area of a well plate.

In Figure 4.13, SW620 cells had a spindle oval shape and a little round shape. This cell line had the fast rate growth. At 72 h of incubation (Figure 4.13D), the density of cells was high and cells were spread almost all over the area of a well plate

4.12 Morphology of treated cancer cell lines

After cell lines were treated with F7F-3 at its IC₅₀ value, the change in cell morphology could be observed in various types. Each cell line had a different of overview death (Figures 4.14-4.18).

4.12.1 Treated BT474 cell line (by composition F7F-3 at $0.50 \pm 0.01 \mu\text{g/mL}$)

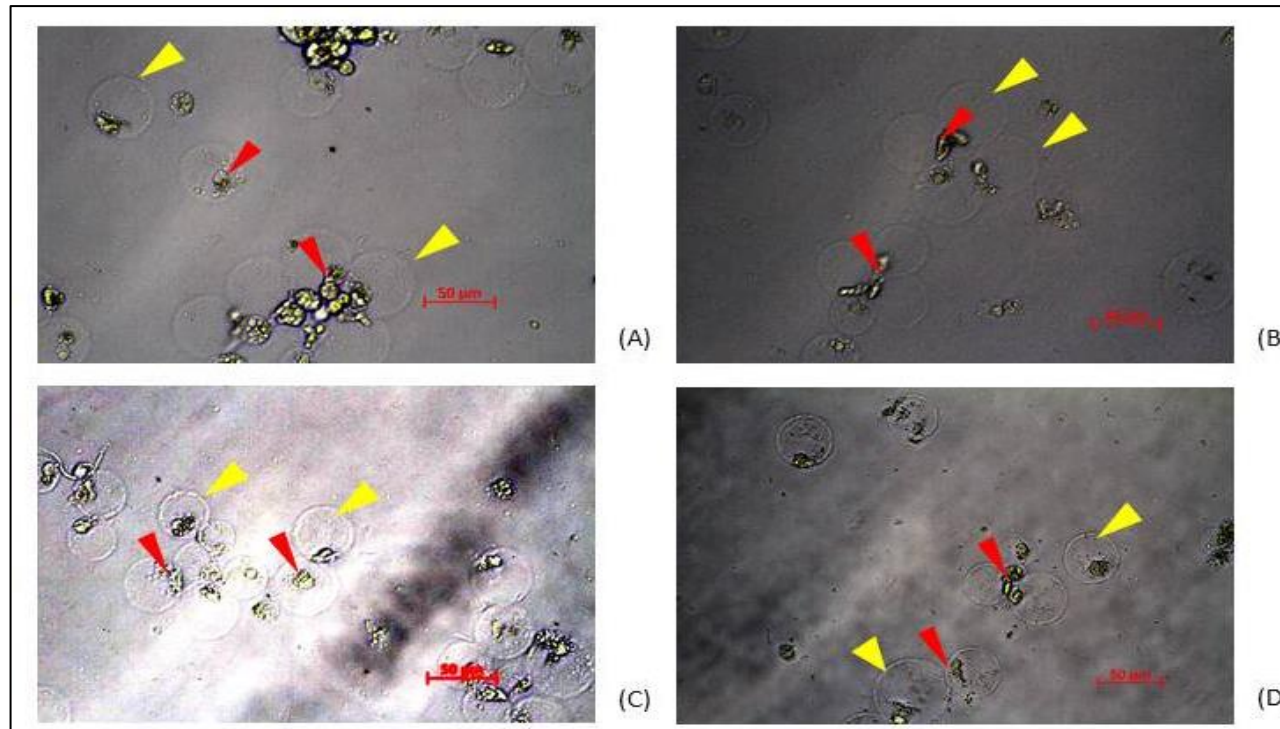


Figure 4.14 The morphology of treated BT474 cell line at 0 h (A), 24 h (B), 48 h (C), and 72 h (D). All images were magnified at 20X and the scale bar was 50 μm . A red arrow indicated shrunken nucleus and organelle while a yellow arrow indicated cell membrane.

4.12.2 Treated Chago cell line (by composition F7F-3 at $0.92 \pm 0.08 \mu\text{g/mL}$)

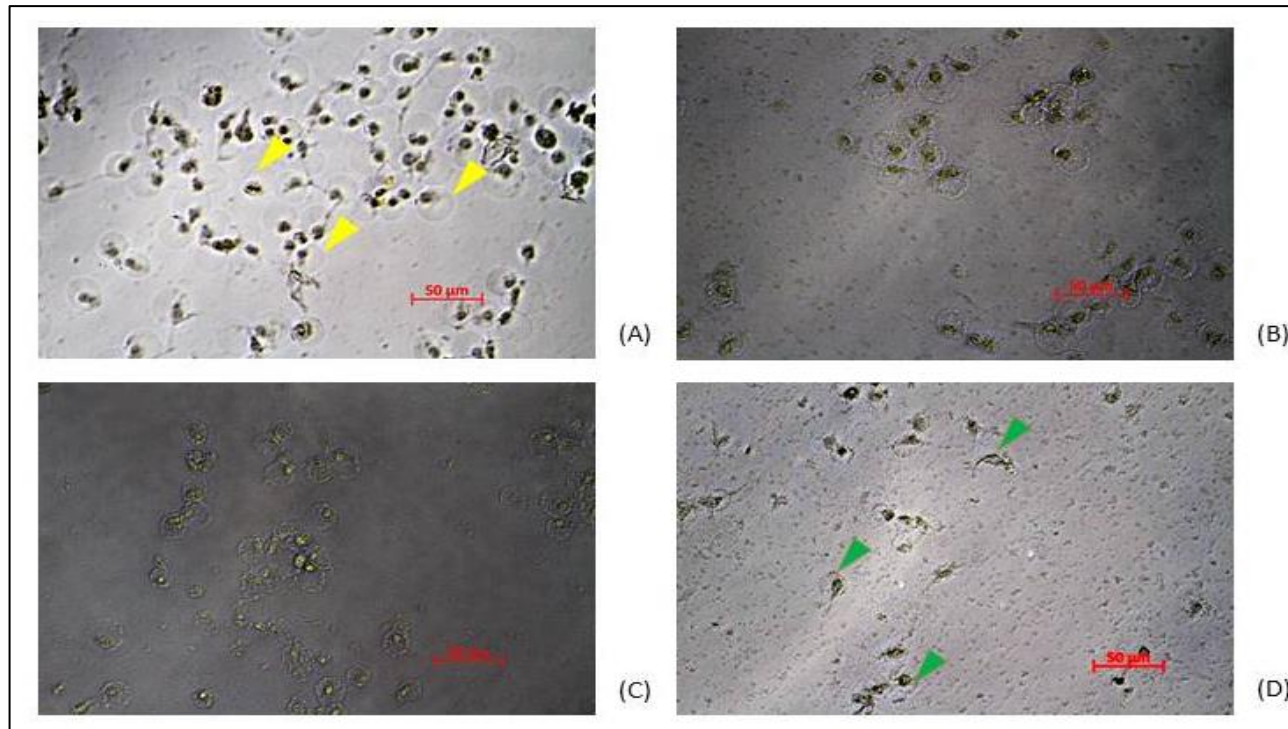


Figure 4.15 The morphology of treated Chago cell line at 0 h (A), 24 h (B), 48 h (C), and 72 h (D). All images were magnified at 20X and the scale bar was 50 μm . A yellow arrow indicated hypertonic cells while a green arrow indicated cell debris.

4.12.3 Treated Hep-G₂ cell line (by composition F7F-3 at $0.39 \pm 0.04 \mu\text{g/mL}$)

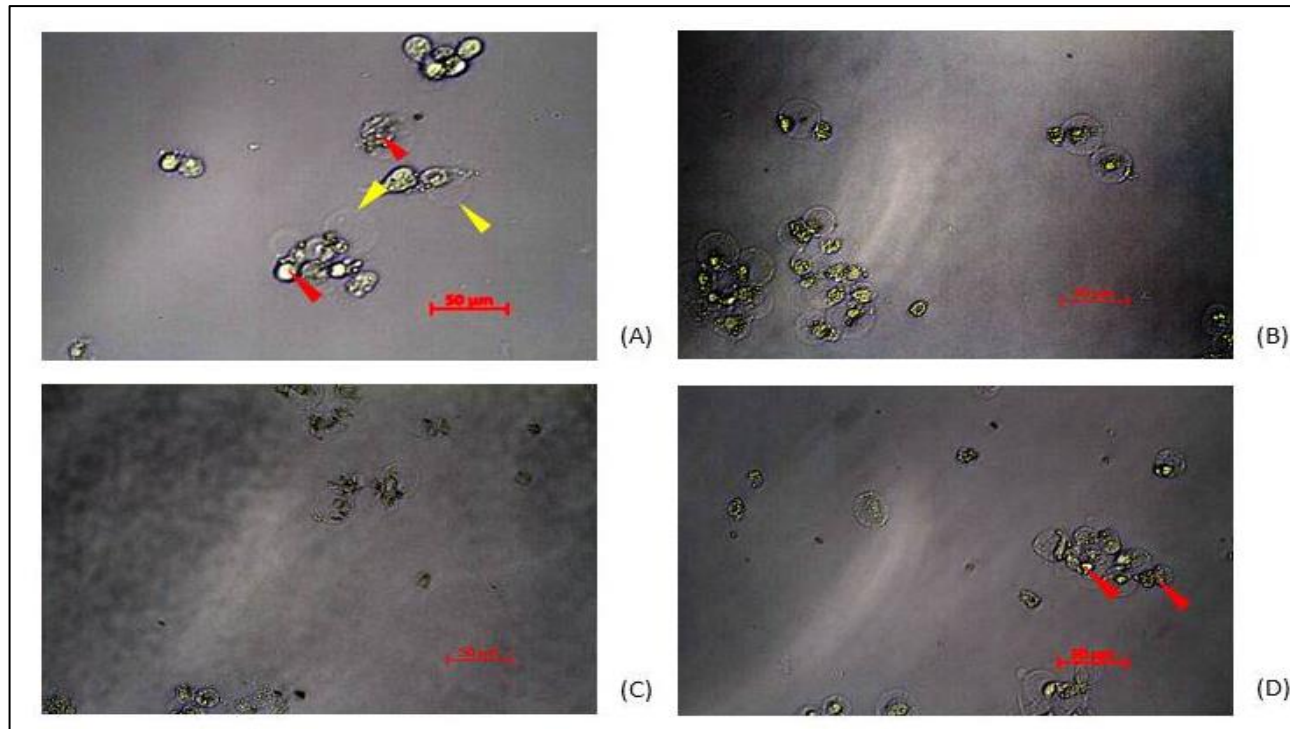


Figure 4.16 The morphology of treated Hep-G₂ cell line at 0 h (A), 24 h (B), 48 h (C), and 72 h (D). All images were magnified at 20X and the scale bar was 50 μm. A red arrow indicated shrunken nucleus and organelle while a yellow arrow indicated cell membrane.

4.12.4 Treated KATO-III cell line (by composition F7F-3 at $0.36 \pm 0.06 \mu\text{g/mL}$)

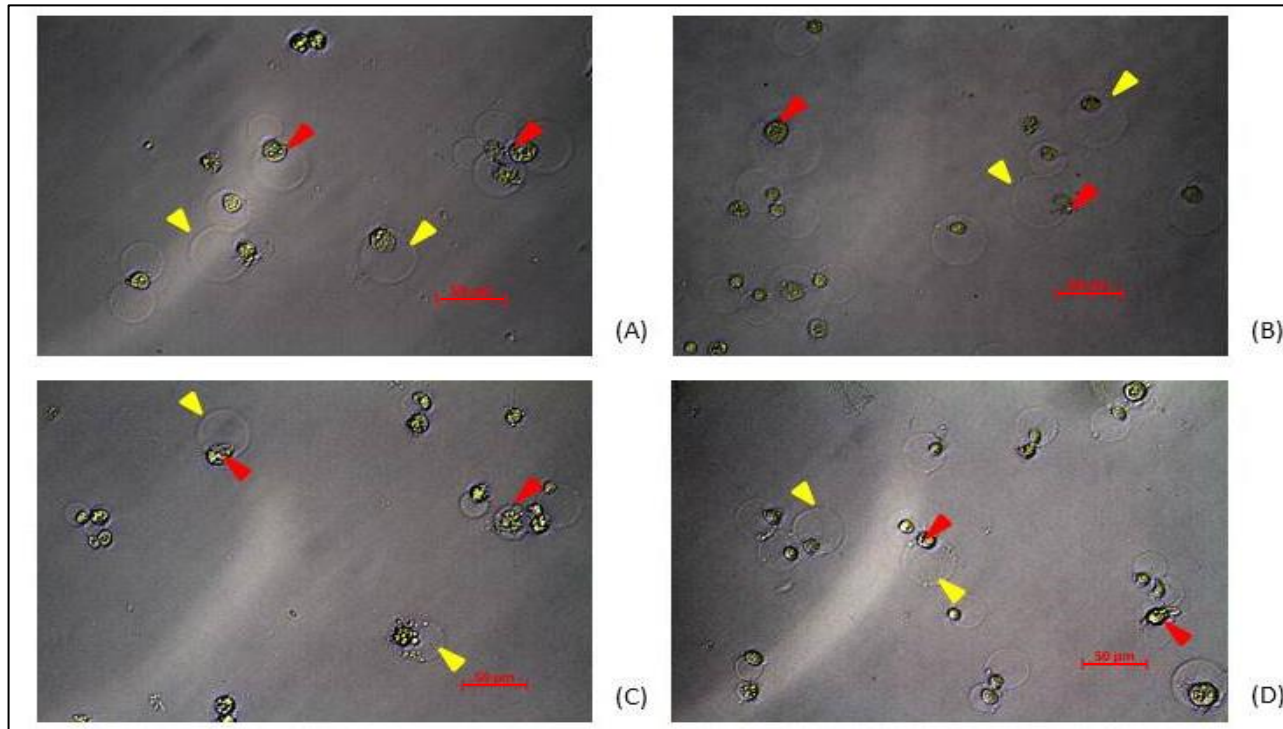


Figure 4.17 The morphology of treated KATO-III cell line at 0 h (A), 24 h (B), 48 h (C), and 72 h (D). All images were magnified at 20X and the scale bar was 50 μm. A red arrow indicated shrunken nucleus and organelle while a yellow arrow indicated cell membrane.

4.12.5 Treated SW620 cell line (by composition F7F-3 at $0.62 \pm 0.16 \mu\text{g/mL}$)

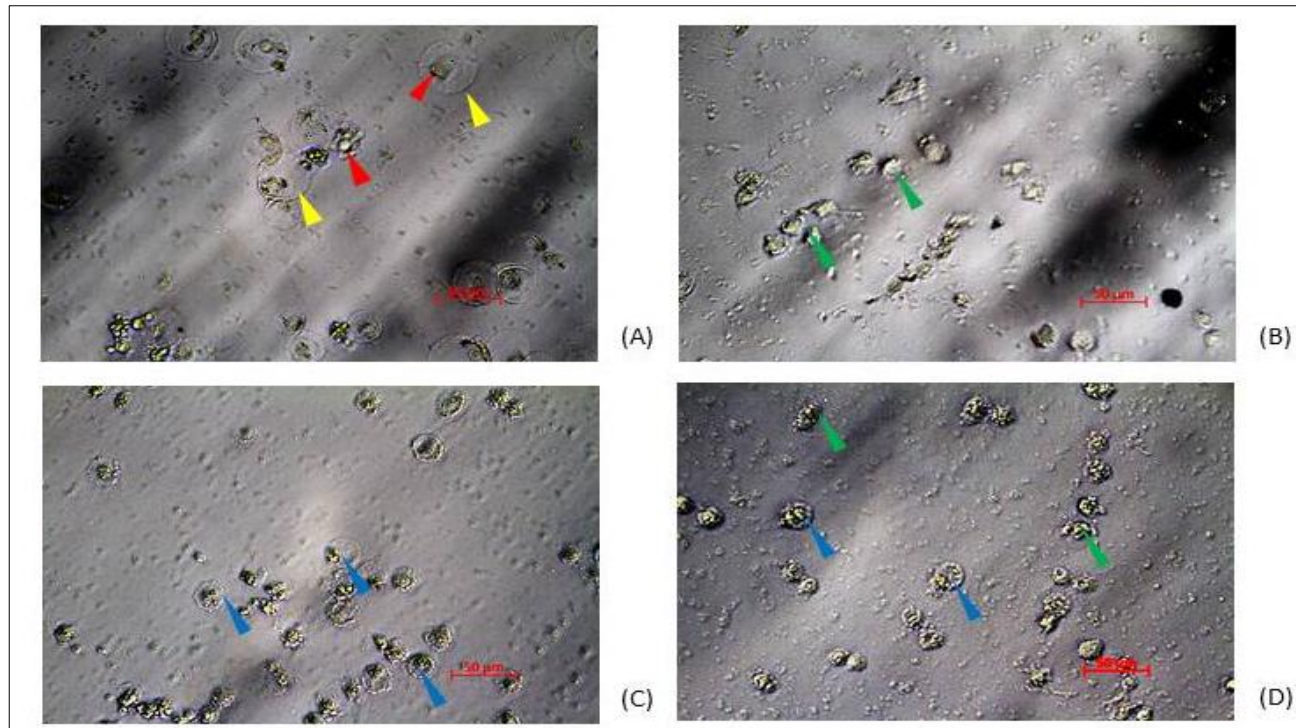


Figure 4.18 The morphology of treated SW620 cell line at 0 h (A), 24 h (B), 48 h (C), and 72 h (D). All images were magnified at 20X and the scale bar was 50 μm . A red arrow indicated shrunken organelle. A yellow arrow indicated cell membrane. A green arrow indicated cell debris while a blue arrow indicated shrunken cell.

Figure 4.14 showed the treated BT474 cell line, at 0 h of incubation (Figure 4.14A), organelles started to shrink so the amount of cytoplasm looked increased. Cells looked round. At 24 h of incubation (Figure 4.14B), the number and the density of cells decreased. The area of organelles was smaller than where was seen at 0 h of incubation. At 48 h of incubation (Figure 4.14C), the number of cells was more decreased. At 72 h of incubation (Figure 4.14D), cell debris were seen. The left over cells looked smaller in size than cells at 0 h of incubation. The number of cells kept decreasing.

Figure 4.15 showed the treated Chago cell line, at 0 h of incubation (Figure 4.15A), cells started to be in a hypertonic form. Organelles started to shrink like the event of BT474 cell line but the treated Chago cells were smaller in size than treated BT474 cells. At 24 h of incubation (Figure 4.15B), the number and the density of cells were rapidly decreased. The shape of cells started to change not to be round. At 48 h of incubation (Figure 4.15C), morphology of death cell could be noticed in various forms. Round shape was disappeared. At 72 h of incubation (Figure 4.15D), only cell debris could be found and the shape of cell debris could not be identified.

Figure 4.16 showed the treated Hep-G₂ cell line, at 0 h of incubation (Figure 4.16A), cells started to be in a hypertonic form like BT474 and Chago cell lines at this period of incubation. However, some cells were still not in a shrinkage form but were attached to each other to form a clump. At 24 h of incubation (Figure 4.16B), the number of shrinkage cells increased but the number of total cells and density decreased. Cells were attached to each other to form a clump. At 48 h of incubation (Figure 4.16C), the morphology remained unchanged. At 72 h of incubation (Figure 4.16D), the number of cell debris increased but dead cells were noticed in some area, not widely dispersed in a well plate.

Figure 4.17 showed the treated KATO-III cell line, at 0 h of incubation (Figure 4.17A), cells started to be in a hypertonic form like BT474 cell line. At 24 h of incubation (Figure 4.17B), the morphology remained unchanged but the density and the number of cells decreased. At 48 h of incubation (Figure 4.17C), the morphology still remained unchanged. At 72 h of incubation (Figure 4.17D), the cell size became smaller than the cell size at 48 h of incubation. Nonetheless, the morphology remained unchanged.

Figure 4.18 showed for SW620 cell line, at 0 h of incubation (Figure 4.18A), cell death started to be noticed by observing the various changed shapes such as

hypertonic, shrank. The cell density and number were rapidly decreased. At 24 h of incubation (Figure 4.18B), cell debris could be visible. More cells were shrinkage. At 48 h of incubation (Figure 4.18C), the number of shrunk cells and cell debris increased. At 72 h of incubation (Figure 4.18D), the number of shrunk cells and cell debris kept increasing.

Overview morphology of all treated cell lines was that cells became hypertonic. Organelles were shrinkage so it made the amount of cytoplasm look increased. That led the cell look round and not broken. Thus, it's very interesting to continue finding the death program of those cell lines.

4.13 Chemical structure of a bioactive compound

According to ^1H NMR spectroscopic data, subfractions F7E, F7F-3 and F8E were similar. Among these 3 samples, F7F-3 was the almost pure exhibited the best antiproliferative activity against 5 cancer cell lines. In addition, the best described morphology of cell death was visible. Thus, F7F-3 was further subjected analysis of the chemical structure. F7F-3 was solid or yellow crystal. Sometimes, it was yellow solid or in oily form. Its structure was analyzed by 1-dimensional and 2-dimensional NMR spectroscopy, including HSQC, HMBC, and COSY. The F7F-3 was identified as **alpha-mangostin** (Figure 4.19) and its NMR data were summarized in Table 4.18.

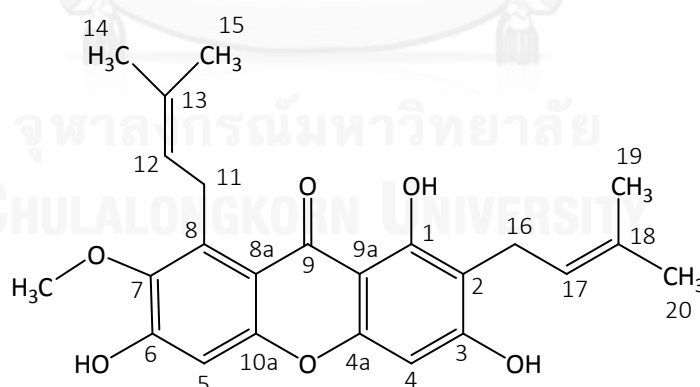


Figure 4.19 The chemical structure of F7F-3 by NMR analysis.

Table 4.17 NMR spectroscopic data of F7F-3.

Position	δ_{H} (^1H NMR) (CDCl_3 , 400 MHz)	δ_{C} (^{13}C NMR) (CDCl_3 , 100 MHz)	δ_{H} (^1H NMR) (CDCl_3 , 400 MHz) from (1)	δ_{C} (^{13}C NMR) (CDCl_3 , 100 MHz) from (1)	H-H-COSY	HMBC
2	-	108.6	-	109.7	-	-
3	-	161.7	-	161.6	-	-
4	6.29 (1H, s)	93.4	6.24 (1H, s)	92.4	-	C2, C3, C4a, C9a
4a	-	155.2	-	154.8	-	-
5	6.83 (1H, s)	101.7	6.74 (1H, s)	101.6	-	C7, C8a, C10a
6	-	155.9	-	155.4	-	-
7	-	142.7	-	142.7	-	-
8	-	137.2	-	137.2	-	-
8a	-	112.4	-	111.7	-	-
9	-	182.2	-	181.8	-	-
9a	-	103.8	-	103.1	-	-
10a	-	154.7	-	155.2	-	-
11	4.09 (2H)	26.7	4.00 (2H)	26.3	H14	C7, C8, C8a, C12, C13
12	5.28 (1H)	123.3	5.18 (1H)	122.1	H11	C12
13	-	132.2	-	131.7	-	-
14	1.77 (3H, s)	18.3	1.61 (3H, s)	25.7	-	C12, C13, C15
15	1.83 (3H, s)	16.9	1.72 (3H, s)	17.7	-	C12, C13, C14
16	3.45 (2H)	21.6	3.28 (2H)	21.3	H19	C1, C2, C3, C17, C18
17	5.28 (1H)	121.6	5.17 (1H)	123.4	H16	C17
18	-	133.8	-	132.6	-	-
19	1.69 (3H, s)	20.9	1.62 (3H, s)	25.7	-	C17, C18, C20
20	1.84 (3H, s)	18.0	1.75 (3H, s)	18.1	-	C17, C18, C19
7-OMe	3.81 (3H, s)	62.2	3.82(3H, s)	61.2	-	C7
1-OH	13.79 (1H, s, OH)	160.8	13.35 (1H, s, OH)	160.2	-	C1, C2, C9a

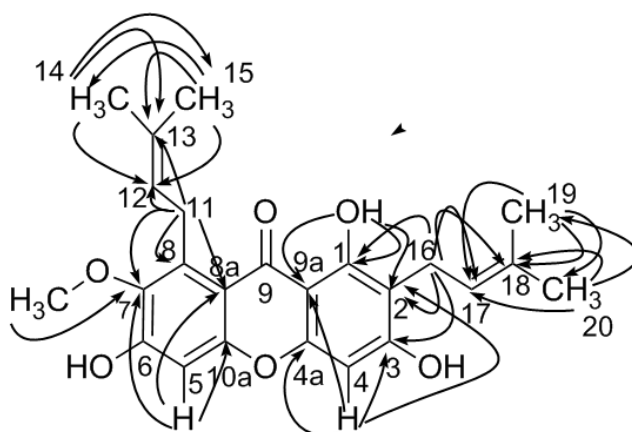


Figure 4.20 HMBC correlation of carbon position of F7F-3.

The chemical structure of compound F7F-3 was analysed according to the spectrum reference from Mahabusarakam et al. (32), Yu et al. (68), Ghazali et al. (1), and Massarani et al. (69). It was identified as **1,3,6-trihydroxy-7-methoxy-2,8-diprenylxanthone or alpha-mangostin** which was one of bioactive compounds in mangosteen (70).

This compound has molecular weight at 410.45 g/mol (atomic weight of Carbon, Hydrogen and Oxygen are 12.010, 1.008 and 15.999, respectively). This compound would be calculated IC_{50} from $\mu\text{g/ml}$ in table 4.12 to $\mu\text{mol/ml}$. The IC_{50} of this compound in $\mu\text{g/mL}$ and $\mu\text{mol/L}$ in table 4.18

Table 4.18 IC_{50} of alpha-mangostin (F7F-3) in $\mu\text{g/mL}$ and $\mu\text{mol/L}$

Cancer cell lines	alpha-mangostin (F7F-3)	
	IC_{50} ($\mu\text{g/ml}$)	IC_{50} ($\mu\text{mol/L}$)
BT474	0.50 ± 0.01	1.22 ± 0.03
Chago	0.92 ± 0.08	2.25 ± 0.20
Hep-G ₂	0.39 ± 0.04	0.94 ± 0.01
KATO-III	0.36 ± 0.06	0.88 ± 0.16
SW620	0.62 ± 0.16	1.50 ± 0.39

Chapter V

Discussion

In this research, honey pot cerumen of *Tetragonula laeviceps* was used to determine the antiproliferative activity on cancer cell lines. As it was the mixture of many bee products such as honey; beeswax; propolis, it was expected to have the better antiproliferative activity, comparing to single bee product. Cerumen was collected from Chantaburi province because there were many types of fruit orchard such as rambutan, mangosteen, durian which were food sources for stingless bees and honeybees. Meantimes, pollination by bees was very important for plants. Hence, in this province, there was a meliniponiculture and apiculture complex for orchard agriculture to increase products. Farmers seemed to prefer stingless bee to honeybee because it could not sting and was less aggressive. That led to a high density of stingless bee population in this province (3).

Since there were a very few research articles on cerumen, many articles about other bee products would be used for the better discussion here.

Cerumen collected from an orchard in Chantaburi province looked dark brown and sticky. However, it was reported that propolis from Brazil looked green (71) and propolis from China looked red (72). In overall, it seemed to be that the character of raw natural products depended on geography or external factors a lot. It might be possible that the color character depended on the color of plant resin. There were some supportive articles as below.

In 2007, Dausch et al. (73) reported *A. mellifera* red propolis collected from many places in northeastern Brazil. Red propolis was extracted by ethanol and was analyzed for chemical compositions by reverse phase HPLC and reverse phase high performance thin layer chromatography. The result showed that there were various types of flavonoid and various compositions such as rutin, liquiritigenin, daiazain, quercetin, luteolin, dalbergin, isoliquiritigenin, formononetin, pinocembrin, pinobanksin-3-acetate, and biochanin. It was found out that main plant resin in red propolis was from *Dalbergia ecastophyllum*. produce red propolis is come from this plants.

In 2012, Shimomura et al. (74) presented propolis from *A. mellifera* in Jeju island, South Korea. This propolis was yellow black. It was originated from resin of

native plants and mixed with wax and old resin within a hive. After it was extracted by MeOH, it was analyzed by reversed phase-HPLC. The chemical components were revealed to be similar to those in *Angelica keiskei*, native plant in Korea. Those 6 main compositions were SS-(+)-laserpitin, (SS)-(-)-isolaserpitin, (-)-selidin, 4-hydroxyderricin, xanthoangelol, and xanthoangelol.

In addition, it was likely that extraction methods played a key role in bioactive compounds and bioactivity of natural products, too.

In 2011, Aspe and Fernandez (75) reported the extraction of *Pinus radiata* bark from Chile. Four different methods of extractions which were conventional maceration (batch), soxlet extraction, ultrasound assisted extraction (UAE), and microwave assisted extraction (MAE) were used. However, the solution of 3:7 between H₂O:acetone was used in all methods. The result showed that, for the first step, soxlet extraction gave the most yield at 12.0%. It was followed by MAE, UAE, and conventional maceration at 10.4%, 9.5%, and 8.0%, respectively. When it was continued to the second and third step, MAE could increase the yield of extract to be 15.2% and a few of solvent volume was used. Next, extracts from soxlet and MAE were used to test for the antioxidant activity by DPPH method. The result showed that both extracts had the better antioxidant activity than pycogenol. The activity was better when MAE extract was more extracted in the further step. The activity of extracts by MAE in the first, second, and third step was 11.6, 9.9, and 7.8 µg/mL, respectively while the activity of extracts by soxlet in the first, second, and third step was 15.4, 14.2, and 14.5 µg/mL, respectively. It showed that soxlet extraction gave the best yield for single extraction while MAE gave the best yield for multiple extractions.

Hence, in this research, cerumen was extracted by 2 methods. The first one was the extracted with 80% methanol, dichloromethane, and hexane, respectively which were followed by Umthong *et al.* (18) and Teerasripreecha *et al.* (19). The second method was the extraction in the reversed order of organic solvents with hexane, dichloromethane, and 80% methanol, respectively. All of 6 crude extracts (CME, CDE, CHE, ReCME, ReCDE, and ReCHE) were obtained. Considering the appearance of those crude extracts (Tables 4.1 and 4.2), CHE looked similar to ReCHE (sticky and waxy form), CDE looked similar to ReCDE (red-brown sticky resin), and CME looked similar to ReCME (brown liquid).

However, the percentage yield among 6 crude extracts was different (Tables 4.1 and 4.2). The percentage yield of CME, CDE, and CHE was 4.858, 51.997, and

23.549, respectively, but the percentage yield of reversed crude extracts was 9,280, 30.100, and 43.370, respectively. Thus, in this research, it supported that a different method for extraction gave a different yield.

Considering the appearance of crude extracts of cerumen, they looked different from crude extracts of propolis although they were from the same species. CME, CDE, and CHE of *T. laeviceps*' propolis were dark brown solid, sticky solid, and sticky liquid, respectively (18). Moreover, CME, CDE, and CHE of *Apis mellifera*'s propolis were hazel, yellow brown as well as sticky, and brown as well as sticky, respectively. The percentage of yield was also different. For CME, CDE, and CHE of *A. mellifera*'s propolis were 25.0, 1.47, and 0.82, respectively (19).

The antiproliferative activity against 5 cancer cell lines like BT474, Chago, Hep-G2, KATO-III, and SW620 was determined by MTT assay which was described in Santos *et al.* (65), Hernandez *et al.* (66), Najafi *et al.* (67), Umthong *et al.* (18) and Teerasripreecha *et al.* (19). The result showed that reversed crude dichloromethane extract (ReCDE) had the overview best activity against 5 cancer cell lines at the IC₅₀ value range of 0.56 – 5.25 µg/mL. CDE also had the good activity at the IC₅₀ value range of 0.55 – 5.04 µg/mL. The IC₅₀ value of reCDE was lower than the IC₅₀ value of CDE from *A. mellifera*'s propolis (43.8 – 53.5 µg/mL for 5 cancer cell lines) (19). Thus, at the crude level, it seemed to be that cerumen was more potential than propolis in term of antiproliferative activity.

Not only CDE of cerumen which was composed of plant resin as a main compound could have the antiproliferative activity, but CDE of other plants was also reported to be active.

In 2006, Kohn *et al.* (76) reported that CDE of *Aspidosperma tomentosum* that was one of Brazillian plants had the antiproliferative activity against 5 cancer cell lines like K562 (leukemia), UACC62 (melanoma), NCI460 (lung cancer), NCI-ADR (drug resistant breast cancer), and MCF-7 (breast cancer). When those cell lines were treated by this extract at 125 µg/mL for 48 h, the growth percentage of K562, UACC 62, NCI460, NCI-ADR, and MCF-7 were 70%, 6%, 2%, -1, and -46%, respectively. Furthermore, when these cell lines were treated by crude 70% ethanol extract for 48 h, the growth percentage of K562, NCI460, NCI-ADR, UACC62, and MCF-7 were 97%, 31%, 19%, 13%, and -18%, respectively.

In 2012, Marchetti *et al.* (77) reported that CDE of *Calea pinnatifida* in Brazil had the antiproliferative activity against 9 cancer cell lines with the IC₅₀ value range of 8.41 - 228.58 µg/mL. This extract was found to be better than crude ethanol extract

in inhibiting the growth of HT-40 cell line with the IC_{50} value of 80.0 $\mu\text{g/mL}$. Nonetheless, other 8 cell lines were not sensitive to this extract at all.

Here, reCDE was purified due to the yield and activity. After silica gel 60G chromatography, it seemed to be that mobile phase and eluting solvents played the major role for the antiproliferative activity. Considering the results as in table 4.4, the pattern of compositions in initial fractions (compositions I-IV, waxy form) could be identified when pure dichloromethane was used as mobile phase in TLC. However, after they were eluted from silica gel column by using the mixed solvents of high percentage of hexane and low percentage of ethyl acetate, the obtained fractions were not active at all.

As the second type, middle fractions (compositions V-XIII) had oily form. The pattern of compositions could be identified when the mixed solvents of 97: 3, 95: 5 of dichloromethane per methanol were used as mobile phase. It showed that the compositions were medium in polarity because they could be eluted from silica gel column by using the mixed solvents of lower percentage of hexane and 100% ethyl acetate. The activity result of various compositions was varied from low to high.

As the last type, remaining fractions (compositions XIV-XVI) contained remaining sediments, solid or pigment form. The composition pattern could be identified when the mixed solvents of 90: 10 of dichloromethane per methanol was used as mobile phase. Although these fractions could be eluted from silica gel column by using the mixed mobile phase of ethyl acetate and methanol or pure methanol, no activity or very low activity was revealed.

The most interesting fractions were fraction VII and VIII because molybdated dipped TLC of these fractions showed a big yellow spot while other parts showed blue or purple patterns (Table 4.4 and appendix D).

After those 16 fractions were tested against 5 cancer cell lines by MTT assay, fraction VII, VIII, and XI had high activity and high yield, especially fraction VII (IC_{50} value of 3.38 – 6.45 $\mu\text{g/mL}$, 379 mg) and fraction VIII (IC_{50} value of 5.37 – 6.46 $\mu\text{g/mL}$, 304 mg). However, IC_{50} values of these fractions were higher than IC_{50} values of ReCDE. It could be observed that, in this case, crude extracts was better than partially purified form.

In 2005, Al Waili (8) reported that the mixture of honey, beeswax, and olive oil in the ratio of 1: 1: 1 (v/v) from United Arab Emirates had antimicrobial activity against *Staphylococcus aureus* and *Candida albicans*. Comparing to only one bee

product, honey was potential to inhibit the growth of both microorganisms, but not beeswax or olive oil.

After fractions VII and VIII were further purified by chromatography by silica gel 60G to give 10 and 9 fractions respectively. They were also different in yield, mass, and appearance (Tables 4.7 and 4.8). The most interesting combined fractions were in subfractions F7E and F8D because the pattern on TLC of these compositions was very yellow and single with various forms such as powder, oil, or crystal. In contrast, a lot of thick patterns were observed on TLC of subfractions F7F and F8E. It represented that there were a lot of compositions which could not be separated.

In order to get a pure bioactive compound, a bioactive combined fraction was purified three times by column chromatography. After it was assayed for the antiproliferative activity, a pure fraction F7F-3 had the highest activity against 5 cancer cell lines with the IC_{50} value range of 0.36 – 0.92 $\mu\text{g/mL}$ (Tables 4.12 and 4.16).

The activity of fraction F7F-3 as a newly found compound in cerumen was compared to the activity of doxorubicin and 5-fluorouracil, present chemotherapeutic drugs. The result showed that 5-fluorouracil could not inhibit the growth of BT474, Hep-G₂, and KATO-III. In this research, 5-fluorouracil could inhibit the growth of SW620 with the IC_{50} value of 5.69 $\mu\text{g/mL}$. The value was quite different from Sharma and Smith (78) which reported that the IC_{50} value of 5-FU for SW620 was only 4 $\mu\text{g/mL}$. The difference was possible that there were variation among cell lines. Alternatively, SW620 cell line used in this research had been subcultured for too many times. Thus, it was possible that the cell line was very weak and could be resistant to the drug. New isolation of SW620 cell line from a patient should be in concerned. For many years already, resistant cancer cell lines had become a severe problem for treatment.

For example, Zhong et al. (79) reported breast cancer cell line (MCF-7) which was resistant to 2 chemotherapeutic drugs which were adriamycin (IC_{50} value of 403.56 $\mu\text{g/mL}$) and docetaxel (IC_{50} value of 68.31 $\mu\text{g/mL}$). In contrast, non-resistant MCF-7 cell line was sensitive to adriamycin with the IC_{50} value of 0.66 $\mu\text{g/mL}$ and docetaxel with the IC_{50} value of 3.08 $\mu\text{g/mL}$. However, resistant cell lines were differently sensitive to 2 types of mi-RNA (microRNA) which were miR-122 and miR-29a. For adriamycin resistant cell lines treated by miR-122 and miR-29a had the IC_{50} values of 295.01 and 282.34 $\mu\text{g/mL}$, respectively. Nonetheless, docetaxel resistant cell lines treated by miR-122 and miR-29a had the IC_{50} values of 20.000 and 29.667 $\mu\text{g/mL}$, respectively. After protein was analysed by western blot, it revealed that resistant cell lines treated by both types of miRNA had more expression of tumor

suppressor protein or PTEN (Phosphate and Tensin homolog protein) than untreated resistant cell lines. From this research, it was possible that some types of resistant cancer cell lines could be alternatively treated.

According to tables 4.16 and 4.18, the IC_{50} values in $\mu\text{mol/L}$ of fraction F7F-3 for BT474, Chago, Hep-G₂, KATO-III and SW620 were 1.22, 2.25, 0.94, 0.88 and 1.50 $\mu\text{mol/L}$, respectively while the IC_{50} values in $\mu\text{mol/L}$ of doxorubicin for BT474, Chago, Hep-G₂, KATO-III and SW620 were 0.77, 0.65, 0.59, 1.03 and 0.12 $\mu\text{mol/L}$, respectively. It obviously showed that fraction F7F-3 had almost the similar potential to doxorubicin in some cancer cell lines. In the future, fraction F7F-3 may be applied to those cancer cell lines resistant to doxorubicin and 5-fluorouracil. Alternatively, if the cost of producing fraction F7F-3 is cheaper than synthesizing both doxorubicin and 5-fluorouracil, this fraction will be more challenging in drug development. Fortunately, after this fraction was tested on normal fibroblast cell line (CRL-1947 as control), low or no cytotoxicity was revealed (Table 4.15).

A bioactive compound, isolated from fractions F7E, F7F-3, and F8E-5, was analyzed to be alpha-mangostin (Figure 4.19). It was the main xanthone in mangosteen. This compound was reported to have a lot of medical and pharmaceutical bioactivities such as antioxidant, antimicrobial, anti-inflammatory, and anticancer activities (70).

From NMR spectroscopic data, the result of ^1H and ^{13}C correlation in HMBC was presented in table 4.17 and figure 4.20. Proton at carbon position 4 (δ_{H} 6.29) has a correlation with carbon position 2, 3, 4a and 9a (δ_{C} 108.6, 161.7, 155.2 and 103.8). Proton at position 5 (δ_{H} 6.83) has a correlation with position 7, 8a and 10a (δ_{C} 142.7, 112.4 and 154.7). 2 protons at position 11 (δ_{H} 4.09) have a correlation with position 7, 8, 8a, 12 and 13 (δ_{C} 142.7, 137.2, 112.4, 123.3 and 132.2). Proton at carbon position 12 (δ_{H} 5.28) has own correlation with position 12 (δ_{C} 123.3). Methyl protons at position 14 (δ_{H} 1.77) have a correlation with position 12, 13 and 15 (δ_{C} 123.3, 132.2 and 16.9). Methyl protons at position 15 (δ_{H} 1.83) have a correlation with position 12, 13, 14 (δ_{C} 123.3, 132.2 and 18.3). 2 protons at position 16 (δ_{H} 3.45) have a correlation with position 1, 2, 3, 17 and 18 (δ_{C} 160.8, 108.6, 161.7, 121.6 and 133.8). Proton at carbon position 17 (δ_{H} 5.28) has own correlation with position 12 (δ_{C} 121.6). Methyl protons at position 19 (δ_{H} 1.69) have a correlation with position 17, 18 and 20 (δ_{C} 121.6, 133.8 and 18.0). Methyl protons at position 20 (δ_{H} 1.84) have correlation with position 17, 18 and 19 (δ_{C} 121.6, 133.8 and 20.9). Methoxy protons (δ_{H} 3.81) have a correlation with position 7 (δ_{C} 66.2). Lastly, hydroxyl proton (δ_{H} 13.79) has a correlation with carbon

position 1, 2 and 9a (160.8, 108.6 and 103.8). All of correlation positions would be designed to compound structure of alpha-mangostin. When comparing with alpha-mangostin spectrum from Ghazali *et al.* (1) in table 4.17. ^1H and ^{13}C spectrum peak have closely of this research F7F-3 compound. It's showed that F7F-3 is alpha-mangostin.a

It was very reasonable to explain why cerumen had this compound. Considering the sampling site, there were plenty of mangosteen trees. They could be a source of plant resin for bees to produce propolis and cerumen. Stingless bee could collect resin from pericarp of mangosteen.

According to table 4.16, the IC_{50} value of fraction F7F-3 against SW620 cell line was $0.62 \pm 0.16 \mu\text{g/mL}$ but in 2011, Watanapokasin *et al.* (80) reported alpha-mangostin from pericarp of mangosteen in Chantaburi had the antiproliferative activity against SW620 with the IC_{50} value of $19.60 \pm 1.53 \mu\text{g/mL}$. This controversial data should be studied for the difference. However, variation in cell line should be in concerned.

Besides the IC_{50} values, the change in morphology of cancer cell lines treated with alpha-mangostin (fraction F7F-3) at its IC_{50} value was performed. The shape of cell, nucleus and organelle condensation, cell shrinking, and cell floating were parameters used to observe here. For some treated cell lines after 72 h incubation, a lot of debris and low cell density could be observed, too. According to figures 4.14-4.18, it could present that alpha-mangostin caused the cell death of those cancer cell lines by apoptosis.

There were some reports supporting that alpha-mangostin could induce the apoptosis of cells.

In 2002, Matsumoto *et al.* (81) reported that alpha-mangostin from pericarp of mangosteen in Indonesia had the antiproliferative activity against human leukemia cell line (HL60) with the IC_{50} value of $6.8 \mu\text{g/mL}$. In addition, after other cell lines such as K562, NB4 and U937 were treated with $10 \mu\text{g/mL}$ of alpha-mangostin, the cell number decreased, the nucleosomal DNA was fragmented, the amount of caspase-3 protein activated from procaspase-3 increased.

In 2011, Watanapokasin *et al.* (80) purposed the mechanism on how alpha-mangostin from pericarp of mangosteen in Chantaburi could induce apoptosis in 3 colorectal cancer cell lines which were COLO205, MIP-101, and SW620. It showed that the cell cycle of those cell lines treated with $20 \mu\text{g/mL}$ of alpha-mangostin would be

arrested before G1 checkpoint. The fragmentation of DNA was occurred. The amount of apoptotic proteins such as Bax, p53, FAS, cytochrome C increased. The caspase-3, caspase-8, and caspase-9 activation rate also increased. It was found that alpha-mangostin could promote the activation of procaspase-8 from extrinsic pathway to induce of apoptosis process.

In this research, cancer cell lines that treated with alpha-mangostin have an apoptotic character. However, for supporting this hypothesis in future. Treated cancer cell line must have a step of flow cytometer to check the cell cycle process and western blot for analyzed apoptotic protein that has any expression and activation or not.

From the above, it could concluded that alpha-mangostin in cerumen of *T. laeviceps* from Chantaburi province could inhibit the growth of cancer cells. It can be a new and alternative source for an alpha-mangostin. However, further experiments must be designed. A mechanism on how it can control the antiproliferative activity must be discovered.

Chapter VI

Conclusions

T. laeviceps cerumen extracted from 2 methods revealed that CME, CDE, and CHE from the first method had a yield percentage at 4.858, 51.997, and 23.459, respectively and reCHE, reCDE, and reCHE from the second method had a yield percentage at 9.280, 30.100, and 43.370, respectively. The result of antiproliferative activity against 5 cancer cell line by MTT assay showed that reCDE had the best activity in the IC_{50} range at 0.56 – 5.24 $\mu\text{g/mL}$. Then, reCDE was purified by silica gel 60G (0.040-0.063 μm) column chromatography in a glass column (5 cm diameter x 50 cm height with 500 mL bulb). It gave 16 different fractions (I-XVI) which were different in mass and yield. All fractions were tested for the antiproliferative activity. The result showed that fractions VII and VIII had the best antiproliferative activity against 5 cancer cell lines in the IC_{50} range of 3.38 – 6.46 $\mu\text{g/mL}$ and 5.36 – 6.60 $\mu\text{g/mL}$, respectively. Both fractions were further purified by silica gel 60G (0.040-0.063 μm) column chromatography in a glass column (3 cm diameter and 60 cm height with 140 mL bulb). Both fractions gave 19 subfractions in total. All subfractions were tested for the antiproliferative activity. The result showed that subfractions F7E, F7F, and F8E had the antiproliferative activity against 5 cancer cell lines in the IC_{50} range of 0.88 – 1.64 $\mu\text{g/mL}$, 0.95 – 1.71 $\mu\text{g/mL}$, and 3.96 – 6.28 $\mu\text{g/mL}$, respectively. Subfractions F7F and F8E still had a lot of compositions so both subfractions were further purified by silica gel 60G (0.040-0.063 μm) column chromatography in a glass column (2.5 cm diameter and 50 cm height with 100 mL bulb). Both subfractions gave 26 compositions in total. All compositions were tested for the antiproliferative activity. The result showed that F7F-3 and F8E-5 had the good antiproliferative activity against 5 cancer cell lines in the IC_{50} range of 0.36 – 0.92 $\mu\text{g/mL}$ and 1.74 – 3.88 $\mu\text{g/mL}$, respectively. Furthermore, doxorubicin, the recent chemotherapeutic drug, had the antiproliferative activity against 5 cancer cell lines in the IC_{50} range of 0.07 – 0.56 $\mu\text{g/mL}$ while, 5-fluorouracil, other recent chemotherapeutic drug, had the antiproliferative activity against Chago and SW620 with the IC_{50} values of 0.38 and 5.69 $\mu\text{g/mL}$. However, BT474, Hep-G₂, and KATO-III were not sensitive to 5-fluorouracil. Bioactive fractions and chemotherapeutic drugs were tested for cytotoxicity with CRL-1943 (fibroblast cell). The result showed that F7F-3 and F7E showed cytotoxic activity against CRL-1943 (fibroblast cell) with the IC_{50} values of 4.56 and 9.01 $\mu\text{g/mL}$ respectively. In contrast, F8E-5 had no cytotoxicity to fibroblast cells. Also, doxorubicin

and 5-fluorouracil had no cytotoxicity to fibroblast cells. Among F7F-3, F7F, and F8E-5, F7F-3 had the best antiproliferative activity against cancer cell lines. Thus, F7F-3 was tested for morphology change of 5 cancer cell lines after they were treated by using concentration IC_{50} values. The result showed that all cell lines had a hypertonic condition. Organelle and nucleus were shrinkage so it made the amount of cytoplasm looked increased. Cell looked round but not broken. Some cells remained like debris. In overall, it showed the event of apoptosis. Subfraction F7E, F7F-3, and F8E-5 were analyzed by 1H NMR spectroscopy. The result showed that 3 bioactive compounds had the similar 1H NMR pattern. Subfraction F7F-3 was the most bioactive compound and gave the most obvious cell death morphology. When it was analyzed by 1-dimensional and 2-dimensional NMR spectroscopy, HSQC, HMBC, and COSY, subfraction F7F-3 was identified as alpha-mangostin the major bioactive compound of pericarp of *Garcinia mangostana* or mangosteen fruit. The suggestion from this research for further step in future is cancer cell line treated with alpha-mangostin will be confirmed for apoptosis by flow cytometry and western blot. At last, in *T. laeviceps* cerumen is a new choice for alpha-mangostin source for developing an effective anti-cancer drug in the future.

REFERENCES

1. Ghazali, M.S.I.A.S., Lian, C.E.G. and Ghani, A.D.K. 2010. Chemical constituent from roots of *Garcinia Mangostana* (Linn.). *International Journal of Chemistry* **2**:134-142.
2. Sakagami, S. and Inoue, T. 1985. Taxonomic Notes on Three Bicolored Tetragonula Stingless Bees in Southeast Asia. *Japanese Journal of Entomology* **53**:174-189.
3. Klakasikorn, A., Wongsiri, S., Deowanish, S. and Duangphakdee, O. 2005. New record of stingless bees (Meliponini: *Trigona*) in Thailand. *The Natural History Journal of Chulalongkorn University* **5**:1-7.
4. Chinh, T.X., Sommeijer, M.J., Boot, W.J. and Michener, C.D. 2005. Nest and Colony Characteristics of Three Stingless Bee Species in Vietnam with the First Description of the Nest of *Lisotrigona carpenteri* (Hymenoptera: Apidae: Meliponini). *Journal of the Kansas Entomological Society* **78**:363-372.
5. Massaro, F.C., Brooks, P.R., Wallace, H.M. and Russell, F.D. 2011. Cerumen of Australian stingless bees (*Tetragonula carbonaria*): gas chromatography-mass spectrometry fingerprints and potential anti-inflammatory properties. *Die Naturwissenschaften* **98**:329-337.
6. Roubik, D.W. 2006. Stingless bee nesting biology. *Apidologie* **37**:124-143.
7. Nolkemper, S., Reichling, J., Sensch, K.H. and Schnitzler, P. 2010. Mechanism of herpes simplex virus type 2 suppression by propolis extracts. *Phytomedicine : International Journal of Phytotherapy and Phytopharmacology* **17**:132-138.
8. Al-Waili, N.S. 2005. Mixture of Honey, Beeswax and olive oil Inhibits growth of *Staphylococcus aureus* and *Candida albicans*. *Archives of Medical Research* **36**:10-13.
9. Voidarou, C., Alexopoulos, A., Plessas, S., Karapanou, A., Mantzourani, I., Stavropoulou, E., Fotou, K., Tzora, A., Skoufos, I. and Bezirtzoglou, E. 2011. Antibacterial activity of different honeys against pathogenic bacteria. *Anaerobe* **17**:375-379.
10. Choudhari, M.K., Punekar, S.A., Ranade, R.V. and Paknikar, K.M. 2012. Antimicrobial activity of stingless bee (*Trigona* sp.) propolis used in the folk medicine of Western Maharashtra, India. *Journal of Ethnopharmacology* **141**:363-367.
11. Boonsai, P., Phuwapraisirisan, P. and Chanchao, C. 2014. Antibacterial Activity of a Cardanol from Thai *Apis mellifera* Propolis. *International Journal of Medical Sciences* **11**:327-336.
12. Saric, A., Balog, T., Sobocanec, S., Kusic, B., Sverko, V., Rusak, G., Likic, S., Bubalo, D., Pinto, B., Reali, D. and Marotti, T. 2009. Antioxidant effects of flavonoid from Croatian *Cystus incanus* L. rich bee pollen. *Food and Chemical Toxicology* **47**:547-554.

13. **Morais, M., Moreira, L., Feas, X. and Estevinho, L.M.** 2011. Honeybee-collected pollen from five Portuguese Natural Parks: palynological origin, phenolic content, antioxidant properties and antimicrobial activity. *Food and Chemical Toxicology* **49**:1096-1101.
14. **Saad Rached, I.C., Castro, F.M., Guzzo, M.L. and de Mello, S.B.** 2010. Anti-inflammatory effect of bee venom on antigen-induced arthritis in rabbits: influence of endogenous glucocorticoids. *Journal of Ethnopharmacology* **130**:175-178.
15. **Maruyama, H., Sakamoto, T., Araki, Y. and Hara H.** 2010. Anti-inflammatory effect of bee pollen ethanol extract from *Cistus* sp. of Spanish on carrageenan-induced rat hind paw edema. *BMC Complementary and Alternative Medicine* **10**:1-11.
16. **Kas'ianenko, V.I., Komisarenko, I.A., Dubtsova, E.A.** 2011. [Correction of atherogenic dyslipidemia with honey, pollen and bee bread in patients with different body mass]. *Terapevticheskii Arkhiv* **83**:58-62.
17. **Jo, M., Park, M.H., Kollipara, P.S., An, B.J., Song, H.S., Han, S.B., Kim, J.H., Song, M.J. and Hong, J.T.** 2012. Anti-cancer effect of bee venom toxin and melittin in ovarian cancer cells through induction of death receptors and inhibition of JAK2/STAT3 pathway. *Toxicology and Applied Pharmacology* **258**:72-81.
18. **Umthong, S., Phuwapraisirisan, P., Puthong, S. and Chanchao, C.** 2011. In vitro antiproliferative activity of partially purified *Trigona laeviceps* propolis from Thailand on human cancer cell lines. *BMC Complementary and Alternative Medicine* **11**:37.
19. **Teerasripreecha, D., Phuwapraisirisan, P., Puthong, S., Kimura, K., Okuyama, M., Mori, H., Kimura, A. and Chanchao, C.** 2012. In vitro antiproliferative/cytotoxic activity on cancer cell lines of a cardanol and a cardol enriched from Thai *Apis mellifera* propolis. *BMC Complementary and Alternative Medicine* **12**:1-17.
20. **Uzel, A., Sorkun, K.Y., Önçağ, Ö., Çoğulu, D., Gençay, Ö. and Salıh, Br.** 2005. Chemical compositions and antimicrobial activities of four different Anatolian propolis samples. *Microbiological Research* **160**:189-195.
21. **Kanwar, J.R., Mahidhara, G. and Kanwar, R.K.** 2011. Antiangiogenic therapy using nanotechnological-based delivery system. *Drug Discovery Today* **16**:188-202.
22. **Michener, D.C.** 2007. *The Bees of the World* 2nd edition. the John Hopkins University Press, Maryland.
23. **Kwapoong, P., Aidoo, K., Combey, R. and Karikari, A.** 2010. *Stingless bees: importance, management and utilization, a training manual for stingless beekeeping.* Unimax MacMillan, Accra, Ghana.

24. Rattanawanee, A. and Chanchao, C. 2011. Bee Diversity in Thailand and the Applications of Bee Products., 133-162, Changing Diversity in Changing Environment. Intech, Vienna.
25. Sakagami, F.S. and Inoue, T. 1987. Stingless bees of the genus *Trigona* (subgenus *Trigonella*) with notes on the reduction of spatha in male genitalia of the subgenus *Tetragonula* (Hymenoptera, Apidae). *Japanese Journal of Entomology* **55**:610-627.
26. Sakagami, S., Inoue, T., Yamane, S. and Salmah, S. 1983. Nest Architecture and Colony Composition of the Sumatran Stingless Bee *Trigona (Tetragonula) laeviceps*. *Japanese Journal of Entomology* **51**:100-111.
27. Wille, A. and Michener, D.C. 1973. The nest architecture of stingless bees with special reference to those of Costa Rica. *Revista de Biologia Tropical* **21**:1-279.
28. Shahzad, A. and Cohrs, R.J. 2012. In vitro antiviral activity of honey against varicella zoster virus (VZV): A translational medicine study for potential remedy for shingles. *Translational Biomedicine* **3**: 1-9.
29. Nemoseck, T.M., Carmody, E.G., Furchner-Evanson, A., Gleason, M., Li, A., Potter, H., Rezende, L.M., Lane, K.J. and Kern M. 2011. Honey promotes lower weight gain, adiposity, and triglycerides than sucrose in rats. *Nutrition Research* (New York, N.Y.) **31**:55-60.
30. Steiner, L.F. and Summerland, S.A. 1943. Xanthone as an ovicide and larvicide for the codling moth. *Journal of Economic Entomology* **36**:435-439.
31. Negi, J.S., Bisht, V.K., Singh, P., Rawat, M.S.M. and Joshi, G.P. 2013. Naturally Occurring Xanthenes: Chemistry and Biology. *Journal of Applied Chemistry* **2013**:1-9.
32. Mahabusarakam, W., Wiriyachitra, P., Taylor, W.C. 1987. Chemical Constituents of *Garcinia mangostana*. *Journal of Natural Products* **50**:474-478.
33. Suksamrarn, S., Komutiban, O., Ratananukul, P., Chimnoi, N., Lartpornmatulee, N. and Suksamrarn, A. 2006. Cytotoxic prenylated xanthenes from the young fruit of *Garcinia mangostana*. *Chemical & pharmaceutical bulletin* **54**:301-305.
34. Nilar, Harrison, L.J. 2002. Xanthenes from the heartwood of *Garcinia mangostana*. *Phytochemistry* **60**:541-548.
35. Sundaram, B.M., Gopalakrishnan, C., Subramanian, S., Shankaranarayanan, D. and Kameswaran, L. 1983. Antimicrobial activities of *Garcinia mangostana*. *Planta Medica* **48**:59-60.
36. Suksamrarn, S., Suwannapoch, N., Phakhodee, W., Thanuhiranlert, J., Ratananukul, P., Chimnoi, N. and Suksamrarn, A. 2003. Antimycobacterial activity of prenylated xanthenes from the fruits of *Garcinia mangostana*. *Chemical & Pharmaceutical Bulletin* **51**:857-859.

37. **Chen, L.G., Yang, L.L., Wang, C.C.** 2008. Anti-inflammatory activity of mangostins from *Garcinia mangostana*. *Food and Chemical Toxicology* **46**:688-693.
38. **Matsumoto, K., Akao, Y., Ohguchi, K., Ito, T., Tanaka, T., Inuma and M., Nozawa, Y.** 2005. Xanthenes induce cell-cycle arrest and apoptosis in human colon cancer DLD-1 cells. *Bioorganic & Medicinal Chemistry* **13**:6064-6069.
39. **Ho, C.K., Huang, Y.L. and Chen, C.C.** 2002. Garcinone E, a xanthone derivative, has potent cytotoxic effect against hepatocellular carcinoma cell lines. *Planta Medica* **68**:975-979.
40. **Liu, Z., Antalek, M., Nguyen, L., Li, X., Tian, X., Le, A. and Zi, X.** 2013. The effect of gartanin, a naturally occurring xanthone in mangosteen juice, on the mTOR pathway, autophagy, apoptosis, and the growth of human urinary bladder cancer cell lines. *Nutrition and Cancer* **65 Suppl 1**:68-77.
41. **Sakai, S.I., Katsura, M., Takayama, H., Aimi, N., Chokethaworn, N. and Suttajit, M.** 1993. The Structure of Garcinone E. *Chemical & Pharmaceutical Bulletin* **41**:958-960.
42. **National Cancer Institute.** 2011. Hospital-based cancer registry. Union Ultraviolet Ltd, Bangkok.
43. **(World Health Organization) WHO** 2012, posting date. GLOBOCAN 2012: Estimated Cancer Incidence Mortality and Prevalence Worldwide in 2012. . http://globocan.iarc.fr/Pages/fact_sheets_cancer.aspx. . [Online.]
44. **Alberts, B., Johnson, A., Lewis, J., Raff, M., Roberts, K. and Walter, P.** 2008. Chapter 18 Apoptosis: Programmed Cell Death Eliminates Unwanted Cells, 1115-1129, *Molecular Biology of the Cell*, Garland Science, New York.
45. **Jacobson, M.D., Weil, M. and Raff, M.C.** 1997. Programmed cell death in animal development. *Cell* **88**:347-354.
46. **Nagata, S.** 2005. DNA degradation in development and programmed cell death. *Annual Review of Immunology* **23**:853-875.
47. **Galonek, H.L. and Hardwick, J.M.** 2006. Upgrading the BCL-2 network. *Nature Cell Biology* **8**:1317-1319.
48. **Jiang, X. and Wang, X.** 2004. Cytochrome C-mediated apoptosis. *Annual Review of biochemistry* **73**:87-106.
49. **Lowe, S.W., Cepero, E. and Evan, G.** 2004. Intrinsic tumour suppression. *Nature* **432**:307-315.
50. **Lavrik, I., Golks, A. and Krammer, P.H.** 2005. Death receptor signaling. *Journal of Cell Science* **118**:265-267.
51. **Boatright, K.M. and Salvesen, G.S.** 2003. Mechanisms of caspase activation. *Current Opinion in Cell Biology* **15**:725-731.

52. Kumar, S. 2007. Caspase function in programmed cell death. *Cell Death and Differentiation* **14**:32-43.
53. Gerhardt, H., Golding, M., Fruttiger, M., Ruhrberg, C., Lundkvist, A., Abramsson, A., Jeltsch, M., Mitchell, C., Alitalo, K., Shima, D. and Betsholtz, C. 2003. VEGF guides angiogenic sprouting utilizing endothelial tip cell filopodia. *The Journal of Cell Biology* **161**:1163-1177.
54. Malik, S., Cusidó, R.M., Mirjalili, M.H., Moyano, E., Palazón, J. and Bonfill, M. 2011. Production of the anticancer drug taxol in *Taxus baccata* suspension cultures: A review. *Process Biochemistry* **46**:23-34.
55. Nicolaou, K.C., Yang, Z., Liu, J.J., Ueno, H., Nantermet, P.G., Guy, R.K., Claiborne, C.F., Renaud, J., Couladouros, E.A. and Paulvannan, K., et al. 1994. Total synthesis of taxol. *Nature* **367**:630-634.
56. Holton, R.A., Kim, H.B., Somoza, C., Liang, F., Biediger, R.J., Boatman, P.D., Shindo, M., Smith, C.C. and Kim, S. 1994. First total synthesis of taxol. 2. Completion of the C and D rings. *Journal of the American Chemical Society* **116**:1599-1600.
57. Holton, R.A., Somoza, C., Kim, H.B., Liang, F., Biediger, R.J., Boatman, P.D., Shindo, M., Smith, C.C. and Kim, S. 1994. First total synthesis of taxol. 1. Functionalization of the B ring. *Journal of the American Chemical Society* **116**:1597-1598.
58. Noordhuis, P., Holwerda, U., Van der Wilt, C.L., Van Groeningen, C.J., Smid, K., Meijer, S., Pinedo, H.M. and Peters, G.J. 2004. 5-Fluorouracil incorporation into RNA and DNA in relation to thymidylate synthase inhibition of human colorectal cancers. *Annals of Oncology* **15**:1025-1032.
59. Momparler, R.L., Karon, M., Siegel, S.E. and Avila, F. 1976. Effect of adriamycin on DNA, RNA, and protein synthesis in cell-free systems and intact cells. *Cancer Research* **36**:2891-2895.
60. Rein, D.T., Breidenbach, M. and Curiel, D.T. 2006. Current developments in adenovirus-based cancer gene therapy. *Future oncology* (London, England) **2**:137-143.
61. Aagaard, L. and Rossi, J.J. 2007. RNAi therapeutics: principles, prospects and challenges. *Advanced Drug Delivery Reviews* **59**:75-86.
62. Alexis, F., Pridgen, E.M., Langer, R. and Farokhzad, O.C. 2010. Nanoparticle technologies for cancer therapy. *Handbook of Experimental Pharmacology* **197**:55-86.
63. Kalishwaralal, K., Sheikpranbabu, S., BarathManiKanth, S., Haribalaganesh, R., RamkumarPandian, S. and Gurunathan, S. 2011. Gold nanoparticles inhibit vascular endothelial growth factor-induced angiogenesis and vascular permeability via Src dependent pathway in retinal endothelial cells. *Angiogenesis* **14**:29-45.

64. Gaspar, V.M., Correia, I.J., Sousa, Â., Silva, F., Paquete, C.M., Queiroz, J.A. and Sousa, F. 2011. Nanoparticle mediated delivery of pure P53 supercoiled plasmid DNA for gene therapy. *Journal of Controlled Release* **156**:212-222.
65. Santos, F.A., Bastos, E.M., Uzeda, M., Carvalho, M.A., Farias, L.M., Moreira, E.S., Braga, F.C. 2002. Antibacterial activity of Brazilian propolis and fractions against oral anaerobic bacteria. *Journal of Ethnopharmacology* **80**:1-7.
66. Hernandez, J., Goycoolea, F.M., Quintero, J., Acosta, A., Castaneda, M., Dominguez, Z., Robles, R., Vazquez-Moreno, L., Velazquez, E.F., Astiazaran, H., Lugo, E. and Velazquez C. 2007. Sonoran propolis: chemical composition and antiproliferative activity on cancer cell lines. *Planta Medica* **73**:1469-1474.
67. Najafi, M.F., Vahedy, F., Seyyedini, M., Jomehzadeh, H.R. and Bozary, K. 2007. Effect of the water extracts of propolis on stimulation and inhibition of different cells. *Cytotechnology* **54**:49-56.
68. Yu, L., Zhao, M., Yang, B., Zhao, Q. and Jiang, Y. 2007. Phenolics from hull of *Garcinia mangostana* fruit and their antioxidant activities. *Food Chemistry* **104**:176-181.
69. Al-Massarani, S., El Gamal, A., Al-Musayeib, N., Mothana, R., Basudan, O., Al-Rehaily, A., Farag, M., Assaf, M., El Tahir, K. and Maes, L. 2013. Phytochemical, Antimicrobial and Antiprotozoal Evaluation of *Garcinia Mangostana* Pericarp and α -Mangostin, Its Major Xanthone Derivative. *Molecules* **18**:10599-10608.
70. Pedraza-Chaverri, J., Cárdenas-Rodríguez, N., Orozco-Ibarra, M. and Pérez-Rojas, J.M. 2008. Medicinal properties of mangosteen (*Garcinia mangostana*). *Food and Chemical Toxicology* **46**:3227-3239.
71. Teixeira, E.W., Negri, G., Meira, R.M., Message, D. and Salatino, A. 2005. Plant Origin of Green Propolis: Bee Behavior, Plant Anatomy and Chemistry. *Evidence-based Complementary and Alternative Medicine : eCAM* **2**:85-92.
72. Hatano, A., Nonaka, T., Yoshino, M., Ahn, M.R., Tazawa, S., Araki, Y. and Kumazawa, S. 2012. Antioxidant Activity and Phenolic Constituents of Red Propolis from Shandong, China. *Food Science and Technology Research* **18**:577-584.
73. Dausch, A., Moraes, C.S., Fort, P. and Park, Y.K. 2008. Brazilian red propolis--chemical composition and botanical origin. *Evidence-based Complementary and Alternative Medicine : eCAM* **5**:435-441.
74. Shimomura, K., Inui, S., Sugiyama, Y., Kurosawa, M., Nakamura, J., Choi, S.J., Ahn, M.R. and Kumazawa, S. 2012. Identification of the plant origin of propolis from Jeju Island, Korea, by observation of honeybee behavior and phytochemical analysis. *Bioscience, Biotechnology, and Biochemistry* **76**:2135-2138.

75. Aspé, E. and Fernández, K. 2011. The effect of different extraction techniques on extraction yield, total phenolic, and anti-radical capacity of extracts from *Pinus radiata* Bark. *Industrial Crops and Products* **34**:838-844.
76. Kohn, H.K., Pizao, P.K., Foglio, M.A., Antonio, M.A., Amaral, M.C.E., Bittric, V. and Carvalho, J.E. 2006. Antiproliferative activity of crude extract and fractions obtained from *Aspidosperma tomentosum* Mart. *A Revista Brasileira de Plantas Medicinai* **8**:110-115.
77. Marchetti, M.G., Silva, A.K., Santos, N.A., Sousa, O.M.I., Tinti, V.S., Figueira, M.G., Foglio, A.M. and Carvalho, E.J. 2012. The anticancer activity of dichloromethane crude extract obtained from *Calea pinnatifida*. *Journal of Experimental Pharmacology* **4**:157-162.
78. Sharma, R.I. and Smith, T.A. 2008. Colorectal tumor cells treated with 5-FU, oxaliplatin, irinotecan, and cetuximab exhibit changes in 18F-FDG incorporation corresponding to hexokinase activity and glucose transport. *Journal of Nuclear Medicine : official publication, Society of Nuclear Medicine* **49**:1386-1394.
79. Zhong, S., Li, W., Chen, Z., Xu, J. and Zhao, J. 2013. MiR-222 and miR-29a contribute to the drug-resistance of breast cancer cells. *Gene* **531**:8-14.
80. Watanapokasin, R., Jarinthanan, F., Nakamura, Y., Sawasjirakij, N., Jaratrungtawee, A. and Suksamrarn, S. 2011. Effects of alpha-mangostin on apoptosis induction of human colon cancer. *World Journal of Gastroenterology* **17**:2086-2095.
81. Matsumoto, K., Akao, Y., Kobayashi, E., Ohguchi, K., Ito, T., Tanaka, T., Iinuma, M. and Nozawa, Y. 2003. Induction of apoptosis by xanthones from mangosteen in human leukemia cell lines. *Journal of Natural Product* **66**:1124-1127.



APPENDICES

จุฬาลงกรณ์มหาวิทยาลัย
CHULALONGKORN UNIVERSITY

Appendix A

Absorbance value at 540 nm of different cancer cell lines treated with crude extracts of *T. laeviceps*'s cerumen

	CME (µg/mL)				ReCME (µg/mL)				CDE (µg/mL)				ReCDE (µg/mL)				CHE (µg/mL)				ReCHE (µg/mL)			
	Ctrl	100	1000	10000	Ctrl	100	1000	10000	Ctrl	100	1000	10000	Ctrl	100	1000	10000	Ctrl	100	1000	10000	Ctrl	100	1000	10000
BT474	0.376	0.386	0.094	0.092	0.804	0.838	0.838	0.075	0.804	0.633	0.081	0.136	0.804	0.676	0.083	0.132	0.435	0.336	0.359	0.073	0.804	0.979	0.528	0.156
	0.386	0.562	0.074	0.085	0.710	0.803	0.818	0.111	0.710	0.666	0.091	0.199	0.710	0.738	0.079	0.107	0.726	0.324	0.395	0.070	0.710	0.888	0.553	0.075
	0.424	0.450	0.100	0.110	0.873	0.774	0.580	0.100	0.873	0.689	0.077	0.189	0.873	0.648	0.080	0.105	0.549	0.386	0.385	0.070	0.873	0.838	0.494	0.074
Mean	0.395	0.466	0.089	0.096	0.796	0.805	0.745	0.095	0.796	0.662	0.083	0.174	0.796	0.687	0.081	0.115	0.570	0.348	0.380	0.071	0.796	0.901	0.525	0.101
Percentage of viable cell	100	117.93	22.67	24.194	100	101.25	93.782	11.983	100	83.379	10.44	21.966	100	86.491	10.12	14.423	100	61.140	66.58	12.444	100	113.42	66.03	12.767
SD	0	18.39	2.85	2.60	0	3.29	14.753	1.88	0	2.92	0.74	3.49	0	4.75	0.19	1.57	0	4.75	2.66	0.26	0	7.30	3.06	4.86
CHACO	1.571	0.833	0.704	0.085	1.571	0.59	0.634	0.08	1.571	0.832	0.736	0.075	1.571	0.965	0.048	0.078	1.571	1.284	0.504	0.07	1.571	0.857	0.609	0.301
	1.739	0.889	0.426	0.09	1.739	0.87	0.55	0.086	1.739	0.776	0.633	0.078	1.739	0.727	0.059	0.091	1.739	1.197	0.65	0.065	1.739	1.051	0.643	0.419
	1.724	1.088	0.239	0.079	1.724	0.998	0.589	0.11	1.724	0.769	0.722	0.068	1.724	0.884	0.063	0.088	1.724	1.323	0.685	0.066	1.724	1.173	0.707	0.476
Mean	1.678	0.936	0.456	0.085	1.678	0.819	0.591	0.092	1.678	0.792	0.697	0.074	1.678	0.859	0.057	0.086	1.678	1.268	0.613	0.067	1.678	1.027	0.653	0.399
Percentage of viable cell	100	55.820	27.20	5.046	100	48.828	35.220	5.482	100	47.219	41.54	4.390	100	51.172	3.377	5.105	100	75.566	36.53	3.993	100	61.204	38.92	23.758
SD	0	6.52	11.39	0.27	0	10.15	2.05	0.77	0	1.68	2.72	0.25	0	5.89	0.38	0.33	0	3.14	4.67	0.13	0	7.75	2.42	4.34
Hep-G ₂	0.580	0.252	0.063	0.066	0.580	0.269	0.139	0.066	0.580	0.152	0.182	0.063	0.580	0.189	0.149	0.084	0.580	0.273	0.12	0.068	0.580	0.245	0.153	0.113
	0.670	0.273	0.077	0.074	0.670	0.208	0.117	0.077	0.670	0.176	0.165	0.067	0.670	0.217	0.076	0.085	0.670	0.409	0.095	0.062	0.670	0.267	0.214	0.208
	0.458	0.197	0.066	0.072	0.458	0.212	0.128	0.067	0.458	0.219	0.17	0.056	0.458	0.173	0.07	0.072	0.458	0.339	0.122	0.064	0.458	0.269	0.205	0.185
Mean	0.569	0.241	0.069	0.071	0.569	0.229	0.128	0.070	0.569	0.182	0.172	0.062	0.569	0.193	0.098	0.080	0.569	0.340	0.112	0.065	0.569	0.260	0.191	0.169
Percentage of viable cell	100	42.296	12.07	12.419	100	40.363	22.496	12.302	100	32.045	30.29	10.896	100	33.919	17.28	14.118	100	59.813	19.74	11.365	100	45.752	33.51	29.643
SD	0	5.63	1.06	0.60	0	4.90	1.58	0.87	0	4.87	1.25	0.80	0	3.20	6.31	1.04	0	9.76	2.16	0.44	0	1.91	4.73	7.11
KATO-III	0.589	0.203	0.154	0.072	0.589	0.275	0.21	0.085	0.589	0.247	0.278	0.08	0.589	0.182	0.065	0.08	0.589	0.286	0.162	0.063	0.589	0.318	0.205	0.089
	0.623	0.333	0.117	0.076	0.623	0.256	0.159	0.08	0.623	0.415	0.148	0.081	0.623	0.242	0.102	0.075	0.623	0.326	0.217	0.06	0.623	0.409	0.179	0.096
	0.549	0.353	0.084	0.07	0.549	0.231	0.197	0.093	0.550	0.381	0.183	0.074	0.549	0.217	0.058	0.075	0.549	0.314	0.203	0.064	0.549	0.438	0.227	0.146
Mean	0.587	0.296	0.118	0.073	0.587	0.254	0.189	0.086	0.587	0.348	0.203	0.078	0.587	0.214	0.075	0.076	0.587	0.309	0.194	0.062	0.587	0.388	0.203	0.110
Percentage of viable cell	100	50.483	20.16	12.379	100	43.271	32.140	14.651	100	59.228	34.58	13.345	100	36.400	12.78	13.061	100	52.584	33.05	10.619	100	66.156	34.70	18.796
SD	0	11.329	4.87	0.42	0	3.07	3.67	0.91	0	12.355	9.36	0.53	0	4.19	3.29	0.40	0	2.86	3.98	0.29	0	8.71	3.34	4.32
SW620	0.967	0.174	0.08	0.063	0.967	0.133	0.086	0.062	0.967	0.083	0.096	0.062	0.967	0.139	0.074	0.096	0.967	0.092	0.083	0.064	0.967	0.114	0.068	0.103
	1.037	0.115	0.095	0.071	1.037	0.118	0.09	0.074	1.037	0.094	0.119	0.064	1.037	0.145	0.064	0.11	1.037	0.118	0.093	0.065	1.037	0.102	0.085	0.107
	0.893	0.100	0.076	0.068	0.893	0.144	0.072	0.068	0.893	0.102	0.091	0.062	0.893	0.084	0.063	0.088	0.893	0.138	0.098	0.061	0.893	0.115	0.087	0.101
Mean	0.966	0.130	0.084	0.067	0.966	0.132	0.083	0.068	0.966	0.093	0.102	0.063	0.966	0.123	0.067	0.098	0.966	0.116	0.091	0.063	0.966	0.110	0.080	0.104
Percentage of viable cell	100	13.423	8.661	6.970	100	13.630	8.558	7.039	100	9.627	10.56	6.487	100	12.698	6.936	10.145	100	12.008	9.455	6.556	100	11.422	8.282	10.732
SD	0	3.31	0.85	0.34	0	1.10	0.80	0.51	0	0.81	1.26	0.1	0	2.84	0.51	0.94	0	1.95	0.65	0.18	0	0.61	0.88	0.26

Absorbance value at 540 nm of different cancer cell lines treated with fractions in reCDE

	Fraction III (µg/mL)				Fraction IV (µg/mL)				Fraction V (µg/mL)				Fraction VI (µg/mL)			
	Control	100	1000	10000	Control	100	1000	10000	Control	100	1000	10000	Control	100	1000	10000
BT474	0.482	0.495	0.804	0.565	0.804	0.565	0.804	0.565	0.804	0.565	0.294	0.077	0.226	0.258	0.185	0.064
	0.473	0.447	0.710	0.567	0.710	0.567	0.710	0.567	0.710	0.567	0.273	0.075	0.218	0.206	0.174	0.070
	0.611	0.537	0.873	0.747	0.873	0.747	0.873	0.747	0.873	0.747	0.295	0.091	0.190	0.218	0.245	0.075
Mean	0.522	0.493	0.796	0.626	0.796	0.626	0.796	0.626	0.796	0.626	0.287	0.081	0.211	0.227	0.201	0.069
Percentage of viable cell	100	94.444	100	78.774	100	78.774	100	78.774	100	78.774	36.103	10.173	100	107.570	95.158	33.118
SD	0	7.04	0	10.74	0	10.74	0	10.74	0	10.74	1.29	0.90	0	10.61	14.69	2.17
CHACO	1.93	2.682	1.838	1.929	1.838	1.929	1.838	1.929	1.838	1.929	0.933	0.094	2.359	2.218	2.131	0.068
	1.765	1.694	1.476	1.359	1.476	1.359	1.476	1.359	1.476	1.359	0.842	0.095	1.991	1.928	1.611	0.070
	1.702	2.824	1.817	2.101	1.817	2.101	1.817	2.101	1.817	2.101	0.869	0.088	2.407	2.542	1.953	0.074
Mean	1.799	2.400	1.710	1.796	1.710	1.796	1.710	1.796	1.710	1.796	0.881	0.092	2.250	2.229	1.898	0.071
Percentage of viable cell	100	133.407	100	105.030	100	105.030	100	105.030	100	105.030	51.534	5.401	100	98.977	84.284	3.133
SD	0	27.94	0	18.53	0	18.53	0	18.53	0	18.53	2.22	0.20	0	11.15	9.58	0.11
Hep-G ₂	0.679	0.569	0.352	0.399	0.352	0.399	0.352	0.399	0.352	0.399	0.168	0.068	0.283	0.192	0.210	0.072
	0.661	0.592	0.452	0.538	0.452	0.538	0.452	0.538	0.452	0.538	0.280	0.080	0.216	0.173	0.121	0.068
	0.625	0.681	0.795	0.534	0.795	0.534	0.795	0.534	0.795	0.534	0.328	0.075	0.241	0.158	0.123	0.067
Mean	0.655	0.614	0.533	0.490	0.533	0.490	0.533	0.490	0.533	0.490	0.259	0.074	0.246	0.174	0.151	0.069
Percentage of viable cell	100	93.740	100	92.019	100	92.019	100	92.019	100	92.019	48.511	13.929	100	70.671	61.404	28.084
SD	0	7.37	0	12.14	0	12.14	0	12.14	0	12.14	12.58	0.88	0	5.66	16.94	0.94
KATO-III	0.736	1.105	0.308	0.379	0.308	0.379	0.308	0.379	0.308	0.379	0.226	0.078	0.427	0.486	0.426	0.065
	0.736	0.769	0.355	0.332	0.355	0.332	0.355	0.332	0.355	0.332	0.200	0.079	0.443	0.400	0.382	0.075
	0.776	0.871	0.404	0.375	0.404	0.375	0.404	0.375	0.404	0.375	0.207	0.086	0.374	0.375	0.351	0.075
Mean	0.749	0.915	0.356	0.362	0.356	0.362	0.356	0.362	0.356	0.362	0.211	0.081	0.415	0.420	0.386	0.072
Percentage of viable cell	100	122.109	100	101.819	100	101.819	100	101.819	100	101.819	59.392	22.770	100	100.631	92.401	17.090
SD	0	18.77	0	6.05	0	6.05	0	6.05	0	6.05	2.99	1.00	0	11.42	7.38	1.15
SW620	1.281	1.411	0.294	0.279	0.294	0.279	0.294	0.279	0.294	0.279	0.158	0.078	0.300	0.367	0.285	0.069
	1.668	1.708	0.386	0.462	0.386	0.462	0.386	0.462	0.386	0.462	0.154	0.096	0.306	0.364	0.268	0.068
	1.653	1.865	0.391	0.477	0.391	0.477	0.391	0.477	0.391	0.477	0.127	0.088	0.332	0.338	0.314	0.080
Mean	1.534	1.661	0.357	0.406	0.357	0.406	0.357	0.406	0.357	0.406	0.146	0.087	0.313	0.356	0.289	0.072
Percentage of viable cell	100	108.301	100	113.618	100	113.618	100	113.618	100	113.618	40.909	24.622	100	114.003	92.455	23.135
SD	0	12.27	0	25.22	0	25.22	0	25.22	0	25.22	3.85	1.91	0	4.13	6.14	1.62

(Continued in the next page)

	Fraction VII (µg/mL)				Fraction VIII (µg/mL)				Fraction IX (µg/mL)				Fraction X (µg/mL)			
	Control	100	1000	10000	Control	100	1000	10000	Control	100	1000	10000	Control	100	1000	10000
BT474	0.482	0.578	0.078	0.098	0.482	0.525	0.078	0.123	0.723	0.789	0.231	0.181	0.723	0.877	1.229	0.15
	0.473	0.492	0.08	0.112	0.473	0.499	0.085	0.124	0.708	0.733	0.226	0.376	0.708	0.685	0.405	0.148
	0.611	0.469	0.081	0.092	0.611	0.551	0.08	0.134	0.59	0.693	0.171	0.231	0.59	0.722	0.364	0.181
Mean	0.522	0.513	0.080	0.101	0.522	0.525	0.081	0.127	0.674	0.738	0.209	0.263	0.674	0.761	0.666	0.160
Percentage of viable cell	100	98.276	15.262	19.285	100	100.575	15.517	24.330	100	109.599	31.074	38.991	100	113.013	98.862	23.701
SD	0	0.05	0.00	1.61	0	4.07	0.56	0.95	0	5.84	4.04	12.28	0	12.35	59.15	2.24
CHACO	2.359	2.101	0.104	0.085	2.359	2.747	0.084	0.101	2.431	3.815	0.438	0.185	2.431	2.636	1.97	0.16
	1.991	2.254	0.137	0.085	1.991	2.615	0.197	0.100	2.522	3.147	0.392	0.195	2.522	3.034	1.466	0.158
	2.407	1.944	0.096	0.086	2.407	1.687	0.084	0.092	2.83	3.768	0.215	0.154	2.83	2.074	1.097	0.148
Mean	2.250	2.100	0.112	0.085	2.250	2.349	0.122	0.374	2.594	3.577	0.348	0.178	2.594	2.58	1.511	0.155
Percentage of viable cell	100	93.222	4.992	3.789	100	104.333	5.400	4.327	100	137.865	13.427	6.861	100	99.499	58.242	5.987
SD	0	5.62	0.78	0.01	0	20.94	2.37	0.17	0	11.73	3.71	0.67	0	15.18	13.79	0.20
Hep-G ₂	0.283	0.112	0.060	0.065	0.283	0.164	0.066	0.082	0.81	0.61	0.114	0.178	0.81	0.572	0.326	0.217
	0.216	0.141	0.063	0.066	0.216	0.171	0.067	0.083	0.818	0.568	0.102	0.172	0.818	0.687	0.264	0.124
	0.241	0.200	0.066	0.071	0.241	0.143	0.068	0.129	0.812	0.522	0.101	0.192	0.812	0.806	0.41	0.137
Mean	0.247	0.151	0.065	0.067	0.247	0.159	0.067	0.098	0.813	0.567	0.106	0.181	0.813	0.688	0.333	0.159
Percentage of viable cell	100	61.391	25.528	27.381	100	64.732	27.097	39.705	100	69.672	12.992	22.213	100	84.631	40.984	19.590
SD	0	14.89	1.01	1.08	0	4.83	0.31	8.83	0	4.42	0.73	1.03	0	11.75	7.36	5.06
KATO-III	0.427	0.420	0.076	0.069	0.427	0.443	0.077	0.101	0.838	0.985	0.327	0.191	0.838	1.113	0.684	0.142
	0.443	0.380	0.067	0.080	0.443	0.410	0.082	0.101	0.871	0.95	0.27	0.252	0.871	1.18	0.398	0.137
	0.374	0.354	0.069	0.077	0.374	0.386	0.080	0.107	0.868	0.995	0.21	0.222	0.868	1.269	0.356	0.14
Mean	0.415	0.385	0.071	0.075	0.415	0.413	0.080	0.103	0.859	0.977	0.269	0.222	0.859	1.187	0.479	0.140
Percentage of viable cell	100	92.780	17.101	18.146	100	99.550	19.127	24.803	100	113.698	31.315	25.805	100	138.223	55.801	16.259
SD	0	6.49	0.94	1.00	0	5.63	0.49	0.69	0	2.25	5.56	2.90	0	7.44	16.97	0.24
SW620	1.281	1.713	0.097	0.109	1.281	1.800	0.096	0.207	1.523	1.683	0.101	0.218	1.523	1.695	0.781	0.142
	1.668	1.854	0.095	0.108	1.668	1.936	0.105	0.203	1.403	1.55	0.136	0.212	1.403	2.369	0.429	0.163
	1.653	1.597	0.103	0.113	1.653	2.109	0.101	0.229	1.39	1.563	0.142	0.208	1.39	2.022	0.373	0.151
Mean	1.534	1.721	0.098	0.11	1.534	1.948	0.101	0.213	1.439	1.599	0.126	0.213	1.439	2.029	0.528	0.152
Percentage of viable cell	100	112.212	6.410	7.171	100	127.01	6.56	13.89	100	111.121	8.781	14.782	100	141.010	36.677	10.565
SD	0	6.85	0.22	0.14	0	8.24	0.24	0.75	0	4.16	1.26	0.29	0	19.13	12.55	0.60

(Continued in the next page)

	Fraction XI (µg/mL)				Fraction XII (µg/mL)				Fraction XIII (µg/mL)				Fraction XIV (µg/mL)			
	Control	100	1000	10000	Control	100	1000	10000	Control	100	1000	10000	Control	100	1000	10000
BT474	0.723	0.76	0.6	0.148	0.723	0.832	0.207	0.181	0.723	0.842	0.261	0.204	0.723	0.694	0.736	0.14
	0.708	0.745	0.438	0.142	0.708	0.826	0.177	0.215	0.708	0.858	0.431	0.192	0.708	0.796	0.934	0.642
	0.59	0.743	0.603	0.141	0.59	0.728	0.135	0.209	0.59	0.808	0.261	0.237	0.59	0.786	0.571	0.301
Mean	0.674	0.749	0.547	0.144	0.674	0.795	0.173	0.202	0.674	0.836	0.318	0.211	0.674	0.759	0.747	0.361
Percentage of viable cell	100	111.232	81.197	21.326	100	118.060	25.680	29.936	100	124.097	47.155	31.321	100	112.617	110.886	53.587
SD	0	1.13	11.44	0.46	0	7.08	4.38	2.20	0	3.095	11.896	2.824	0	6.81	22.03	31.07
CHACO	2.431	2.488	1.956	0.202	2.431	2.691	0.524	0.172	2.431	3.809	1.54	0.197	2.431	2.05	2.763	0.121
	2.522	2.558	2.244	0.134	2.522	2.736	0.236	0.176	2.522	3.873	1.066	0.237	2.522	1.416	2.505	0.122
	2.83	2.539	2.153	0.133	2.83	2.677	0.53	0.189	2.83	3.41	1.527	0.196	2.83	3.265	2.658	0.111
Mean	2.594	2.528	2.117	0.156	2.594	2.701	0.43	0.179	2.594	3.697	1.378	0.210	2.594	2.244	2.642	0.118
Percentage of viable cell	100	97.456	81.627	6.026	100	104.124	16.575	6.900	100	142.516	53.103	8.095	100	86.483	101.837	4.548
SD	0	1.14	4.63	1.24	0	0.97	5.29	0.28	0	7.90	8.50	0.74	0	29.57	4.08	0.19
Hep-G ₂	0.81	0.662	0.591	0.186	0.81	0.683	0.233	0.132	0.81	0.562	0.568	0.211	0.81	0.759	0.739	0.168
	0.818	0.829	0.749	0.133	0.818	0.722	1.039	0.161	0.818	0.745	0.111	0.223	0.818	0.568	0.63	0.142
	0.812	0.864	0.766	0.14	0.812	0.697	0.255	0.148	0.812	0.707	0.275	0.263	0.812	0.704	0.665	0.121
Mean	0.813	0.785	0.702	0.153	0.813	0.701	0.509	0.147	0.813	0.671	0.318	0.232	0.813	0.677	0.678	0.143
Percentage of viable cell	100	96.517	86.312	18.812	100	86.148	62.582	18.074	100	82.541	39.099	28.566	100	83.238	83.361	17.664
SD	0	10.84	9.69	2.89	0	1.98	46.09	1.46	0	9.69	23.24	2.73	0	9.87	5.59	2.36
KATO-III	0.838	1.145	0.676	0.146	0.838	0.922	0.507	0.184	0.838	0.909	0.723	0.255	0.838	0.528	0.576	0.265
	0.871	1.054	0.912	0.137	0.871	0.754	0.196	0.213	0.871	1.137	0.525	0.2	0.871	1.161	0.753	0.257
	0.868	0.961	0.798	0.145	0.868	1.066	0.505	0.215	0.868	1.091	0.688	0.189	0.868	0.798	0.688	0.241
Mean	0.859	1.053	0.795	0.142	0.859	0.914	0.403	0.204	0.859	1.046	0.645	0.215	0.859	0.846	0.672	0.254
Percentage of viable cell	100	122.623	92.588	16.608	100	106.403	46.876	23.749	100	121.731	75.126	24.990	100	96.508	78.269	29.608
SD	0	8.74	11.22	0.47	0	14.84	17.01	1.65	0	11.46	10.04	3.36	0	30.19	8.51	1.16
SW620	1.523	1.625	0.726	0.129	1.523	2.031	0.656	0.15	1.523	1.906	0.849	0.319	1.523	1.504	1.942	0.102
	1.403	0.907	1.021	0.128	1.403	1.988	0.615	0.178	1.403	1.994	0.802	0.199	1.403	1.52	1.867	0.104
	1.39	1.667	1.152	0.135	1.39	1.404	0.696	0.167	1.39	2.132	0.848	0.207	1.39	1.462	1.933	0.108
Mean	1.439	1.400	0.966	0.131	1.439	1.808	0.656	0.165	1.439	2.011	0.833	0.242	1.439	1.495	1.914	0.105
Percentage of viable cell	100	97.289	67.169	9.082	100	125.649	45.575	11.469	100	139.759	57.901	16.798	100	103.939	133.040	7.275
SD	0	24.24	12.38	0.21	0	19.88	2.30	0.80	0	6.47	1.52	3.81	0	1.70	2.32	0.17

Absorbance value at 540 nm of different cancer cell lines treated with compound and active compound from fraction VII and VIII

	F7E (µg/mL)								F7F (µg/mL)					
	Control	15.625	31.25	62.5	125	250	500	1000	Control	62.5	125	250	500	1000
BT474	0.491	0.672	0.586	0.545	0.166	0.192	0.061	0.062	0.153	0.112	0.122	0.099	0.062	0.056
	0.641	0.675	0.626	0.616	0.068	0.078	0.065	0.068	0.288	0.204	0.114	0.092	0.071	0.077
	0.601	0.616	0.672	0.498	0.130	0.099	0.067	0.067	0.222	0.196	0.123	0.068	0.075	0.056
Mean	0.578	0.654	0.628	0.553	0.121	0.123	0.064	0.066	0.221	0.171	0.120	0.086	0.069	0.063
Percentage of viable cell	100	113.350	108.782	95.814	21.040	21.295	11.155	11.363	100	77.225	54.148	39.065	31.373	28.507
SD	0	4.73	6.11	8.45	7.03	8.59	0.45	0.44	0	18.83	1.82	6.01	2.46	4.48
CHACO	2.900	2.909	1.839	2.236	0.624	1.076	0.086	0.067	1.737	1.807	1.235	0.313	0.123	0.057
	2.746	2.218	2.201	2.070	1.067	0.739	0.079	0.069	1.698	1.776	0.969	0.195	0.092	0.057
	2.775	2.271	1.447	1.746	0.779	0.710	0.081	0.073	1.836	1.901	1.257	0.186	0.131	0.057
Mean	2.807	2.466	1.829	2.017	0.823	0.842	0.082	0.070	1.757	1.828	1.154	0.231	0.115	0.057
Percentage of viable cell	100	87.857	65.157	71.854	29.330	29.975	2.912	2.483	100	104.041	65.661	13.166	6.564	3.244
SD	0	11.18	10.97	7.24	6.53	5.92	0.11	0.09	0	3.02	7.45	3.29	0.96	0.00
Hep-G ₂	0.763	0.629	0.537	0.563	0.148	0.089	0.060	0.070	0.583	0.357	0.358	0.190	0.064	0.08
	0.674	0.591	0.605	0.612	0.124	0.119	0.064	0.070	0.512	0.398	0.266	0.115	0.095	0.072
	0.555	0.544	0.598	0.545	0.122	0.255	0.061	0.069	0.410	0.46	0.29	0.182	0.088	0.08
Mean	0.664	0.588	0.580	0.573	0.131	0.154	0.062	0.070	0.502	0.405	0.305	0.162	0.082	0.077
Percentage of viable cell	100	88.528	87.354	86.365	19.776	23.210	9.318	10.473	100	80.731	60.731	32.359	16.412	15.415
SD	0	5.24	4.56	4.30	1.74	10.87	0.24	0.09	0	8.44	7.77	6.70	2.65	0.75
KATO-III	0.500	0.679	0.939	0.412	0.087	0.106	0.057	0.057	0.287	0.206	0.094	0.069	0.057	0.06
	0.562	0.765	0.747	0.460	0.069	0.110	0.063	0.062	0.248	0.286	0.092	0.063	0.062	0.058
	0.749	0.698	0.714	0.518	0.078	0.088	0.062	0.063	0.279	0.362	0.093	0.059	0.056	0.064
Mean	0.604	0.714	0.800	0.463	0.078	0.101	0.061	0.061	0.271	0.285	0.093	0.064	0.058	0.061
Percentage of viable cell	100	118.309	132.511	76.754	12.942	16.819	10.077	10.066	100	104.914	34.275	23.464	21.499	22.359
SD	0	6.12	16.38	7.18	1.27	1.59	0.42	0.38	0	23.47	0.30	1.51	0.97	0.92
SW620	1.968	1.913	1.907	1.500	1.266	0.322	0.136	0.061	0.989	0.878	0.32	0.075	0.073	0.072
	1.875	1.433	1.433	1.873	1.176	0.203	0.076	0.064	1.411	0.926	0.338	0.088	0.068	0.085
	1.761	1.687	1.687	1.559	1.308	0.242	0.082	0.065	1.39	0.858	0.504	0.086	0.083	0.087
Mean	1.868	1.678	1.676	1.644	1.250	0.256	0.098	0.063	1.263	0.887	0.387	0.083	0.074	0.081
Percentage of viable cell	100	89.826	89.704	87.295	66.929	13.668	5.256	3.402	100	70.238	30.660	6.570	5.910	6.438
SD	0	10.51	10.36	9.42	2.95	2.65	1.44	0.09	0	2.26	6.56	0.45	0.49	0.53

(Continued in the next page)

	F8E (µg/mL)						F7F-3 (µg/mL)							
	Control	62.5	125	250	500	1000	Control	15.625	31.25	62.5	125	250	500	1000
BT474	0.298	0.202	0.129	0.291	0.110	0.079	0.166	0.122	0.224	0.067	0.082	0.087	0.067	0.072
	0.251	0.108	0.194	0.152	0.205	0.064	0.270	0.288	0.174	0.073	0.082	0.085	0.071	0.065
	0.259	0.228	0.109	0.237	0.165	0.071	0.287	0.328	0.197	0.071	0.081	0.095	0.069	0.067
Mean	0.269	0.179	0.144	0.227	0.160	0.071	0.241	0.246	0.198	0.070	0.082	0.089	0.069	0.068
Percentage of viable cell	100	66.634	53.434	84.202	59.372	26.500	100	102.116	82.241	29.073	33.831	36.902	28.548	28.064
SD	0	19.14	13.59	21.27	14.23	2.21	0	36.93	8.42	1.05	0.12	1.77	0.76	1.27
CHACO	1.165	1.488	1.059	0.642	0.574	0.086	2.225	3.230	1.440	2.359	0.317	0.083	0.081	0.065
	1.162	0.856	1.375	0.704	0.285	0.080	2.283	2.302	1.821	1.645	0.419	0.084	0.087	0.074
	1.441	0.881	1.245	0.713	0.951	0.082	2.047	1.676	1.569	1.630	0.198	0.084	0.087	0.068
Mean	1.256	1.075	1.226	0.686	0.603	0.083	2.185	2.402	1.610	1.878	0.311	0.084	0.085	0.069
Percentage of viable cell	100	85.583	97.771	54.643	48.035	6.574	100	109.953	73.689	85.953	14.243	3.846	3.884	2.734
SD	0	23.27	10.36	2.53	21.68	0.19	0	29.22	7.23	15.58	4.14	0.02	0.12	0.21
Hep-G ₂	0.258	0.200	0.169	0.076	0.083	0.064	0.299	0.209	0.170	0.087	0.064	0.068	0.064	0.069
	0.267	0.215	0.188	0.133	0.106	0.063	0.311	0.167	0.171	0.073	0.066	0.069	0.066	0.068
	0.212	0.167	0.177	0.153	0.151	0.060	0.286	0.194	0.170	0.076	0.065	0.073	0.069	0.069
Mean	0.246	0.194	0.178	0.121	0.113	0.062	0.299	0.190	0.170	0.078	0.065	0.070	0.066	0.068
Percentage of viable cell	100	78.937	72.528	49.144	46.211	25.326	100	63.548	56.955	26.247	21.729	23.458	22.242	22.878
SD		8.14	3.17	13.38	11.50	0.77	0	5.77	0.07	2.10	0.36	0.79	0.59	0.22
KATO-III	0.168	0.132	0.167	0.090	0.069	0.060	0.515	0.307	0.247	0.126	0.083	0.061	0.071	0.070
	0.151	0.128	0.165	0.124	0.069	0.062	0.510	0.306	0.326	0.135	0.087	0.070	0.056	0.066
	0.194	0.150	0.133	0.133	0.087	0.062	0.555	0.300	0.307	0.141	0.090	0.071	0.059	0.060
Mean	0.171	0.137	0.155	0.116	0.075	0.061	0.527	0.304	0.293	0.134	0.087	0.068	0.062	0.065
Percentage of viable cell	100	79.949	90.599	67.544	43.885	35.888	100	57.689	55.708	25.408	16.498	12.891	11.828	12.391
SD	0	5.51	9.17	10.80	4.93	0.69	0	0.59	6.38	1.22	0.55	0.86	1.23	0.75
SW620	1.605	2.538	2.020	2.377	0.786	0.061	0.318	0.228	0.242	0.180	0.080	0.110	0.079	0.070
	1.473	1.670	2.003	1.868	0.546	0.057	0.269	0.303	0.290	0.086	0.089	0.066	0.065	0.067
	1.904	1.678	1.778	1.880	0.621	0.061	0.271	0.231	0.199	0.094	0.332	0.076	0.081	0.067
Mean	1.661	1.962	1.933	2.042	0.651	0.060	0.286	0.253	0.243	0.120	0.167	0.084	0.075	0.068
Percentage of viable cell	100	118.156	116.434	122.962	39.219	3.612	100	88.634	85.192	42.047	58.386	29.385	26.258	23.679
SD	0	24.54	6.64	14.28	6.06	0.13	0	12.47	12.89	14.94	40.83	6.52	2.51	0.49

(Continued in the next page)

	F7F-4 (µg/mL)							F7F-5 (µg/mL)							F7F-6 (µg/mL)						
	Ctrl	31.25	62.5	125	250	500	1000	Ctrl	31.25	62.5	125	250	500	1000	Ctrl	31.25	62.5	125	250	500	1000
BT474	0.249	0.289	0.294	0.299	0.185	0.103	0.076	0.491	0.406	0.604	0.681	0.453	0.174	0.055	0.376	1.380	0.680	0.502	0.300	0.141	0.063
	0.237	0.282	0.261	0.248	0.164	0.125	0.072	0.641	0.548	0.828	0.301	0.366	0.197	0.058	0.386	0.918	0.710	0.458	0.403	0.176	0.077
	0.281	0.323	0.250	0.242	0.251	0.103	0.076	0.601	0.680	0.642	0.316	0.282	0.175	0.070	0.424	1.003	0.513	0.453	0.235	0.107	0.082
Mean	0.256	0.298	0.268	0.263	0.200	0.110	0.074	0.577	0.545	0.692	0.433	0.367	0.182	0.061	0.395	1.100	0.634	0.471	0.313	0.141	0.074
Percentage of viable cell	100	116.6																			
	100	82	104.865	102.948	78.166	43.107	29.099	100	94.388	119.782	74.970	63.520	31.480	10.509	100	278.331	160.388	119.132	79.098	35.759	18.744
SD	0	6.96	7.25	10.01	14.45	4.16	0.71	0	19.36	16.92	30.41	12.07	1.82	1.11	0	50.80	21.90	5.61	17.45	7.16	2.09
CHACO	2.123	2.034	2.598	1.895	1.966	1.779	0.179	2.900	2.240	1.815	3.376	2.397	1.891	0.992	1.304	1.455	1.315	1.530	1.452	1.430	0.564
	1.912	1.806	1.464	2.334	1.873	1.900	0.737	2.746	2.528	1.911	2.301	1.984	1.909	1.032	1.207	1.496	1.302	1.629	1.239	1.347	0.161
	1.986	1.659	1.975	1.263	1.771	1.693	0.484	2.775	2.513	1.665	1.522	1.679	1.325	0.884	1.498	1.801	1.258	1.426	1.442	1.454	0.139
Mean	2.007	1.833	2.012	1.831	1.870	1.791	0.466	2.807	2.427	1.797	2.400	2.020	1.708	0.970	1.337	1.584	1.292	1.528	1.378	1.410	0.288
Percentage of viable cell	100	91.32																			
	100	6	100.262	91.204	93.166	89.223	23.241	100	86.455	64.010	85.489	71.972	60.849	34.541	100	118.510	96.638	114.337	103.085	105.519	21.550
SD	0	7.70	23.11	21.92	3.97	4.24	11.37	0	4.72	3.60	27.08	10.49	9.66	2.22	0	11.53	1.85	6.21	7.37	3.45	14.63
Hep-G ₂	0.245	0.207	0.112	0.159	0.137	0.087	0.070	0.763	0.462	0.632	0.687	0.636	0.414	0.170	0.236	0.574	0.487	0.435	0.570	0.092	0.077
	0.237	0.249	0.198	0.181	0.101	0.084	0.071	0.674	0.493	0.508	0.644	0.555	0.380	0.083	0.264	0.464	0.347	0.498	0.392	0.088	0.084
	0.262	0.179	0.213	0.189	0.170	0.099	0.077	0.555	0.386	0.505	0.595	0.484	0.422	0.130	0.316	0.554	0.313	0.394	0.323	0.082	0.099
Mean	0.248	0.212	0.174	0.176	0.136	0.090	0.072	0.664	0.447	0.548	0.642	0.558	0.405	0.128	0.272	0.531	0.382	0.442	0.428	0.088	0.087
Percentage of viable cell	100	85.47																			
	100	0	70.442	71.250	54.956	36.332	29.195	100	67.311	82.589	96.697	84.085	61.040	19.264	100	195.253	140.647	162.774	157.623	32.258	31.841
SD	0	11.71	17.89	5.13	11.37	2.51	1.25	0	6.72	8.92	5.65	9.34	2.74	5.36	0	17.67	27.67	15.62	38.30	1.50	3.40
KATO-III	0.384	0.565	0.451	0.392	0.389	0.261	0.137	0.749	0.461	0.542	0.580	0.583	0.453	0.065	0.413	1.031	0.582	0.640	0.469	0.141	0.090
	0.469	0.551	0.439	0.417	0.364	0.250	0.130	0.500	0.584	0.593	0.606	0.564	0.462	0.068	0.302	0.762	0.670	0.472	0.703	0.124	0.107
	0.415	0.462	0.452	0.372	0.363	0.322	0.136	0.562	0.542	0.521	0.771	0.642	0.320	0.079	0.338	0.514	0.446	0.351	0.345	0.141	0.091
Mean	0.422	0.526	0.447	0.394	0.372	0.278	0.134	0.604	0.529	0.552	0.652	0.596	0.412	0.070	0.351	0.769	0.566	0.488	0.507	0.135	0.096
Percentage of viable cell	100	124.6																			
	100	17	105.953	93.202	88.149	65.767	31.833	100	87.621	91.420	108.045	98.758	68.196	11.672	100	219.087	161.229	138.990	144.450	38.534	27.243
SD	0	10.79	1.41	4.39	2.89	7.44	0.83	0	8.49	4.96	13.99	5.46	10.72	0.97	0	60.23	26.27	33.80	41.82	2.35	2.19
SW620	0.268	0.210	0.335	0.238	0.167	0.279	0.094	2.218	1.473	1.758	1.892	1.710	1.522	0.4402	1.592	1.800	1.862	1.264	1.051	0.396	0.109
	0.228	0.254	0.237	0.214	0.152	0.215	0.106	1.667	2.107	1.569	1.994	1.496	1.007	0.1942	1.683	1.877	1.408	1.455	0.973	0.248	0.092
	0.273	0.230	0.326	0.209	0.108	0.151	0.101	1.667	1.347	1.797	2.067	1.540	1.089	0.3386	1.900	1.701	1.369	1.359	1.102	0.174	0.125
Mean	0.257	0.231	0.299	0.220	0.142	0.215	0.100	1.851	1.642	1.708	1.984	1.582	1.206	0.324	1.725	1.793	1.546	1.359	1.042	0.273	0.109
Percentage of viable cell	100	90.18																			
	100	8	116.660	85.848	55.517	83.847	39.168	100	88.742	92.276	107.234	85.475	65.161	17.526	100	103.917	89.627	78.752	60.419	15.816	6.295
SD	0	6.97	17.13	4.90	9.76	20.50	1.92	0	17.97	5.39	3.87	4.98	12.21	5.45	0	4.17	12.96	4.51	3.09	5.36	0.79

(Continued in the next page)

	F8E-5 (µg/mL)								F8E-6 (µg/mL)						F8E-7 (µg/mL)					
	Control	15.25	31.25	62.5	125	250	500	1000	Control	62.5	125	250	500	1000	Control	62.5	125	250	500	1000
BT474	0.464	0.599	0.567	0.464	0.363	0.113	0.084	0.068	0.259	0.277	0.268	0.173	0.081	0.059	0.259	0.277	0.327	0.188	0.154	0.089
	0.538	0.573	0.629	0.473	0.347	0.116	0.089	0.095	0.324	0.278	0.201	0.112	0.077	0.058	0.324	0.158	0.279	0.174	0.110	0.084
	0.448	0.533	0.457	0.513	0.554	0.122	0.088	0.095	0.354	0.237	0.251	0.110	0.102	0.055	0.354	0.255	0.275	0.170	0.127	0.062
Mean	0.483	0.568	0.551	0.483	0.421	0.117	0.087	0.086	0.312	0.264	0.240	0.132	0.087	0.057	0.312	0.230	0.294	0.177	0.130	0.078
Percentage of viable cell	100	117.597	114.010	99.959	87.163	24.191	18.024	17.762	100	84.551	76.816	42.201	27.810	18.376	100	73.718	94.124	56.848	41.806	25.107
SD	0	5.63	14.69	4.38	19.47	0.84	0.49	2.64	0	6.17	9.13	9.44	3.58	0.66	0	16.57	7.55	2.44	5.81	3.70
CHACO	1.30	1.595	1.991	2.676	1.304	1.259	0.099	0.096	2.014	1.981	2.255	1.892	1.054	0.094	2.014	2.328	2.344	1.980	2.110	1.393
	1.137	1.607	1.283	1.984	1.481	1.322	0.126	0.100	2.166	1.924	1.880	1.639	1.681	0.110	2.166	2.262	2.144	1.818	1.535	1.203
	1.214	1.346	1.332	2.008	1.468	1.129	0.090	0.096	2.014	1.829	1.846	2.044	1.045	0.102	2.014	2.259	2.013	1.634	1.593	1.318
Mean	1.218	1.516	1.535	2.222	1.418	1.236	0.105	0.098	2.065	1.911	1.994	1.858	1.260	0.102	2.065	2.283	2.167	1.811	1.746	1.305
Percentage of viable cell	100	124.509	126.061	182.503	116.429	101.525	8.636	8.061	100	92.572	96.560	89.981	61.018	4.942	100	110.571	104.953	87.698	84.564	63.196
SD	0	9.88	26.52	26.32	6.60	6.58	1.27	0.13	0	3.05	8.97	8.14	14.41	0.31	0	1.53	6.58	6.83	12.51	3.77
Hep-G ₂	0.330	0.321	0.278	0.311	0.239	0.082	0.069	0.080	0.377	0.385	0.340	0.402	0.149	0.075	0.377	0.457	0.412	0.318	0.353	0.299
	0.355	0.330	0.270	0.315	0.229	0.102	0.087	0.063	0.465	0.392	0.472	0.423	0.152	0.133	0.465	0.336	0.315	0.194	0.292	0.176
	0.271	0.277	0.295	0.294	0.169	0.087	0.067	0.061	0.341	0.246	0.417	0.337	0.282	0.069	0.341	0.417	0.297	0.338	0.365	0.202
Mean	0.319	0.310	0.281	0.307	0.212	0.090	0.074	0.068	0.394	0.341	0.410	0.387	0.194	0.092	0.394	0.403	0.341	0.283	0.336	0.226
Percentage of viable cell	100	97.144	88.158	96.213	66.555	28.308	23.350	21.299	100	86.484	103.905	98.174	49.197	23.415	100	102.215	86.534	71.834	85.292	57.202
SD	0	7.29	3.31	2.92	9.76	2.78	2.84	2.75	0	17.13	13.79	9.28	15.71	7.37	0	12.71	12.83	16.16	8.14	13.42
KATO-III	0.543	0.495	0.447	0.585	0.349	0.141	0.104	0.068	0.543	0.577	0.498	0.480	0.242	0.104	0.543	0.580	0.607	0.472	0.381	0.132
	0.498	0.452	0.400	0.541	0.444	0.121	0.135	0.072	0.498	0.463	0.558	0.461	0.207	0.107	0.498	0.496	0.495	0.462	0.350	0.106
	0.478	0.449	0.493	0.532	0.459	0.113	0.080	0.073	0.478	0.494	0.576	0.476	0.137	0.103	0.478	0.529	0.614	0.538	0.329	0.111
Mean	0.506	0.465	0.447	0.553	0.417	0.125	0.107	0.071	0.506	0.511	0.544	0.472	0.196	0.104	0.506	0.535	0.572	0.490	0.353	0.116
Percentage of viable cell	100	91.922	88.222	109.145	82.395	24.656	21.042	14.004	100.941	107.394	93.285	38.613	20.600	100.941	100	105.669	112.924	96.846	69.781	22.990
SD	0	4.13	7.45	4.59	9.58	2.31	4.43	0.46	9.51	6.63	1.60	8.63	0.33	9.51	0	0.03	0.05	0.03	0.02	0.01
SW620	1.875	1.913	1.907	1.460	1.266	0.322	0.136	0.061	0.781	1.036	0.952	0.430	0.074	0.070	0.781	0.836	1.082	0.292	0.111	0.093
	1.761	1.747	1.433	1.873	1.176	0.203	0.076	0.064	0.874	1.192	0.780	0.076	0.073	0.074	0.874	1.245	1.122	0.285	0.103	0.078
	1.751	1.827	1.687	1.559	1.308	0.241	0.082	0.065	1.205	1.143	0.758	0.136	0.077	0.102	1.205	1.280	0.872	0.291	0.129	0.088
Mean	1.795	1.829	1.676	1.631	1.250	0.255	0.098	0.064	0.953	1.124	0.830	0.214	0.074	0.082	0.953	1.120	1.025	0.289	0.114	0.086
Percentage of viable cell	100	101.870	93.320	90.814	69.627	14.219	5.468	3.539	100	117.894	87.118	22.483	7.810	8.604	100	117.523	107.597	30.345	11.979	9.059
SD	0	3.79	10.78	9.80	3.07	2.76	1.50	0.09	0	6.83	9.11	16.24	0.20	1.48	0	21.17	11.52	0.33	1.14	0.69

Absorbance value at 540 nm of different cancer cell lines and CRL-1947 (fibroblast) treated with doxorubicin and 5-fluorouracil

	Doxorubicin ($\mu\text{g/mL}$)						5-Fluorouracil ($\mu\text{g/mL}$)					
	Control	0.1	1	10	100	1000	Control	0.1	1	10	100	1000
BT474	0.577	0.790	0.531	0.425	0.181	0.300	0.458	0.570	0.612	0.476	0.377	0.304
	0.860	0.715	0.576	0.49	0.238	0.338	0.647	0.598	0.622	0.544	0.520	0.319
	0.852	0.699	0.570	0.502	0.245	0.391	0.660	0.592	0.698	0.551	0.460	0.317
Mean	0.763	0.735	0.559	0.472	0.222	0.343	0.588	0.586	0.644	0.524	0.452	0.313
Percentage of viable cell	100	96.304	73.269	61.885	29.038	44.939	100	99.513	109.438	88.971	76.882	53.220
SD	0	5.21	2.61	4.42	3.76	4.93	0	1.88	6.55	5.77	10.01	1.08
CHACO	2.738	3.160	2.324	1.525	0.459	0.145	1.681	1.853	1.491	0.949	0.498	0.449
	3.270	3.348	2.619	1.664	0.569	0.174	1.378	1.713	1.724	1.050	0.510	0.480
	2.066	2.454	1.993	1.836	0.559	0.124	2.134	2.098	1.820	1.045	0.618	0.547
Mean	2.691	2.987	2.312	1.675	0.529	0.148	1.731	1.888	1.679	1.015	0.542	0.492
Percentage of viable cell	100	110.999	85.917	62.237	19.664	5.493	100	109.066	96.969	58.617	31.317	28.413
SD	0	14.30	9.49	4.73	1.84	0.75	0	9.20	7.97	2.68	3.10	2.35
Hep-G ₂	0.456	0.461	0.413	0.291	0.088	0.155	0.409	0.398	0.419	0.340	0.246	0.208
	0.471	0.413	0.392	0.327	0.076	0.120	0.378	0.453	0.379	0.383	0.278	0.222
	0.494	0.452	0.443	0.261	0.085	0.140	0.382	0.471	0.466	0.314	0.280	0.203
Mean	0.474	0.442	0.416	0.293	0.083	0.139	0.390	0.441	0.421	0.346	0.268	0.211
Percentage of viable cell	100	93.316	87.800	61.845	17.484	29.255	100	113.021	108.028	88.688	68.690	54.121
SD	0	4.407	4.340	5.681	1.034	3.045	0	7.96	9.12	7.24	4.05	2.13
KATO-III	0.913	0.926	0.905	0.604	0.360	0.366	0.703	0.686	0.587	0.596	0.485	0.422
	0.906	0.929	0.842	0.570	0.360	0.438	0.588	0.648	0.599	0.645	0.471	0.368
	0.912	0.891	0.891	0.529	0.335	0.495	0.643	0.672	0.556	0.663	0.504	0.356
Mean	0.910	0.915	0.879	0.567	0.352	0.433	0.645	0.669	0.581	0.635	0.487	0.382
Percentage of viable cell	100	100.538	96.587	62.345	38.636	47.565	100	103.744	90.082	98.469	75.531	59.253
SD	0	1.91	2.95	3.37	1.33	5.81	0	2.48	2.81	4.43	2.06	4.45
SW620	2.108	2.000	1.523	0.789	0.227	0.397	1.755	2.275	1.943	2.422	1.191	0.616
	2.126	2.020	1.664	0.838	0.239	0.359	1.686	2.076	1.640	2.777	1.259	0.676
	2.237	2.216	1.599	0.798	0.222	0.394	1.926	2.090	1.962	2.090	1.075	0.657
Mean	2.157	2.077	1.595	0.808	0.230	0.383	1.789	2.147	1.848	2.430	1.175	0.649
Percentage of viable cell	100	96.320	73.973	37.483	10.643	17.758	100	120.008	103.315	135.795	65.666	36.301
SD	0	4.56	2.67	1.00	0.34	0.80	0	5.05	8.25	15.69	4.24	1.40
CRL-1947	0.282	0.343	0.6533	0.355	0.343	0.454	0.202	0.481	0.481	0.408	0.326	0.247
	0.314	0.478	0.5454	0.345	0.346	0.467	0.226	0.417	0.258	0.258	0.476	0.27
	0.312	0.508	0.4038	0.290	0.341	0.5	0.331	0.321	0.342	0.342	0.409	0.463
Mean	0.303	0.443	0.534	0.330	0.343	0.474	0.253	0.406	0.360	0.336	0.404	0.327
Percentage of viable cell	100	146.205	176.293	108.911	113.311	156.326	160.606	142.424	132.806	159.552	129.117	160.606
SD	0	23.68	33.72	9.43	0.68	6.39	25.99	36.35	24.26	24.25	38.28	25.99

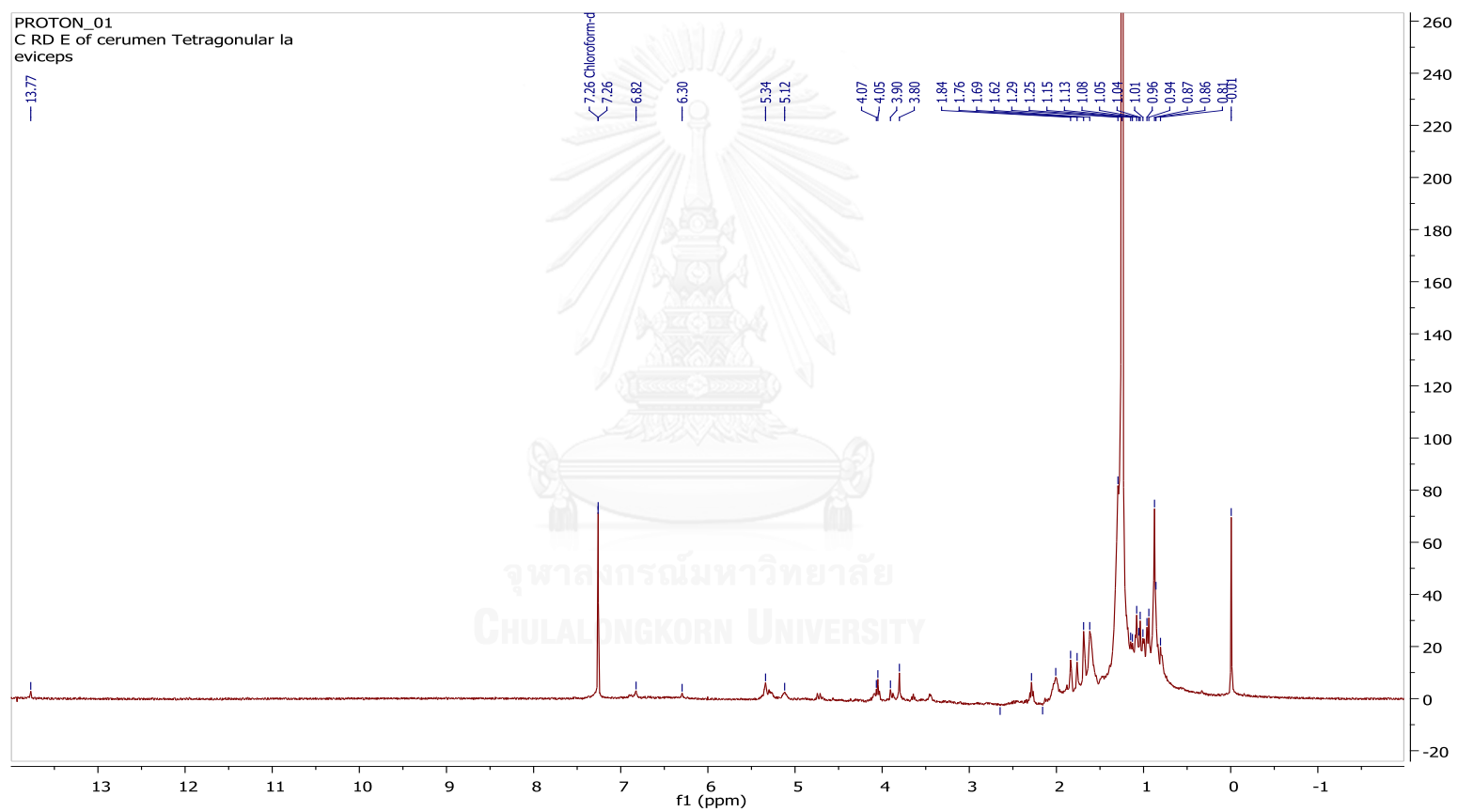
Absorbance value at 540 nm of CRL-1947 treated with active compounds

	F7E (µg/mL)							F7F-3 (µg/mL)							F8E-5 (µg/mL)						
	Ctrl	31.25	62.5	125	250	500	1000	Ctrl	31.25	62.5	125	250	500	1000	Ctrl	31.25	62.5	125	250	500	1000
CRL-1947	0.202	0.580	0.287	0.253	0.308	0.245	0.101	0.202	0.339	0.400	0.439	0.316	0.124	0.078	0.202	0.257	0.302	0.351	0.423	0.481	0.167
	0.226	0.473	0.340	0.234	0.359	0.182	0.103	0.226	0.325	0.325	0.421	0.179	0.112	0.067	0.226	0.406	0.340	0.298	0.333	0.531	0.132
	0.331	0.374	0.269	0.350	0.520	0.199	0.122	0.331	0.321	0.428	0.522	0.172	0.109	0.115	0.331	0.321	0.292	0.257	0.355	0.441	0.087
Mean	0.253	0.476	0.299	0.279	0.395	0.209	0.108	0.253	0.328	0.384	0.460	0.222	0.115	0.087	0.253	0.328	0.311	0.302	0.370	0.484	0.129
Percentage of viable cell	100	187.95 8	118.05 0	110.30 3	156.29 8	82.516	42.793	100	129.80 2	151.93 7	181.96 3	87.800	45.375	34.282	100	129.65 7	122.97 8	119.28 9	146.23 2	191.43 6	50.870
SD	0	33.36	11.81	20.16	35.70	10.55	3.77	0	3.04	17.23	17.36	26.15	2.58	8.08	0	24.14	8.06	15.08	15.13	14.58	12.97

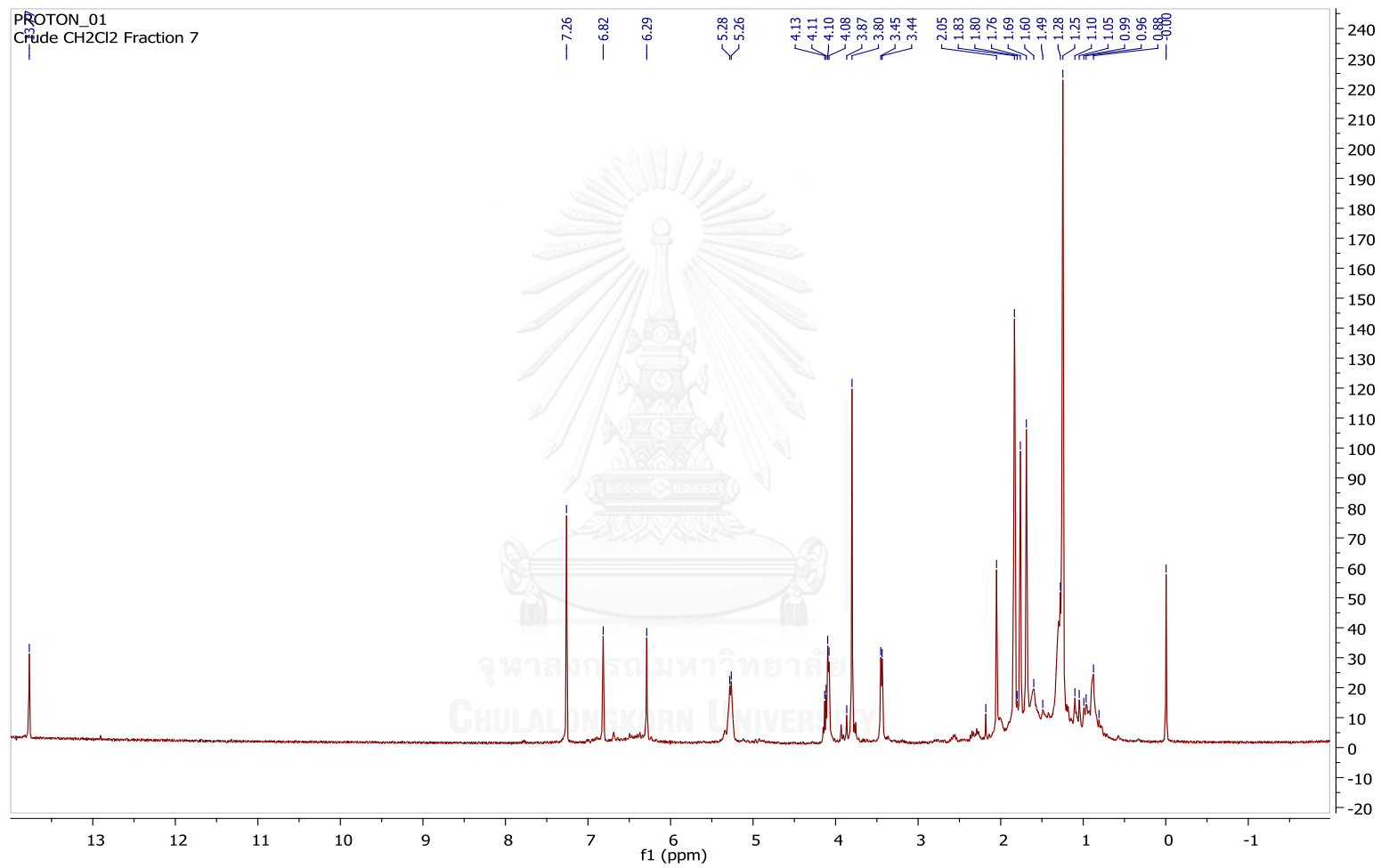


Appendix B

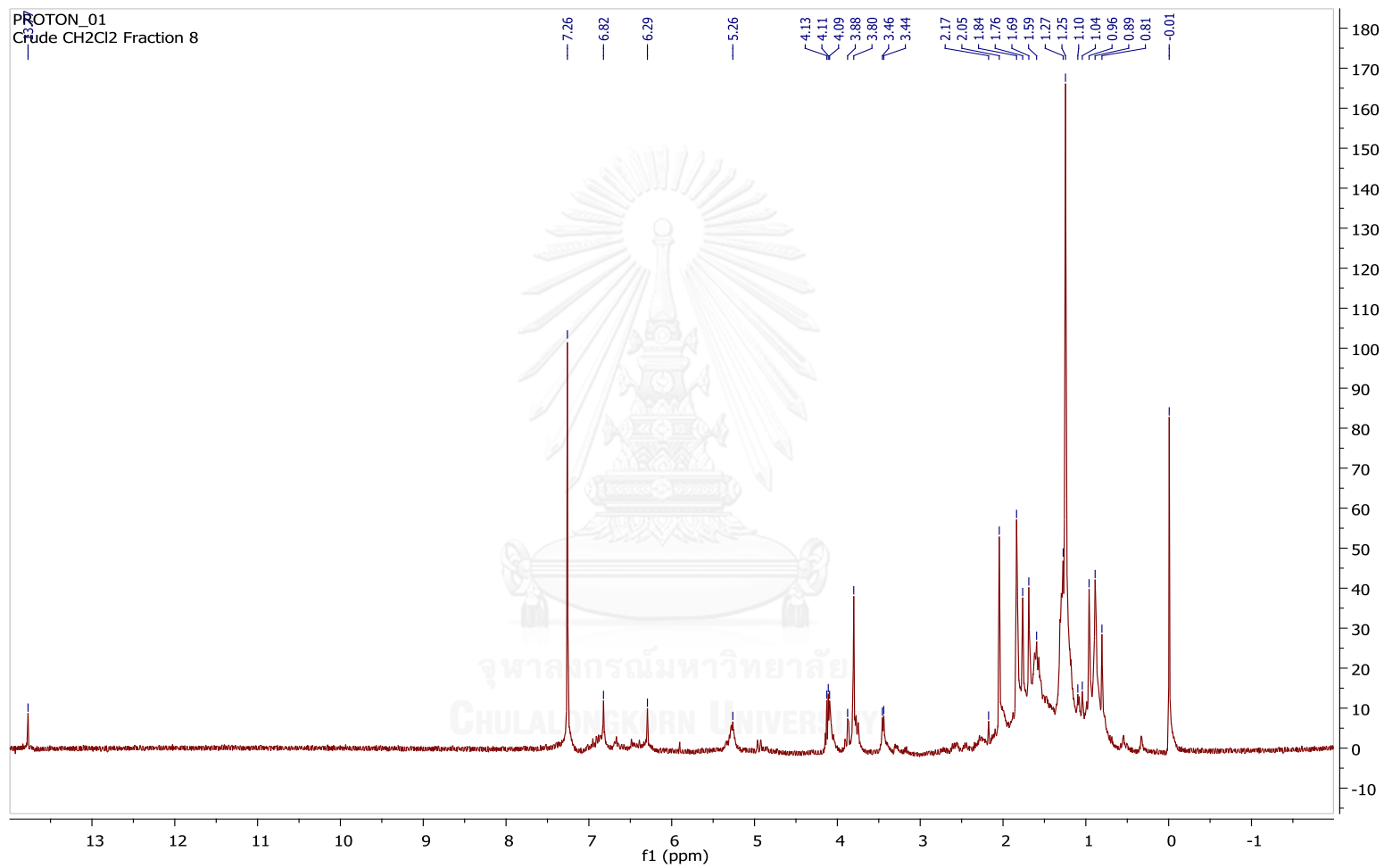
Nuclear magnetic resonance spectrum (NMR spectrum)



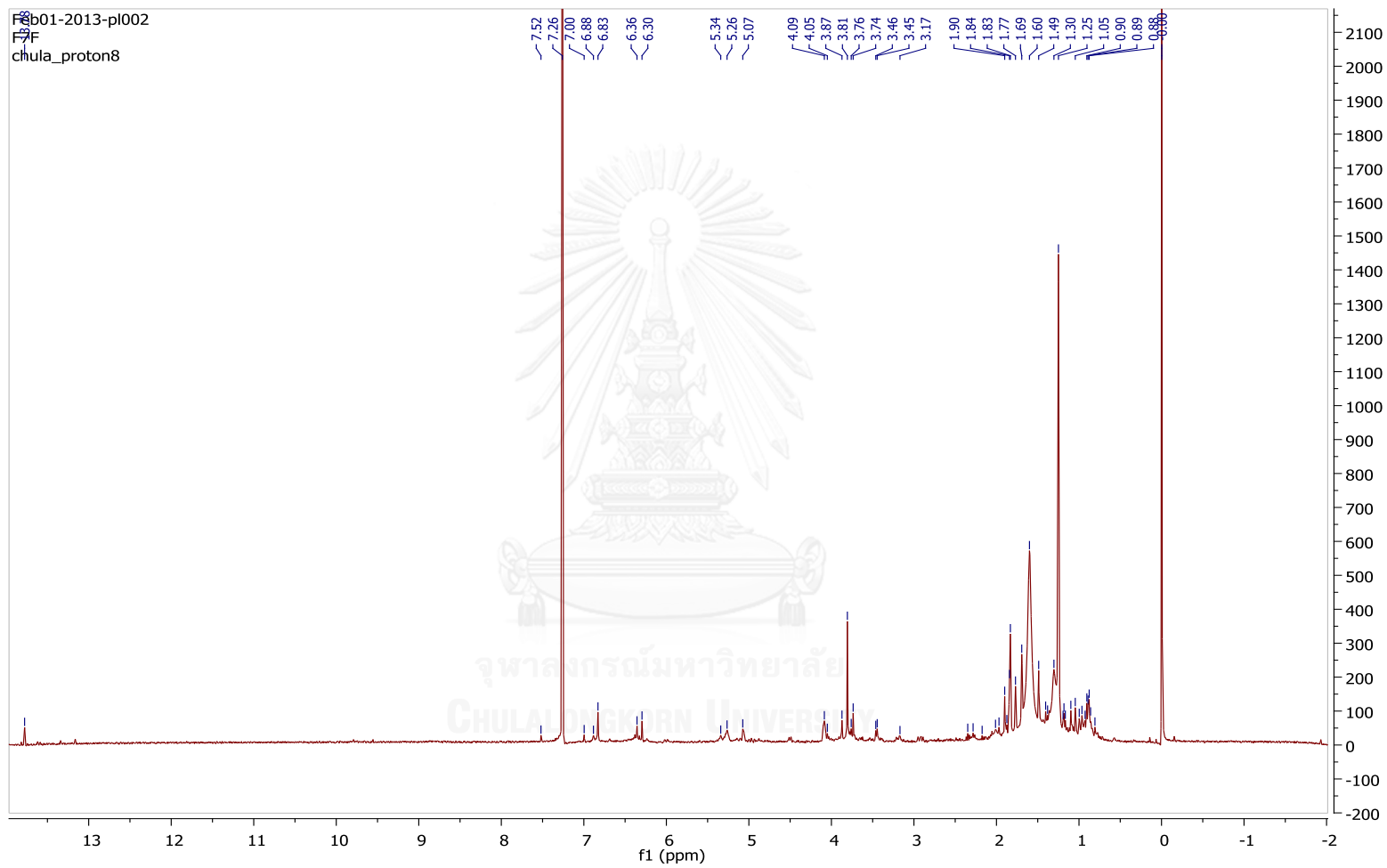
B1. ^1H NMR spectrum of reverse crude dichloromethane extracted (reference peak of CDCl_3 = 7.26 ppm).



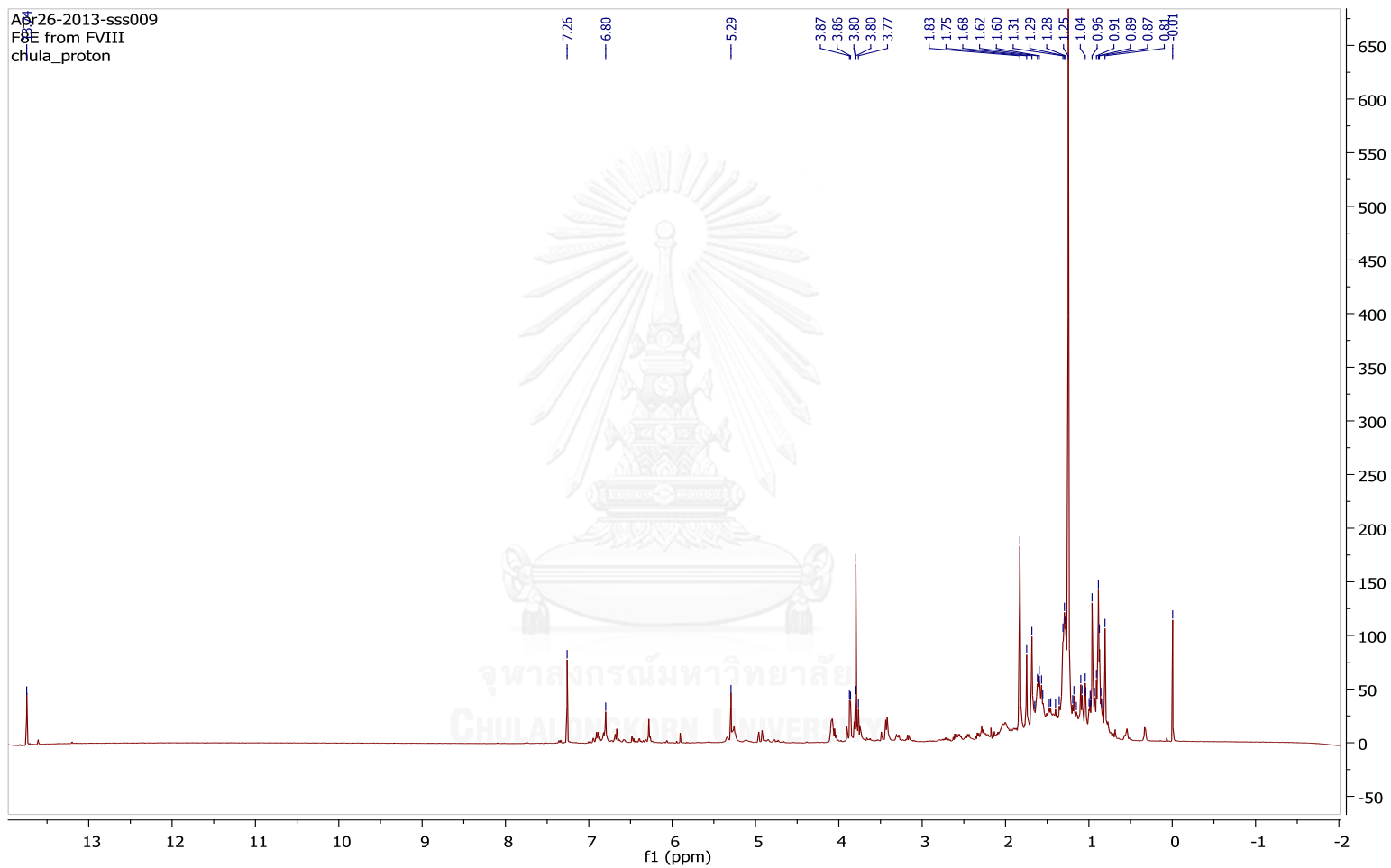
B2. ¹H NMR spectrum of Fraction VII (reference peak of CDCl₃ = 7.26 ppm).



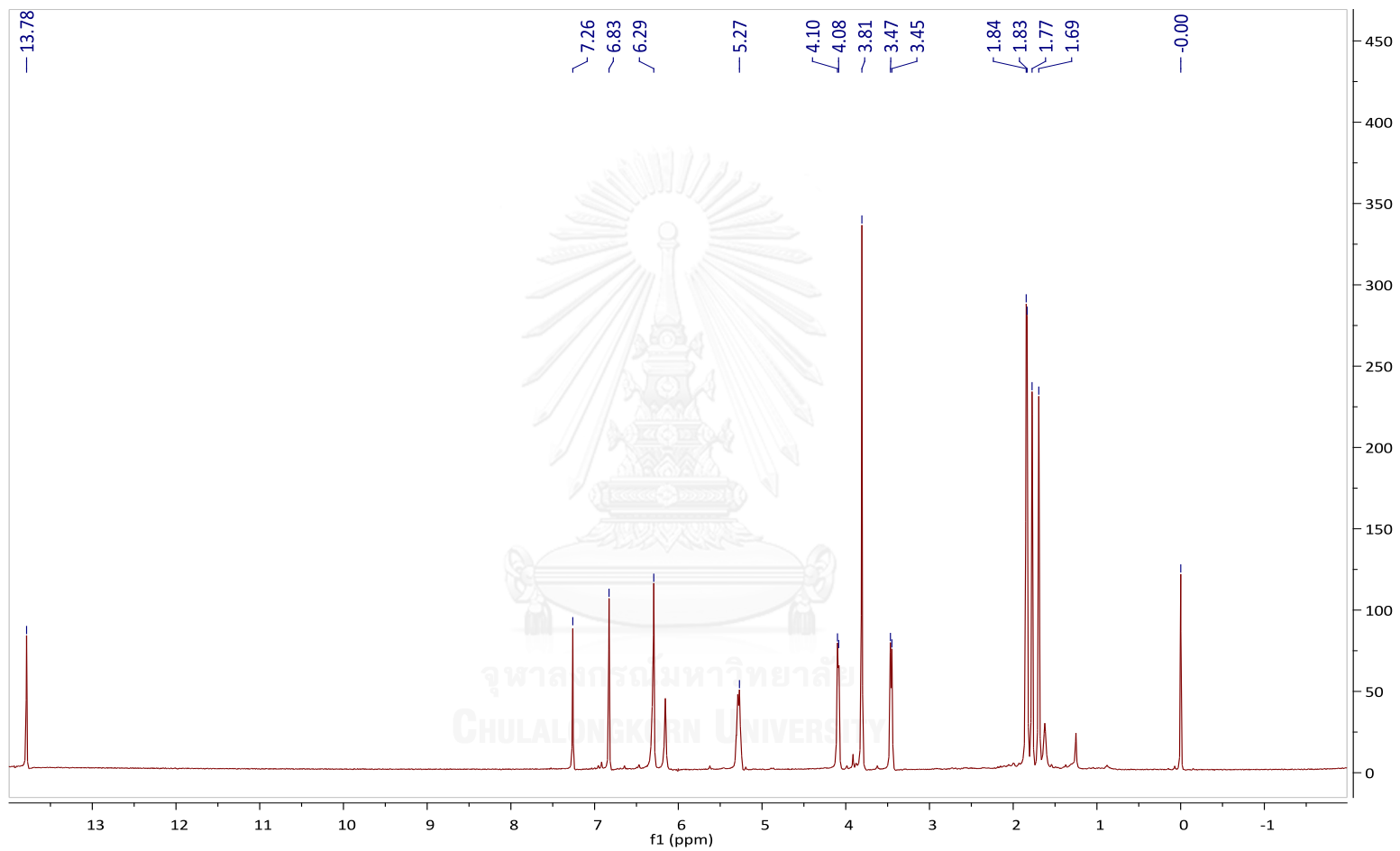
B3. ¹H NMR spectrum of Fraction VIII (reference peak of CDCl₃ = 7.26 ppm).



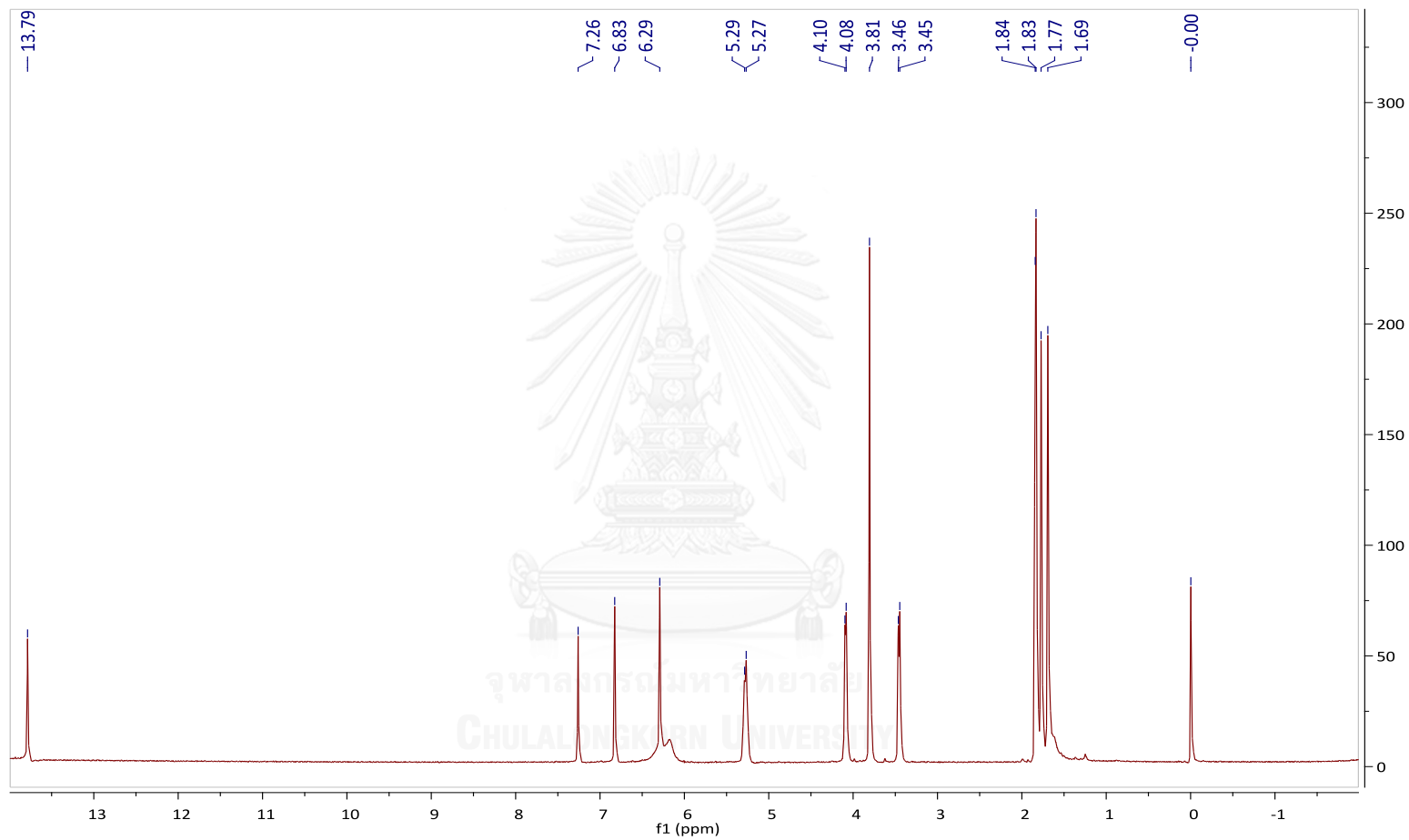
B4. ^1H NMR spectrum of subfraction F7F (reference peak of $\text{CDCl}_3 = 7.26$ ppm).



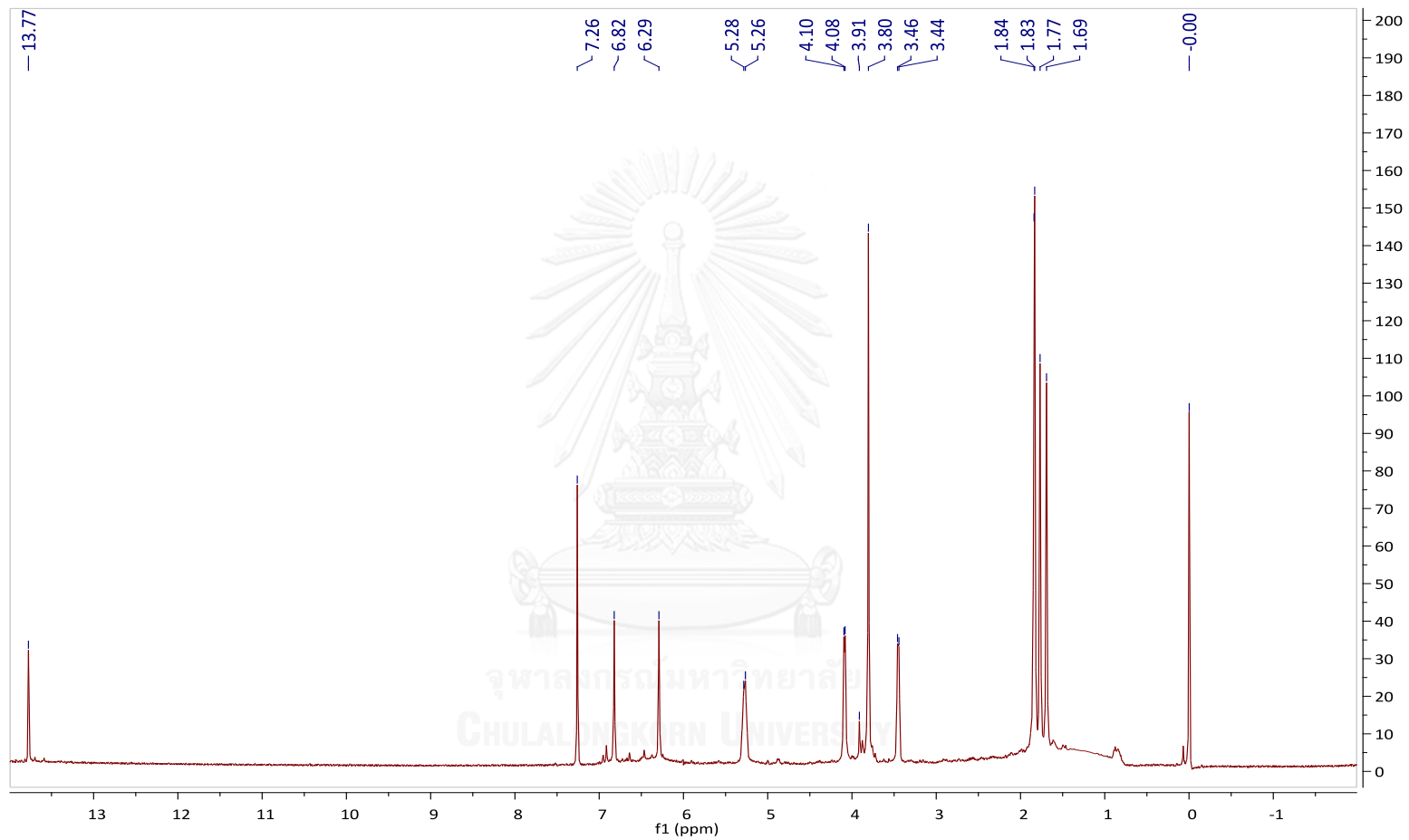
B5. ^1H NMR spectrum of subfraction F8E (reference peak of $\text{CDCl}_3 = 7.26$ ppm).



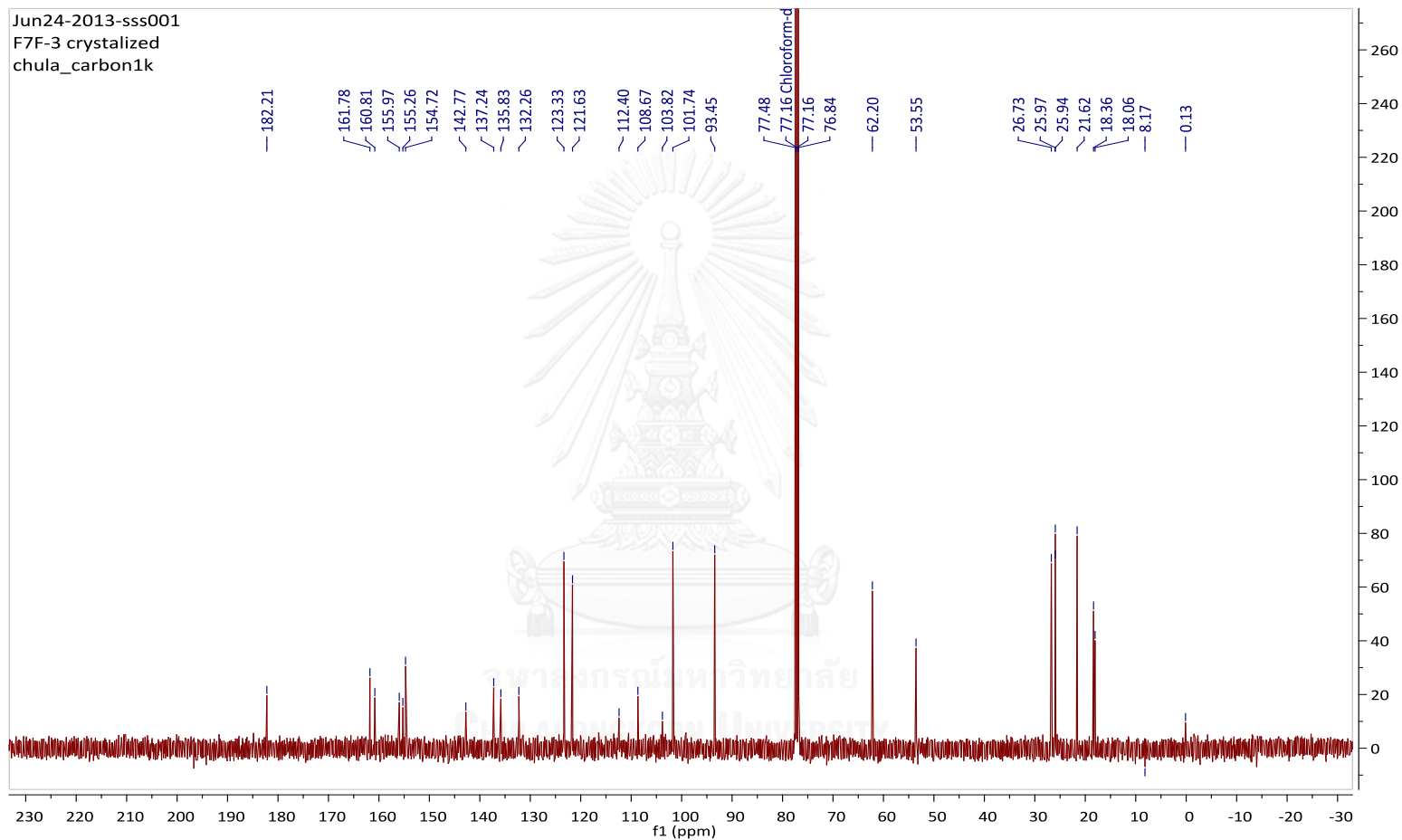
B6. ^1H NMR spectrum of F7E (reference peak of $\text{CDCl}_3 = 7.26$ ppm).



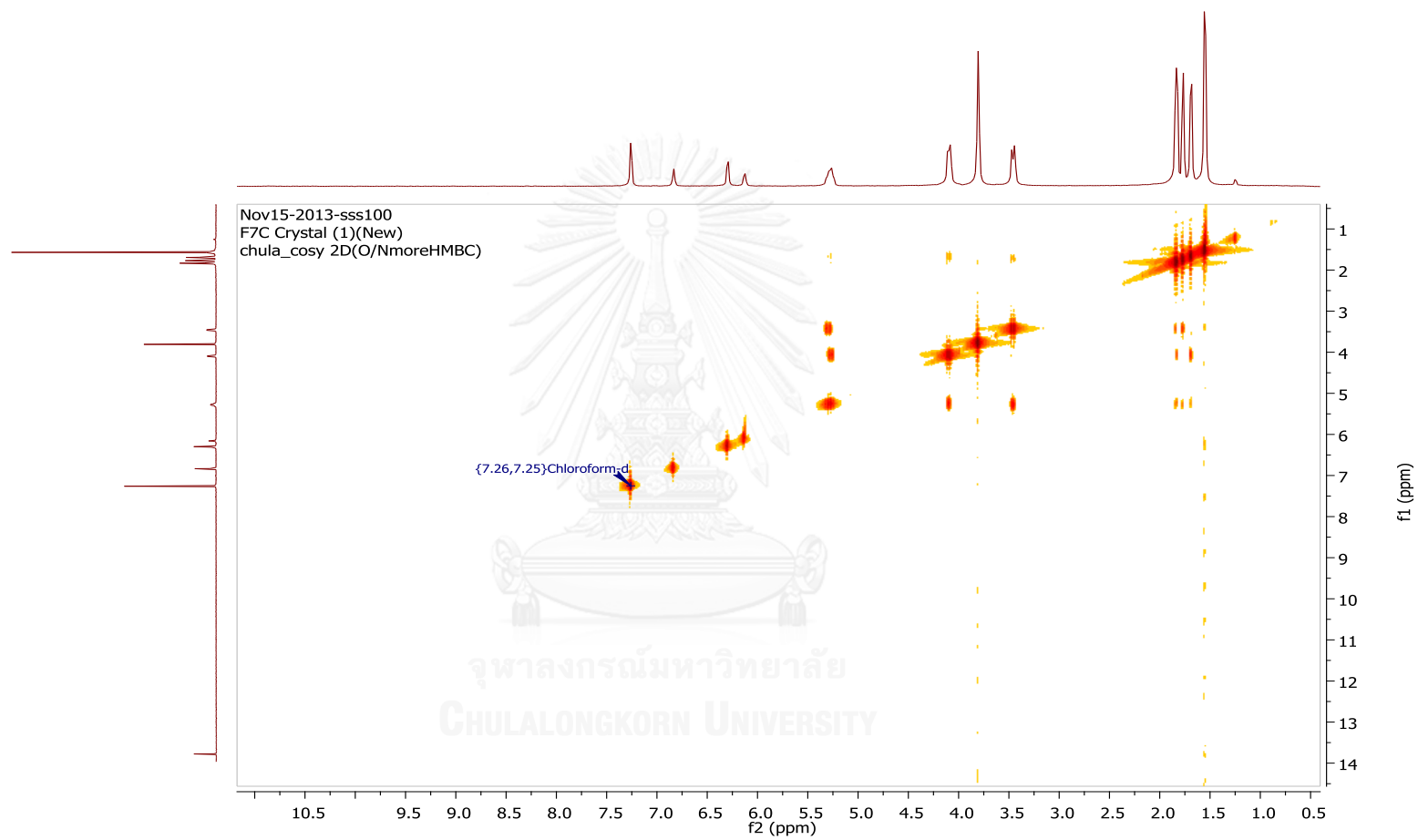
B7. ^1H NMR spectrum of F7F-3 (reference peak of $\text{CDCl}_3 = 7.26$ ppm).



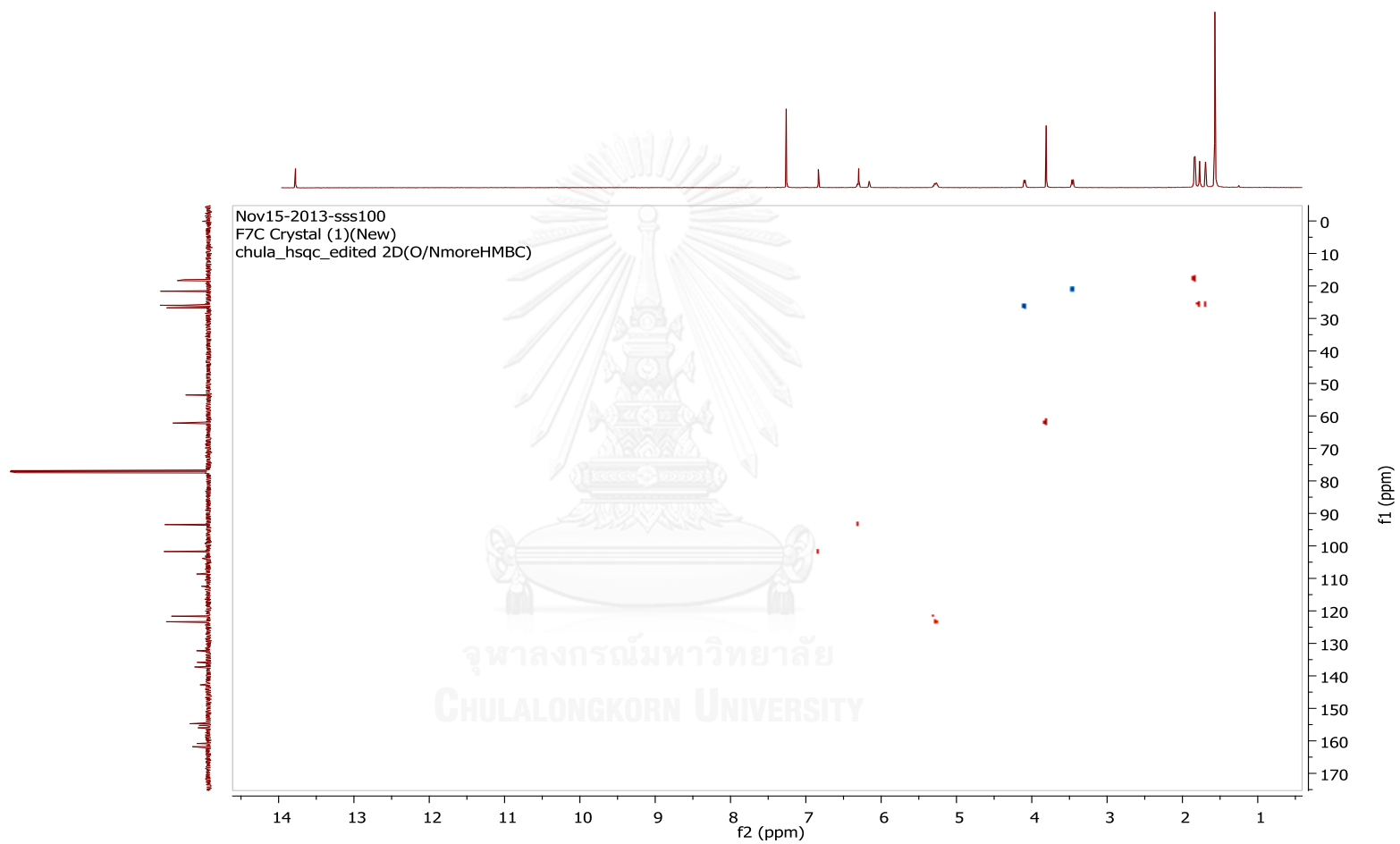
B8. ^1H NMR spectrum of F8E-5 (reference peak of $\text{CDCl}_3 = 7.26$ ppm).



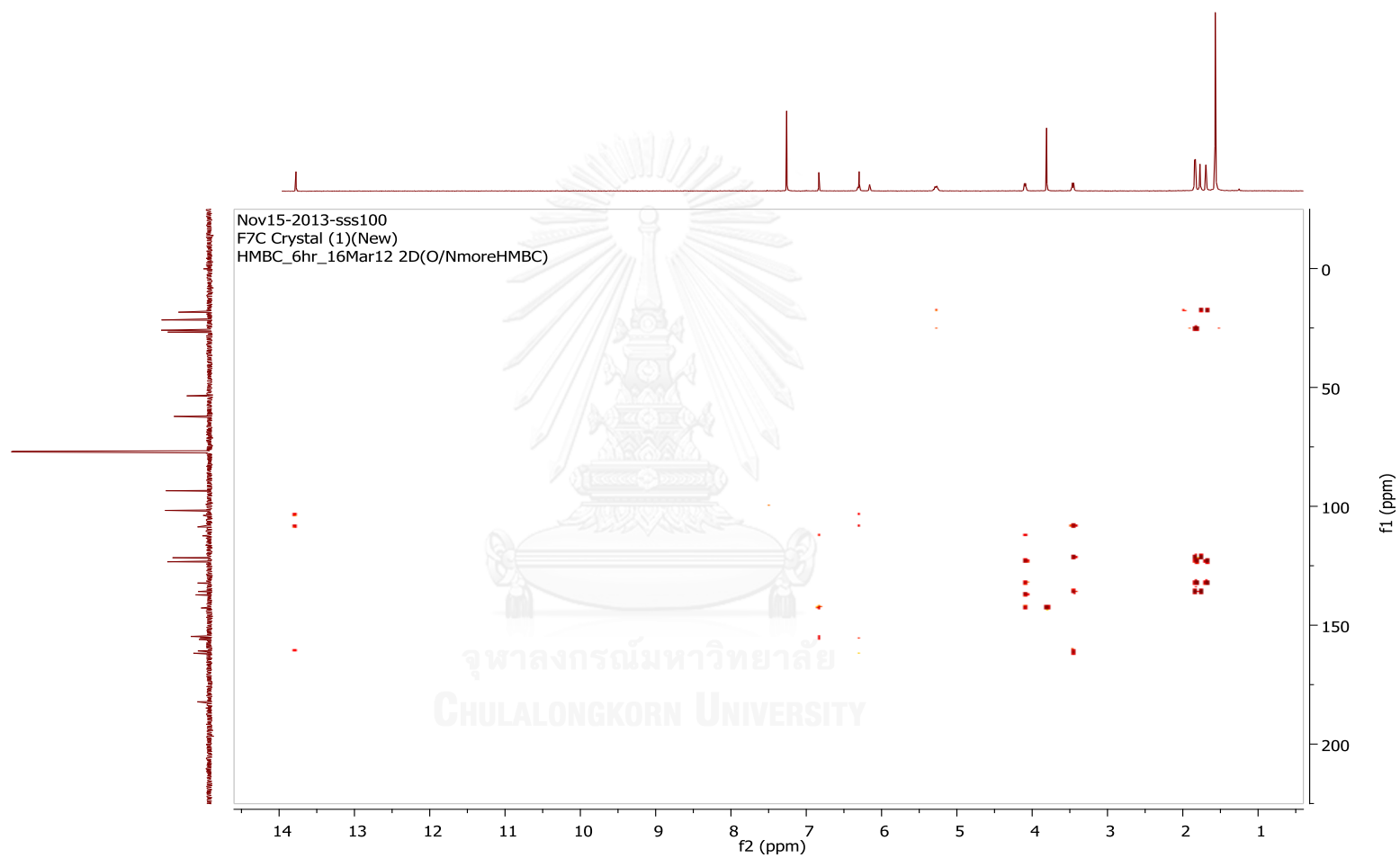
B9. ^{13}C NMR spectrum of F7F-3 (reference peak of $\text{CDCl}_3 = 77.16$ ppm).



B10. Correlation spectroscopy (COSY) spectrum of F7F-3.



B11. heteronuclear single quantum coherence spectroscopy (HSQC) spectrum of F7F-3.



B12. heteronuclear multiple bond correlation (HMBC) spectrum of F7F-3.

Appendix C

Cell culture and reagent preparation

1. Cell counting by haemocytometer

One drop of cells was transferred into a haemocytometer. Cells were counted under a light microscope.

Cell concentration (cells/mL) = the average number of cells from 4 corners x dilution factor x 10^4

2. RPMI 1640 medium

RPMI 1640 powder	10.4 g
NaHCO ₃	2 g
Ultrapure d-H ₂ O	1 L
Fetal bovine serum	5 mL

2.1 Dissolve RPMI powder and NaHCO₃ in ultrapure d-H₂O.

2.2 Adjust pH to be 7.2 by 2 N HCL.

2.3 Filter the solution by 0.22 µm millipore for sterilization.

2.4 Save in a bottle and keep at 4 °C.

2.5 Add 5 mL of fetal bovine serum to 95 mL fresh medium to make 5% (v/v) medium before use.

3. Freezing RPMI 1640 medium (100 mL)

RPMI 1640 fresh medium	65 mL
Fetal bovine serum	25 mL
Analytical grade DMSO	10 mL

4. Trypsin-EDTA preparation

Phosphate buffer saline	0.01 M
Ethylene diamine tetraacetic acid (EDTA)	0.01% (v/v)
Trypsin powder	0.05% (w/v)

After all ingredients are mixed, it will be filtered by 0.22 μm millipore for sterilization and stored at 0 $^{\circ}\text{C}$ until use.

5. Ceric ammonium molybdate dipping reagent for TLC preparation

d-H ₂ O	200 mL
Conc. H ₂ SO ₄	10 mL
(NH ₄) ₆ Mo ₇ O ₂	10 g
Ce(SO ₄).4H ₂ O	0.4 g

5.1) Gently fill conc. H₂SO₄ to 100 mL of d-H₂O.

5.2) Add 10 g of (NH₄)₆Mo₇O₂ to the solution.

5.3) Add 0.4 g of Ce(SO₄).4H₂O to the solution.

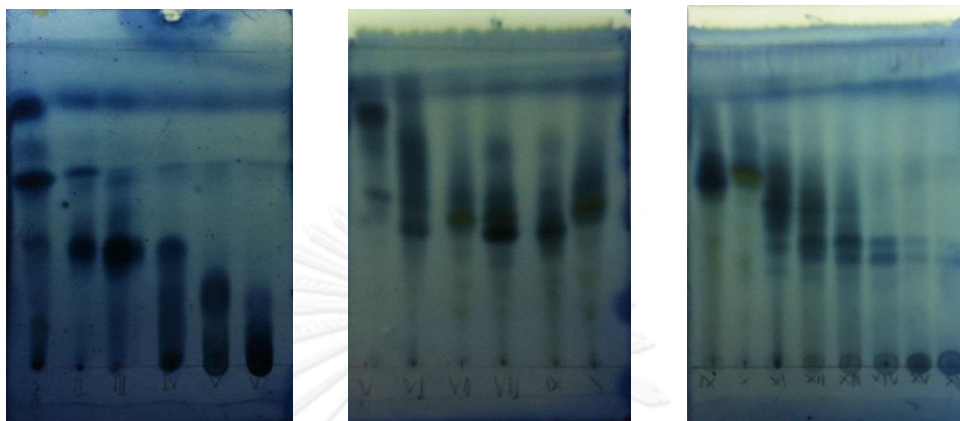
5.4) Adjust the final volume with d-H₂O to be 200 mL.

6. MTT (5 mg/ml) preparation in final volume of 10 mL

MTT powder	50 mg
Sterilized normal saline	10 mL

Appendix D

1. Thin layer chromatography pattern of fractions from reverse crude dichloromethane extracted.

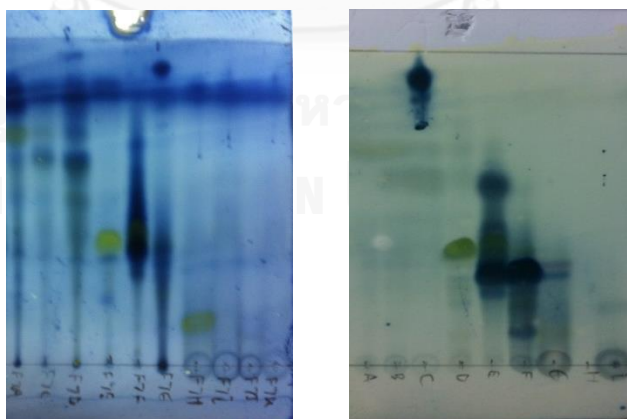


Left TLC: Fraction I-VI pattern in mobile phase system of 100% dichloromethane.

Center TLC: Fraction V-X pattern in mobile phase system of 95% dichloromethane and 5% methanol(v/ v).

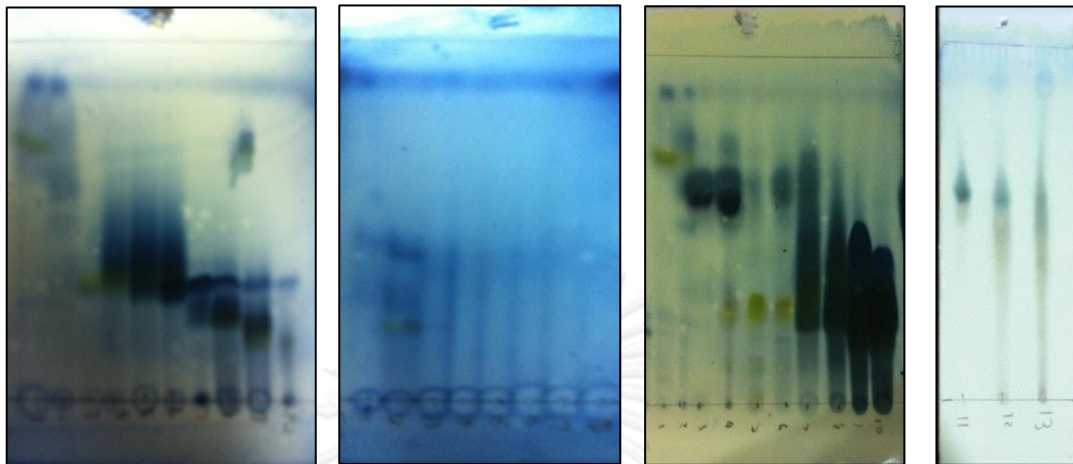
Right TLC: Fraction IX- XVI pattern in mobile phase system of 90% dichloromethane and 10% methanol(v/ v).

2. Thin layer chromatography pattern of chemical compositions from fraction VII and VIII



Left TLC Fraction F7A-F7K pattern from left to right. Right TLC Fraction F8A- F8I pattern from left to right. Both condition used mobile phase system of 95% of dichloromethane and 5% methanol (v/ v).

3. Thin layer chromatography pattern of chemical composition from F7F and F8E



Left TLC: Chemical composition pattern of F7F-1 to F7F-10 from left to right.

Center left TLC: Chemical composition pattern of F7F-11 to F7F-13 from left to right (F7F-13 after merge with all 6 right pattern).

Center right TLC: Chemical composition pattern of F8E-1 to F8E-10 from left to right.

Right TLC: Chemical composition pattern of F8E-11 to F8E-13 from left to right.

Mobile phase system of left and center right is 97% dichloromethane and 3% methanol(v/ v). F8E-11 to F8E-13 (right TLC) use 90% dichloromethane and 10% methanol(v/ v). F7F-11 to F7F-13 (center left) use 95% dichloromethane and 5% methanol(v/ v).

All TLC plate in this research using ceric ammonium molybdate for reagent to identified pattern

VITA

Mr. Pongvit Nugitrangson was born on May 27, 1988, in Bangkok, Thailand. He was graduated with grade 12 from Saint Gabriel College in Bangkok, Thailand, in 2007. In 2011, He was graduated with a Bachelor Degree in Biology from Department of Biology, Faculty of Science, Chulalongkorn University. At present, he is a graduate candidate in Master's Degree, Program in Biotechnology, Faculty of Science, Chulalongkorn University.

Presentations:

Nugitrangson, P., Chanchao, C., Pornpakakul, S., and Puthong, S. (2013) The chemical composition and antiproliferative activities of cerumen: the case of stingless bee *Tetragonula laeviceps* in Thailand. The 28th National Graduate Research

Conference, Bangkok, Thailand. p. 492-499. (Best oral presentation award)

Nugitrangson, P., Chanchao, C., Pornpakaul, S., and Puthong, S. (2014) Chemical composition and antiproliferative activity of cerumen from stingless bee *Tetragonula laeviceps* in Chantaburi province. Abstract. The 18th Biological Sciences Graduate Congress, Kuala Lumpur, Malaysia. 43. (January 6-7, 2014)

Nugitrangson, P., Chanchao, C., Pornpakakul, S., and Puthong, S. (2012) Chemical composition and antiproliferative activity of cerumen from stingless bee *Tetragonula laeviceps* in Chantaburi province. Abstract. The 17th Biological Sciences Graduate Congress, Bangkok, Thailand. BT-OR 10, 47. (December 8-10, 2012)